TRIBHUVAN UNIVERSITY

INSTITUTE OF ENGINEERING

PULCHOWK CAMPUS

THESIS NO.   M-371-MSREE-2020-2023

Structural Analysis of The Bifurcations at Phukot Karnali Hydropower Project

by

Purushottam Khatiwada

A THESIS

SUBMITTED TO THE DEPARTMENT OF MECHANICAL AND AEROSPACE ENGINEERING IN PARTIAL FULFILLMENT OF THE REQUIREMENTS FOR THE DEGREE OF MASTERS OF SCIENCE IN RENEWABLE ENERGY ENGINEERING

DEPARTMENT OF MECHANICAL AND AEROSPACE ENGINEERING

LALITPUR, NEPAL

October, 2023

COPYRIGHT

The author has consented to the availability of their thesis for public scrutiny at the library of the Department of Mechanical and Aerospace Engineering, Pulchowk Campus, Institute of Engineering. Additionally, the author has granted permission for extensive reproduction of this thesis for scholarly purposes, subject to approval by the professor who supervised the research documented herein, or, in their absence, by the Head of the Department under which the thesis was conducted. It is explicitly understood that proper acknowledgment of the author of this thesis and the Department of Mechanical and Aerospace Engineering, Pulchowk Campus, Institute of Engineering, must be accorded in any utilization of the thesis material. Unauthorized reproduction, publication, or commercial exploitation of this thesis without the prior consent of the Department of Mechanical and Aerospace Engineering, Pulchowk Campus, Institute of Engineering, and written authorization from the author is strictly prohibited.
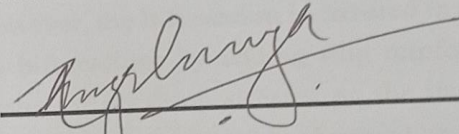
Requests for permission to replicate or employ any portion of this thesis, either in full or in part, should be directed to the following address:

Head,

Department of Mechanical and Aerospace Engineering,

Institute of Engineering Pulchowk Campus

Lalitpur, Kathmandu

Nepal

APPROVAL PAGE

TRIBHUVAN UNIVERSITY

INSTITUTE OF ENGINEERING

PULCHOWK CAMPUS

DEPARTMENT OF MECHANICAL AND AEROSPACE ENGINEERING

"Structural Analysis of The Bifurcations at Phukot Karnali Hydropower Project," has been submitted by Mr. Purushottam Khatiwada as part of the prerequisites for obtaining a Master's degree in Renewable Energy Engineering. We recommend its acceptance by the Institute of Engineering.

Supervisor:

Prof. Dr. Tri Ratna Bajracharya

Department of Mechanical and Aerospace Engineering

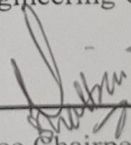Institute of Engineering Pulchowk Campus

External Examiner:

Er. Anil Sapkota

Junior Professor

Nepal Engineering College, Bhaktapur

Committee Chairperson:

Asst. Prof. Dr. Sudip Bhattarai

Head, Department of Mechanical and Aerospace Engineering

Institute of Engineering Pulchowk Campus

Tribhuvan University
Institute of Engineering
Department of Mechanical and Aerospace Engineering
Pulchowk Campus

Date: October 5, 2023

ABSTRACT

The research is based on the structural analysis of bifurcations located in the intake manifold of Phukot Karnali Hydropower Project. The analysis is done with Finite Element Approach (FEM) Approach by making use of Ansys Mechanical 2020 R1. The geometry of the bifurcation is based on the original design data and recommended dimensions including bifurcation angle, cone length and pipe thickness from previous research on the same hydropower project. From literatures it is found that the suggested thickness of the pipe is 130 mm for the first bifurcation and 70 mm for the second bifurcation by conducting structural simulation of the pipe without adding any structural elements. At the actual hydropower site however, the bifurcation is covered in concrete. Firstly, structural analysis is conducted on the two bifurcations by adding ring reinforcements around the inlet and outlet pipes. The maximum value of resulting stresses on the two models found to either be borne by the rings or the maximum displacement seen is observed on the joints of the reinforcements. Therefore, the models for the analysis with concrete blocks are simplified. From the results of the analysis the observed value of maximum stress on the concrete is much lower then the allowable value, the process is repeated with thinner (reduced by 10mm in each model) pipes to assess the rate of changing stress values. It is found that with 100 mm thick first bifurcation and 70 mm thick second bifurcation exerts maximum principal stress on the concrete block (Grade M40) such that the safety factor of the concrete block are 2.067 and 2.057 respectively when considering the permissible stress as 10 MPa (direct stress limit for M40 grade concrete) beyond which the block will develop cracks. Approximately 94.09-ton material can be saved using 100 mm pipe instead of 130 mm pipe for first bifurcation.

ACKNOWLEDGEMENT

CONTENTS

LIST OF TABLES

LIST OF FIGURES

LIST OF ABBREVIATIONS

CAD   : Computer Aided Drawing
CFD   : Computational Fluid Dynamics
NEAEC   : Nepal Electricity Authority Engineering Company
MW   : Megawatts
MPa   : Megapascals
FEM   : Finite Element Method
ASTM   : American Society for Testing and Materials
FOS   : Factor of Safety
SST   : Shear Stress Transport
3D   : Three Dimensional
masl   : meters above sea level

CHAPTER 1: INTRODUCTION

1.1 Overview

Penstock is the component in the hydropower system that converts the potential head of water into pressure head and kinetic head as the water moves from the reservoir to the turbines in hydropower plants (Kumar & Singhal, 2015). A large capacity hydropower plant has a combination of small turbines rather than one large capacity turbine. The rationale behind it is to avoid zero energy generation during the time of repair and maintenance of the turbines. However, if there are multiple turbines, the turbines can be repaired in turn and the loss in energy generation is manageable. Generally, the multiple turbines used are of the same capacity so that the loss is constant during the down time of each turbine. Even though there are many turbines used, each turbine doesn't have its own penstock (Dhakal & Shrestha, 2023). The simple reason behind it being the high material cost from which the pipe is constructed (Neupane & Luitel, 2022).

Manifold is the term used for the penstock that divides the single inlet from the reservoir into equal flow rates to the turbines. Manifold has components such as bifurcation and trifurcations. Bifurcation is the component that divides a flow into two smaller flows (as shown in Figure 1.1) and using successive bifurcations enables the division of flows to multiple turbines as well (Nepal Government, 2006). Trifurcation is a component that divides one flow into three smaller flows (Aguirre et al., 2019). For example, if there are three turbines must be operated, there are two options. Either a trifurcation is selected that has three equal diameter pipes that are joined at a single point, or a manifold is designed which has two bifurcations such that the flow divided at one bifurcation is directed to another bifurcation as shown in Figure 1.2.
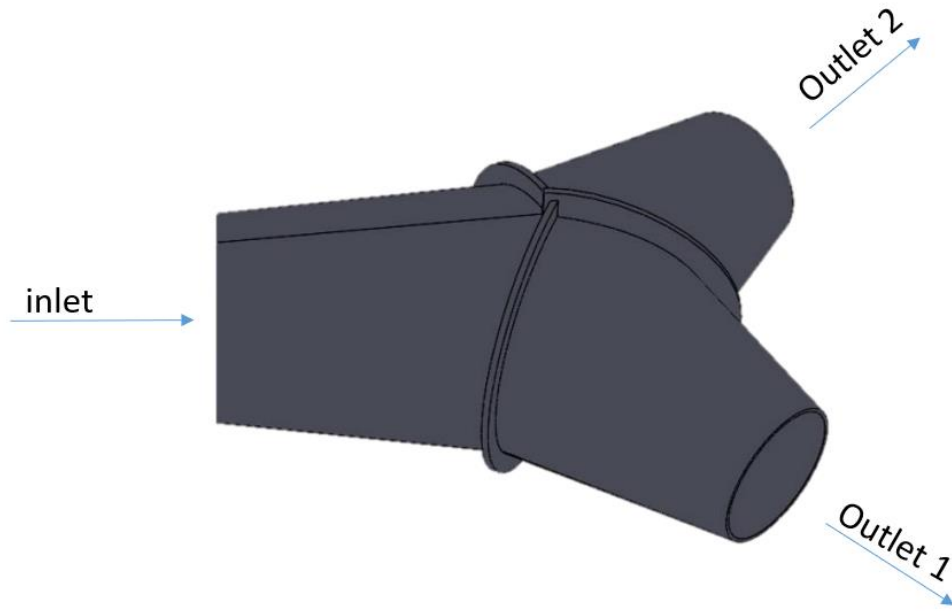
Figure 1.1 Bifurcation with reinforcements (Sharma & Neupane, 2023)
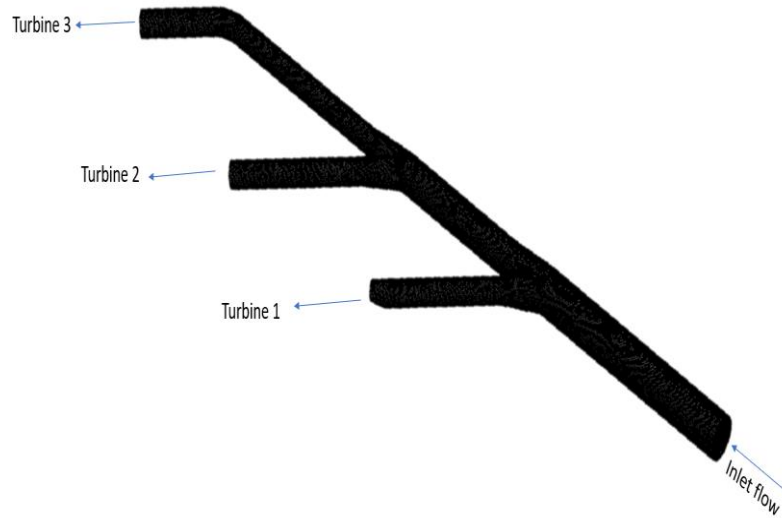
Figure 1.2 Manifold with successive bifurcations

A trifurcation (Aguirre Rodriguez & Camacho, 2014) may seem like the most feasible option, but the stress exerted at the trifurcation point is very high as the number of branched penstocks increases as opposed to a bifurcation. That is since the more complex the shape of a conduit is, the more is the stress concentration (Dhakal & Shrestha, 2023). Therefore, a manifold is preferred as the design is similar even when the number of turbines increases.

A manifold is slightly longer than the trifurcation so the material cost may be slightly high (*Penstock Branch Design*, 2009).

The design and selection of the type of manifold used in the construction is very important to determine strength of the conduit and the flow behavior of the fluid. Constructing the structural components is very expensive so there must be a tradeoff between optimum values of head loss, stresses on the pipes and the cost of construction (Kumar & Singhal, 2015) (Dhakal & Shrestha, 2023). Stresses within a bifurcation tend to be notably elevated, ranging from 3 to 9 times higher than the stresses experienced in conventional pipeline segments (Adamkowski & Kwapisz, 2004). It is very difficult to obtain the optimum head loss with the highest structural strength with just the classical numerical approach. There is the provision of experimental approach as well to ensure it but is found to be very costly when cases like hydropower are to be researched (Bureau of Indian Standards, 1995).

1.2 Problem statement

The research is focused on taking the case study of bifurcations at Phukot Karnali Hydropower Project. Two similar manifolds are designed for the project where there are six turbines of 79 MW each. Each manifold supplies water to three turbines. The design for which has been done by NEAEC.

The analysis if fluid flow is conducted by (Dangi et al., 2022) for the manifold followed by the initial structural simulation of the bifurcation pipes. Several models of the manifold having varying cone length and bifurcation angle are simulated and the best option among them is recommended based on the head loss results. For that, the flow behavior of the fluid is studied in the branched sections and hence the regions of extreme values of pressure and velocity of the fluid are found. Based on the values and the most suitable material chosen, structural analysis is also performed that suggests thickness of 130 mm for first bifurcation and 70 mm for second bifurcation (2nd branch). However, the design thickness was lower than that which means that using the pipe of suggested thickness increases the cost of construction of the bifurcation.

1.3 Rationale

In the actual site, the manifold has many structural components that also help in decreasing the head loss and handling the high pressure exerted by the flow. The point where the flow gets branched in a bifurcation is reinforced with ring girder and external stiffeners. The primary purpose of the stiffening ring is to avert penstock instability resulting from external pressure (Bai et al., 2013). That can help in bringing the suggested thickness of the manifold. The cost of the construction of the manifold can be reduced considerably since

the thickness of the pipe required with other reinforcements is a lot less than with the components analyzed in isolation.

The rationale of the research is that concrete block that surrounds the pipe supports the pipe in bearing the fluid forces inside the pipe and hence the suggested thickness of the pipe may not be required (D. Ji & Li, 2014).

1.4 Objective

The objective of this research is to conduct the structural analysis of the bifurcations in the intake manifold of 480-MW Phukot Karnali hydropower project.

The specific objectives of the research are:

-To model the manifold that supplies the water to the three turbines and conduct CFD on it to compare the head loss in the three outlet pipes

-To conduct structural analysis of pipe along with the supporting members and observe the impact of the members on the stress and deformation of the pipe

-To assess the trend of changing stresses in the bifurcation assembly and suggest the minimum thickness of the pipe required considering a suitable safety factor

1.5 Limitations

The analysis is more focused on the interaction of force between the layers of pipe and concrete, thus other parts welded to pipe structure like ring girders and sickle plates aren't considered. The main cause that prompted the limitation was that the thickness of the components is chosen arbitrarily in the original design as well and a separate analysis can be done by varying the thickness of the components. To compensate for the limitation, the target factor of safety assumed for concrete is higher than normally taken.

CHAPTER 2: LITERATURE REVIEW

The structural strength of a penstock is a very important factor to consider while designing the penstock which can have severe consequences if not designed properly. A study is conducted (Adamkowski, 2001) for the cause of a rupture occurred in Lapino hydropower plant. The pipe was constructed with different materials on either side of the bifurcating point. i.e., concrete, and welded steel. The plant operated with two gensets that were identical to each other. Each set consisted of two Francis turbines sharing a common shaft and hence the generator. The rupture occurred at the steel pipe which induced flood in the whole powerhouse. The cause was found to be the welding joints used in the steel pipe were of low quality and even the reinforcements that supported the pipe lacked strength.

(Thapa et al., 2016) Techniques of Finite Element Method and Computational Fluid Dynamics are used to study the flow behavior and structural stability of bifurcations of Kulekhani III Hydropower project. Suitable thickness and reinforcements were given to the bifurcation component and the structural simulation was performed using FEM. The thickness of the sickle plate used in the model is taken from a suitable guess. ASTM A36 type steel is chosen that has a yield stress of 250 MPa and the pipe must withstand design pressure equal to 1.54 MPa (including the surge pressure). The section is supposed to be a simply-supported beam that has its free ends provided with fixed supports. Prevailing design codes are used as reference standard to compare the stress and deformation values obtained from the structural simulation. The maximum stress that is obtained from the simulation is 108 MPa. The results found to be satisfactory were recommended for the further fabrication process.

Trifurcations make it harder to limit the high losses in a power plant. Thus, the losses are quantified as a function of flow rate by using techniques of CFD. k- ω model is preferred for the turbulence model. The difference in pressure is calculated by applying the energy equation between each outlet (3 meters each) and inlet (4.5 meters) successively. The volumetric rate varies from 20 to 65 m^3 per second. The head loss decreases with increasing volumetric flow within the range mentioned (Aguirre Rodriguez & Camacho, 2014).

A case study taken for CFD is of Solukhola Dudhkoshi hydropower project which generates 86 MW. Three different types of manifolds are simulated in the research in order to find the most optimum manifold option in terms of head loss (Kandel & Luintel, 2019). The head loss is calculated by recording the pressure and velocity values in the three branches of each type of manifold option. The domains are divided into tetrahedron shape elements. The Shear Stress Transport model was adopted for the turbulence during the

problem setup. The inlet is chosen to be mass flow inlet type whereas outlet is taken as pressure outlet. The problem defined was a steady state type. The results were optimum in case of trifurcation type manifold among the three manifolds. The head loss between any two sections of the same pipe is the difference between the pressure and velocity heads of the two sections considered.

$$\Delta h = \frac{\Delta p}{w} + \frac{\Delta v^2}{2g} + \Delta z \qquad \text{...............................} \qquad \text{Equation 2.1}$$

Also written,

Δh = loss in pressure head + loss in kinetic (or velocity head) + loss in potential head

Where,

Δh is the difference in total head between two sections.

Δp is the difference in pressure values in the two sections.

w is the specific weight of the fluid

Δv^2 is the difference in the square of velocities in the two sections.

g is the acceleration due to gravity

Δz is the difference in height of the two sections.

All head losses are measured in meter (m)

There are other minor losses which are generally not included in the calculation, but they are found to have a profound impact on the overall productivity of low head hydropower projects. Head loss must be minimized because it equates to financial gains as the project life lengthens (Mallik & Paudel, 2010).

The part where the flow is divided must carefully be designed since small deviation in any of its design variables brings huge change in the head loss that occurs inside it (Koirala et al., 2017). The design of manifold is subject to different variables such as flow rates, material strength, location of the powerhouse, head, etc. along with the variables of bifurcation such as branch angle, cone length, the cross section of the inlet and branch conduits, properties of material used. When the flow is being branched at a particular bifurcation, a component called sickle plate is provided. It is a thin plate that is located exactly at the point where the flows get separated. It helps in avoiding the internal lining

of the pipe being corroded due to the sand particles hitting the surface when the flow is separated (Mallik & Paudel, 2010).

The thickness of the penstock pipe is found out by the formula.

$$t = \frac{P \text{ x } D}{2 \text{ x } \sigma \text{ x } J}$$ …………………………………………… Equation 2.2

Where,

"P" is the mean effective internal pressure at the center of the pipe measured in MPa

"D" units in diameter measured in meters

"J" is the Joint efficiency that is dependent on the external stiffeners whose value lies between 0 and 1

"σ" represents the allowable stress value for the material chosen that is also measured in MPa
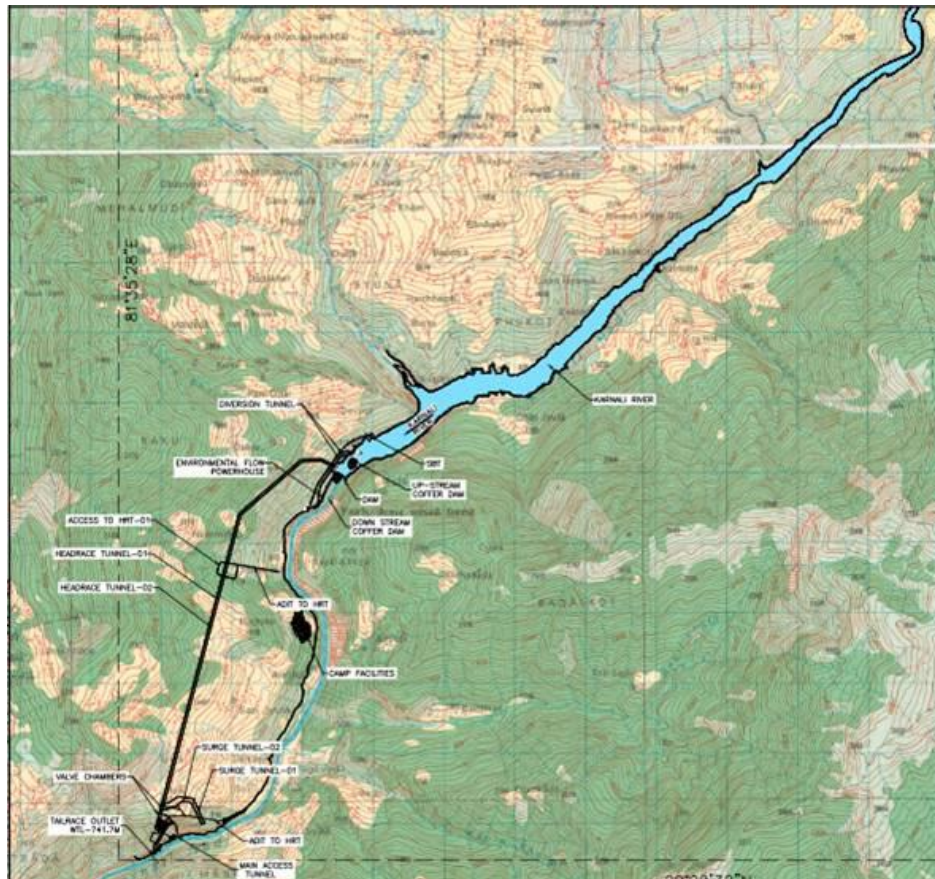
*Figure 2.1 Map of the hydropower area (*Vidhyut Utpadan Company Limited*, 2023)*

The source of hydropower starts when Karnali and Sanigad rivers meet one and half kilometers upstream from the head work. It's design head is 168.3 meter and is a type of peaking Run-of-river hydropower project. The catchment area for the river basin is 16,902 square kilometers shown in Figure 2.1.

There are three turbines arranged to be connected by two successive bifurcations in each manifold. A research article focusing on the flow behavior of the fluid at the three bifurcations using CFD is taken as the basis for this research (Dangi et al., 2022). CFD uses governing equations of fluid flow to iteratively calculate the flow behavior of any fluid in its boundary conditions. (Ferziger & Perić, 2002) It focuses on finding the best cone length and bifurcation angle for the bifurcations in the manifold followed by structural simulation to determine the optimal thickness of the bifurcations. Successive bifurcations are preferred over trifurcations in all but one of the hydropower projects in Nepal.

Structural analysis of any component is based on the principles of Finite Element Method. FEM involves the technique of fragmenting the component into several smaller parts known as elements. Elements are connected to each other through breaking points which are also known as nodes. Applying the equilibrium concept is done for each of the elements and that calculation is executed through stiffness matrix. (Inc, 2018) Calculation by hand when the number of elements is very high is very tough and time consuming hence high computational power devices are used in such cases. The equations that are required to solve the problem are defined based on loads applied and the supports. The main results obtained and observed in such simulations are deformation and stress (Adamkowski & Kwapisz, 2004).

(Sharma & Neupane, 2023) Seti Nadi Hydropower Project is chosen as subject of case study for structural analysis of bifurcation. Circumferential stress is exerted on the pipe due to the flow pressure. It is directly proportional to the diameter of the pipe and inversely proportional to its thickness (Bhavan & Marg, 2000).

$$\sigma = \frac{P \times R}{t} \qquad \text{..} \quad \text{Equation 2.3}$$

where,

σ is allowable Hoop stress measured in MPa

P is Mean effective Pressure exerted on the inner walls measured in MPa

R is inner radius of pipe measured in meters

t is thickness of pipe measured in meters

A design of bifurcation is accepted only when the allowable stress is less than either 2/3 of yield strength or 1/3 of ultimate tensile strength whichever is lesser. For ensuring maximum reliability of the bifurcation structure, different reinforcements are integrated into it internally and externally. Ring girders are a type of external reinforcement whereas sickle plate is a type of internal reinforcement (Bai et al., 2013).

(Karakouzian et al., 2019) Pipes made of concrete are subjected sudden pressure changes. It may be due to valve opening/closing, fluid level in reservoir changing etc. Radial and axial both kinds of stresses are exerted in the pipe.

(Bhavan & Marg, 2000) A proper factor of safety is required during the design of concrete structures because of deviation from the standard procedures. It is usually recommended to have factor of safety above 3 for both bending and direct compression.

The permissible stress for concrete in compression is given as 13.0 MPa for bending stress and 10.0 for direct stress. The permissible value for direct stress is taken in this case because there is no steel reinforcement in the concrete that surrounds the pipe which causes bending.

The thickness of pipes is given by the handbook (Wingate, 2007)

$$t = \frac{P \times R}{\sigma_a \times \eta - 0.6 \times P}$$ ……………………………… Equation 2.4

Where,

t = thickness of pipe measured in meters

P = mean effective pressure at the center of the pipe measured in MPa

R = radius of the pipe measured in meters

σ_a = allowable stress measured in MPa

η = joint efficiency whose values lies between 0 and 1

(Z. Zhang et al., 2020) When the tensile stress acting upon a concrete pipe surpasses its ultimate strength, it initiates the formation of initial cracks. These cracks then progressively propagate due to the ongoing external load, ultimately resulting in the pipe losing its ability to bear weight. The primary strength theory in material mechanics, often applied to materials prone to brittleness, posits that material failure occurs once the Maximum principal stress (σ_1) surpasses the permissible stress (σ).

CHAPTER 3: METHODOLOGY

3.1 Validation with CFD

3.1.1 Data collection

Firstly, the data used for the design of the manifold is obtained from the NEA Engineering company. Also, the data regarding the CFD analysis of the manifold is collected.
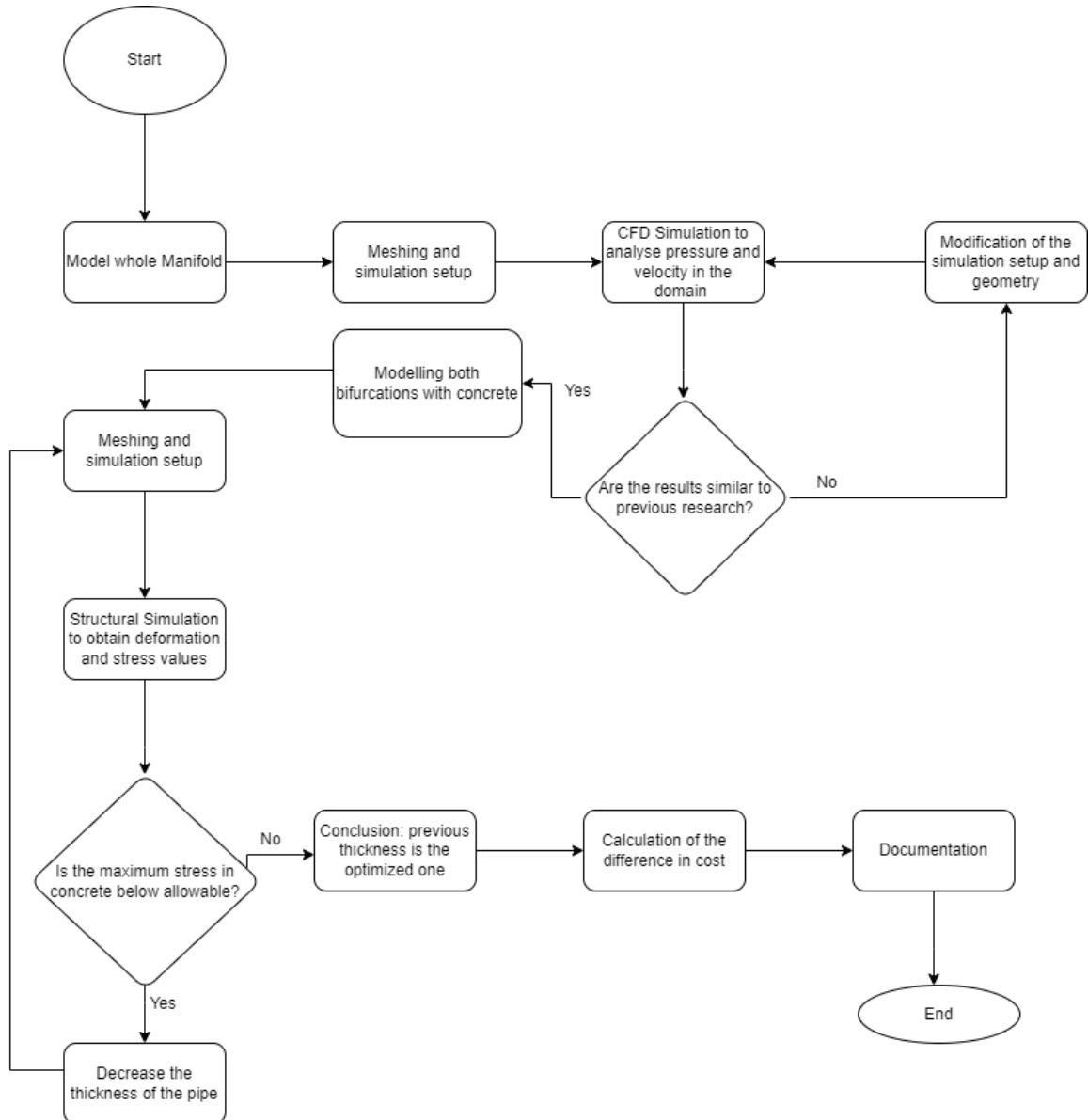
Figure 3.1 Methodology diagram

Then the CFD analysis is performed followed by the structural analysis of bifurcations with and without the addition of concrete block. The detailed steps of the analysis are shown in Figure 3.1.

3.1.2 Modelling the fluid domain.

The dimensions available from the previous research (suggested for least head loss) must be used to construct the manifold that supplies the water to the three turbines. The CAD drawing is constructed in Ansys SpaceClaim shown in Figure 3.2. It consists of two bifurcations which are a little complex to construct because of the conical cross section where the inlet and outlet pipes join. The main inlet pipe is 6.5-meter diameter which decreases to 5.3 meters after the first bifurcation. The 5.3-meter pipe bifurcates into two 3.75-meter pipes to form the second bifurcation. The pipe that supplies water to the third turbine bends at 11.25-meter radius after the second bifurcation. The bifurcation angle is 30 degrees and cone length are 9 meters for the optimized model in the research. Tools like revolve and tangent are used to create cylinder or cone shaped pipes. It is found that the bifurcation point doesn't coincide with the point where the axis of the three pipes meets.
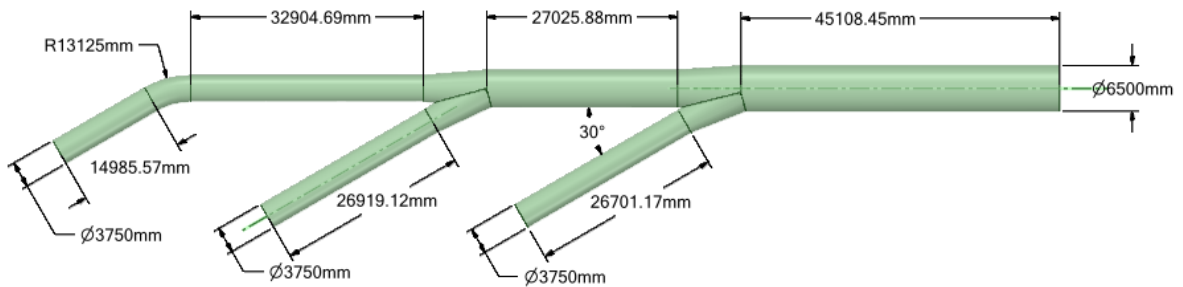
Figure 3.2 Manifold Model (with 9-meter cone length) constructed in SpaceClaim

3.1.3 Meshing

The geometry conducted is meshed considering it as the fluid domain. Tetrahedral elements are chosen because they work best in fluid simulations. Unstructured mesh is used to accommodate complex shapes in the manifold (Inc, 2018). 10 inflation layers are used to represent the boundary layer adjacent to the walls of the manifold. The first inflation layer is 3 mm thick. The mesh quality target is kept as 0.8 such that the best quality elements have their qualities nearly equal to 1 and it does not take long time to mesh as well. The final mesh distribution at the inlet cross section is shown in Figure 3.3. The mesh independence test must be performed by taking pressure and velocity values at a certain plane in the domain to find out the optimum size of the elements.
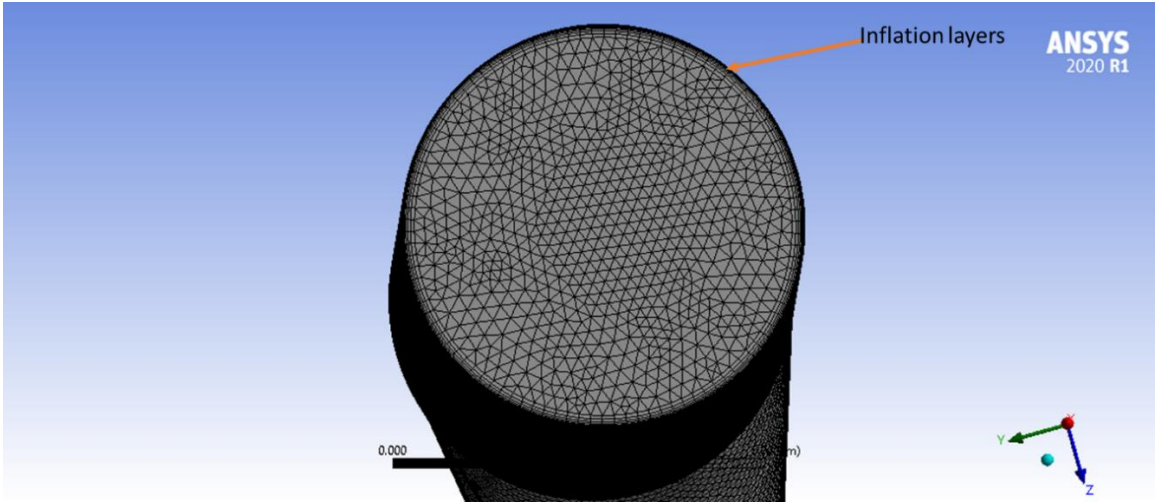
Figure 3.3 Mesh distribution in the inlet cross section
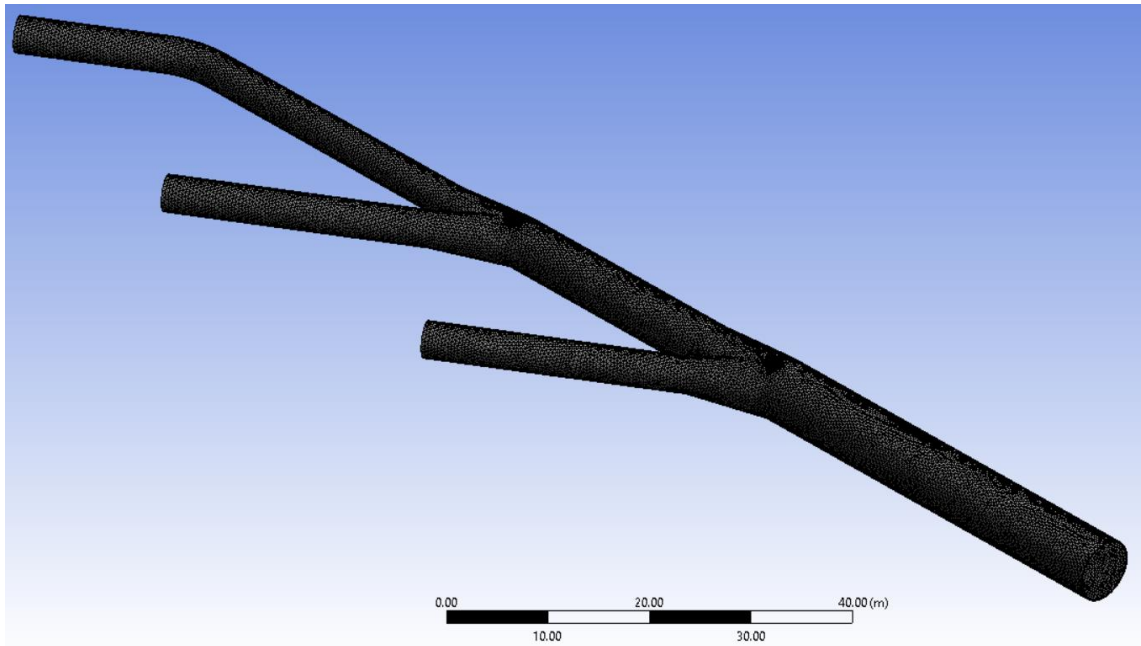
Figure 3.4 Meshed Manifold
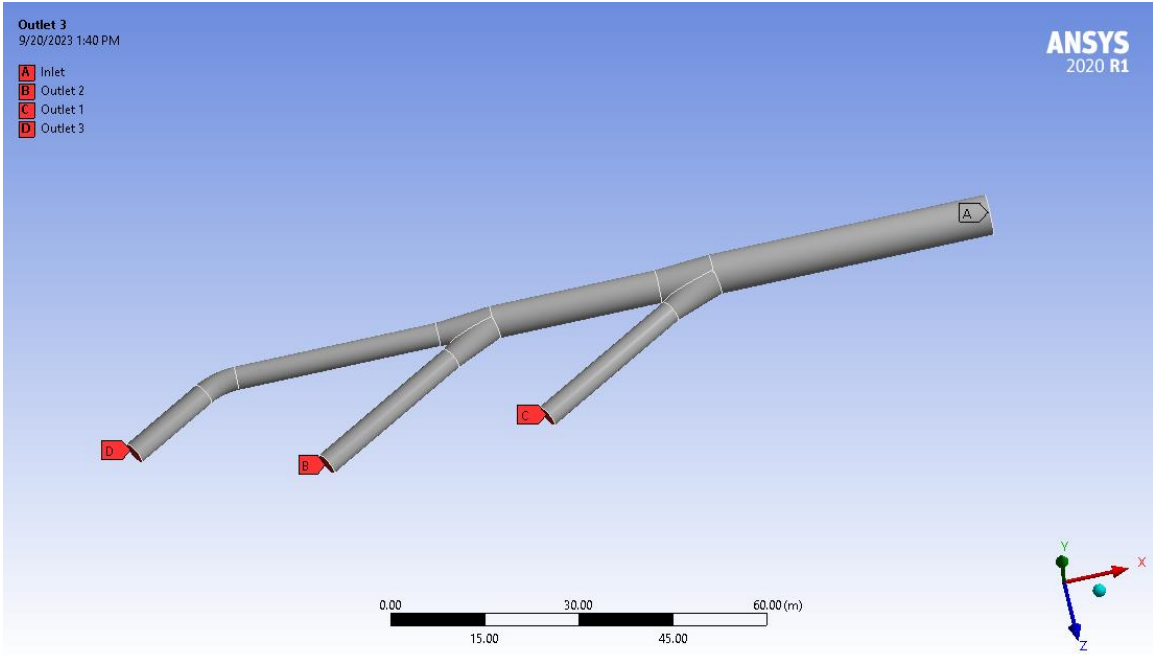
Figure 3.5 Inlet and outlets in the manifold

3.1.4 Problem setup and simulation

The CFD simulation must be performed to reproduce the results of the previous simulation. For that the boundary conditions taken in the previous research are all taken, and fluid simulations are to be performed. Pressure based solver is chosen and the turbulence model chosen is SST k-ω because of the turbulent nature of the flow in the domain being modelled and the optimized computational time. The material is defined as water in the whole domain. After that the boundary conditions are defined taking the design of discharge 348 cubic meter per second (*Vidhyut Utpadan Company Limited*, 2023). The design head at the inlet is 169 meters. The liquid pressure corresponding to that is 1,654,906 pascals. Therefore, the inlet boundary condition is chosen as pressure inlet. The flow in the outlet penstocks is 58 cubic meters per second each. The outlets are chosen as mass flow outlet type and the value is taken as 58,000 kilograms per second. The No slip condition is entered at all the walls. For the solution purpose, the output values of pressure and velocities at the three outlets and a section just upstream of the first bifurcation are recorded by creating a file for each of them and then the simulation is performed. These values are crucial for performing the mesh independence test. The test started with a course mesh of 0.9 meters with the total elements reaching 227,886. The eight variables (pressure and velocity at four sections shown in Figure 3.6) are noted after the solution converges. After that the mesh is made finer and the simulation process is repeated. The process of making a finer mesh is repeated till error reaches less than 1 percent between succeeding and preceding iterations.

14
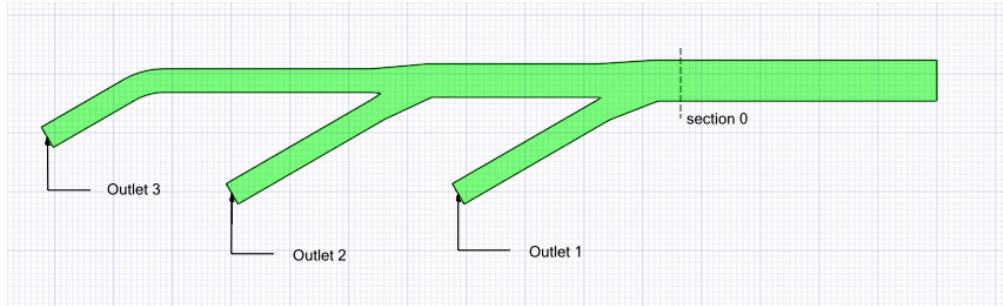
Figure 3.6 Variables recorded for these sections.

3.1.5 Result analysis

Once the mesh independence test is completed, the results tab is opened in the workbench for the best type of mesh created. The values of pressure and velocity are recorded by creating a section by using the offset tool parallel to the three outlets and one other section (just before the first bifurcation) parallel to the main inlet. The values extracted area used to calculate the head loss values. The values for the section before bifurcation are taken as the reference (named as section 0) and three head losses are calculated by deducting the variables for the other three sections (named as section1, section2 and section3 in Figure 3.7). These head loss values are compared with that of the similar geometry simulated in the previous research. The manifold geometry is validated when the head loss values for each of the three sections with respect to section 0 are similar.
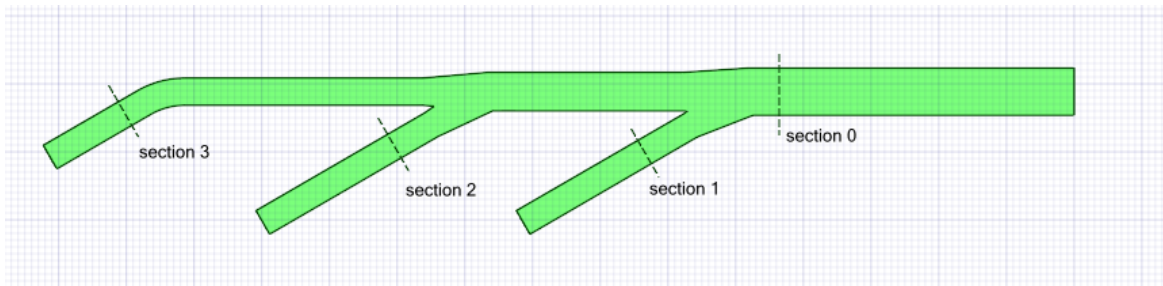
Figure 3.7 Sections for calculating head losses.

3.2 Structural Analysis

3.2.1 Geometry of pipe and other components

Then the two bifurcations made of pipe must be modelled separately using the SpaceClaim software available on Ansys workbench. It is to be noted that structural steel is the preferred material for constructing penstock pipes in high head power plants and they are generally made up of steel sheets (Dhakal & Shrestha, 2023). The modelling process must be same as that followed for the fluid domain used in the fluid simulation. The branching angle in both models is 30 degrees and the cone length is 9 meters. The inlet of the first bifurcation

15

is 6.5 which slowly decreases such that the diameters of the outlet pipe at the two branches are 5.3 and 3.75 meters respectively. The thickness of the first bifurcation is taken as 130 mm and second bifurcation is 70 mm as suggested by the previous research. The thickness values are more than the standard values calculated for each section of the branching in the original design. The original design is 60 mm thickness for the first bifurcation and 50 mm for the second. The thicknesses are calculated in accordance to exceed both the par values of Indian and ASME standards for pipe thickness. Other than that, in each of the bifurcations, a sickle plate (thickness 120 mm for first and 100 mm for second bifurcation) is constructed and inserted inside the pipe aligning with the bifurcation plane. Sickle plate has the primary function of dividing the flow and protecting the vulnerable weld joint at the branches (*Welded Steel Penstocks - USBR Monograph 3*, 1977). The sickle plate is designed using the coordinates that are calculated using the ellipse method. The coordinates are available in the original design file. The curve that lies midway through inward and outward radius of the sickle plate is aligned with the bifurcation arc modelled earlier. After that two C shaped rings are placed surrounding the two outlet pipes and an additional O ring is constructed wrapping the inlet pipe. The rings are made of rectangular cross section because they are more economic and reasonable (Bai et al., 2013). All the rings are 120 mm wide and 120 mm high. The final model containing the pipe parts in first bifurcation is shown in Figure 3.8.

41
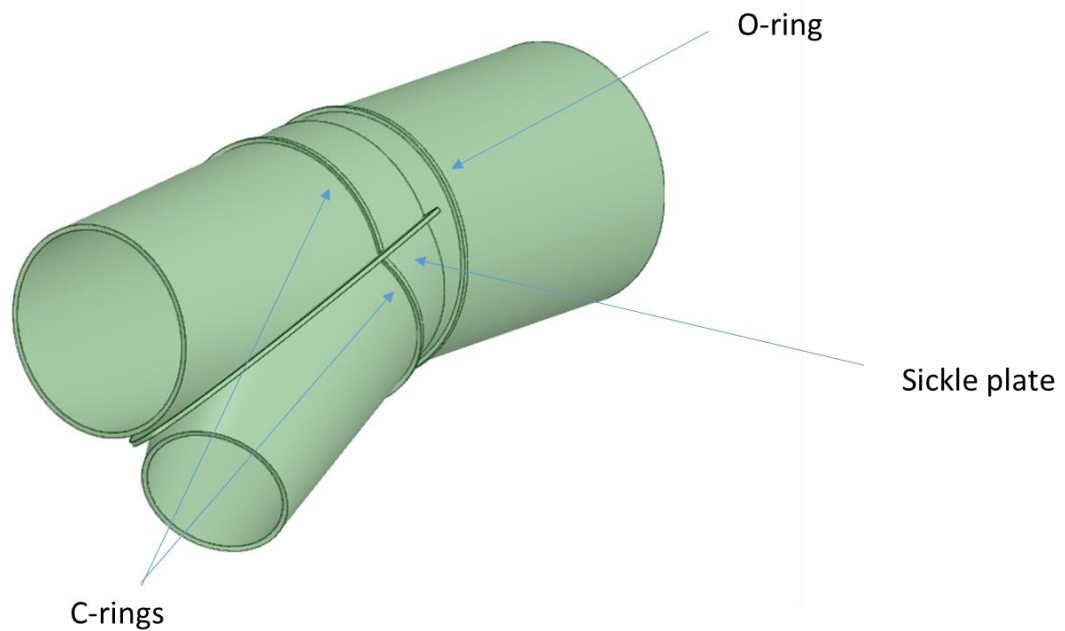
Figure 3.8 First Bifurcation pipe model

Apart from the geometry data suggested in the research, the supports (anchor blocks) are represented by a block that completely covers the bifurcation structure as shown in Figure 3.9. The pipe without sickle plate and rings are covered with a concrete block. That completes the modelling processes required for the structural simulation.
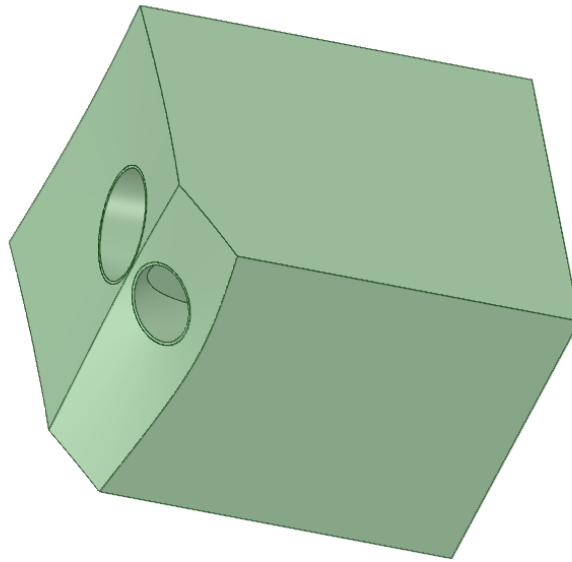
Figure 3.9 First bifurcation completely covered in concrete block.

3.2.2 Model

In contrast to the CFD techniques for fluid flow simulation, structural analysis uses techniques of Finite Element Method (FEM). FEM is used for analyzing solid structures and it discretizes it into several elements connected through common point called Nodes. It helps in determining the accurate values of the stresses at different points where the calculation by hand would have been very tedious. The workbench is opened, and a new project is created using the static structural tab. Firstly the pipe only is simulated. The first option on the structural window is engineering data that contains the data of the material properties. Generally structural steel is chosen in such large hydropower projects for penstocks. It already has the default material as structural steel and its properties available in library is shown in Table 3-1. The properties match with E 250 type steel listed in IS 2062:2011(Standard 2062, 2011).

Table 3-1 Properties of steel in Ansys library

Ultimate tensile strength	460 MPa
Yield strength	250 MPa

Density	7850 kg/m^3
Shear Modulus	77 GPa
Bulk Modulus	167 GPa
Young's modulus	200 GPa
Coefficient of thermal expansion	0.000012 C^{-1}
Poisson's ratio	0.3

After that in the geometry tab, the geometry of bifurcation pipe only is uploaded. After the model option is available which opens Ansys Mechanical, which is the default application available for meshing, simulation setup and solution. The different components of the pipe are named as inlet, outlet1, outlet2, inner walls, outer walls, sickle plate, O ring, C ring etc. The named selection option is helpful when the meshing for the different components must be done separately and to define the boundary conditions. The meshing process is done in which the different faces are meshed according to their respective sizes. Face meshing option is used for the rings and sickle plate using the same size. Remaining parts are meshed using the body sizing option and that size is varied in the mesh independence test. The element distribution type chosen is the unstructured tetrahedron for the pipe surface and the sickle plate for the complex shape and contact they share. The target mesh quality for the elements generated is taken as 0.7. The mesh distribution is as shown in Figure 3.10.
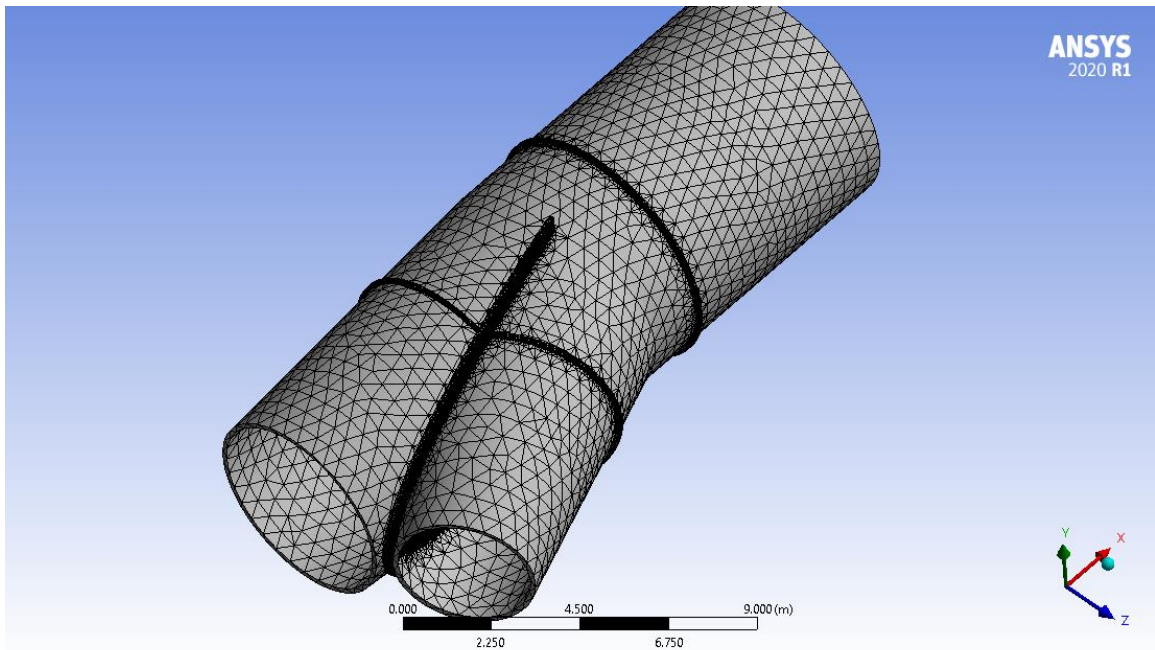
Figure 3.10 Meshed First Bifurcation (coarse)

18

Then the boundary conditions are defined, providing fixed support at the inlet and both outlets as shown in Figure 3.11. A pressure of 2.32 MPa (shown in Figure 3.12) is defined to be exerted on the inner walls of the pipe and the inner parts of the sickle plate. Von-mises stress and deformation variables are defined for the result whose contours must be observed. Other than that, Average stresses on outlets are also defined for the results so that the mesh independence test can be performed. After that the solution is run.
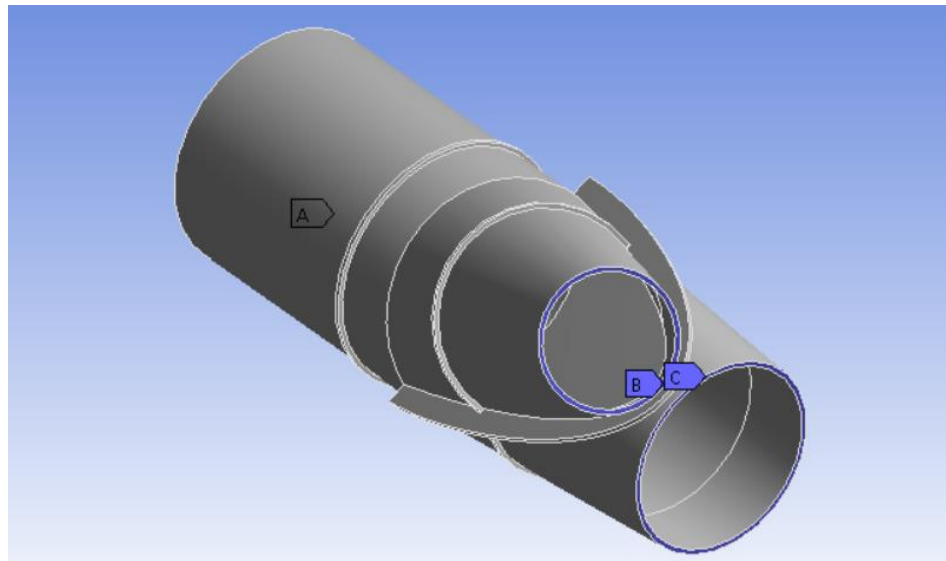
Figure 3.11 Fixed support boundary conditions on the inlet and outlet
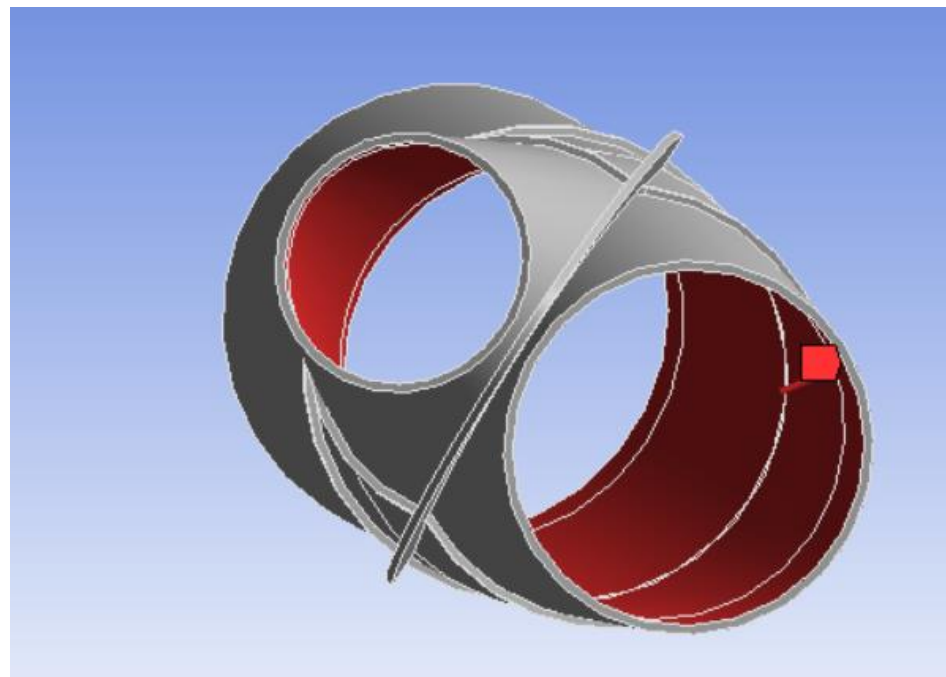
Figure 3.12 Pressure boundary condition on the inner walls

19

For the geometry with concrete block covering the pipe, all the steps are similar except the fact that the material must be chosen in the engineering data option and there is option of adding concrete in the general materials category. The properties of concrete available in library is as shown in Table 3-2.

Table 3-2 Properties of concrete from the Ansys Library

Ultimate tensile strength	5 MPa
Yield strength	0 MPa
Density	2300 kg/m^3
Shear Modulus	12.712 GPa
Bulk Modulus	15.625 GPa
Young's modulus	30 GPa
Coefficient of thermal expansion	0.000014 C^{-1}
Poisson's ratio	0.18
Ultimate compressive strength	41 MPa

The meshing process for the concrete block and pipe geometry is done by using contact sizing method. Apart from that the center of influence method is used for the mesh of concrete block. That assures finer mesh in the pipes and in the interface of the concrete and pipe layer. Also, additional boundary conditions are required for the concrete block. Apart from the ends of the pipe, all but top face of the concrete block is provided with fixed support and acceleration due to gravity is applied in the Negative Y direction (Wang et al., 2017). Pressure at the inner walls is taken same as in pipes only case. In the model tab, the material must be assigned for the two bodies as concrete and structural steel. Other than that, the rest of the process is the same.

Figure 3.13 Mesh distribution for concrete block and pipe (second bifurcation)
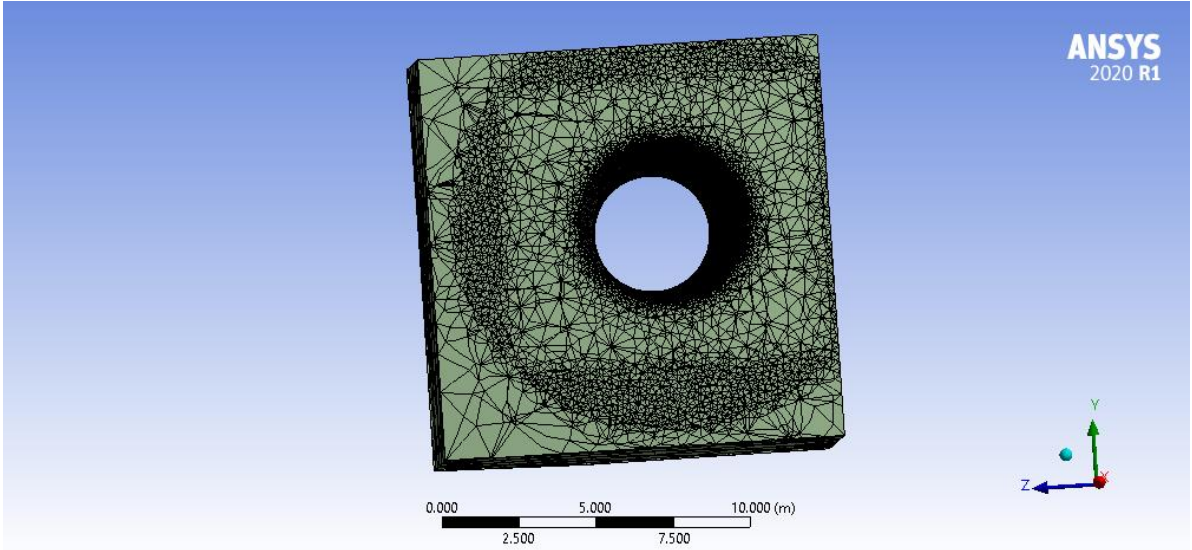
Figure 3.14 Mesh cross section
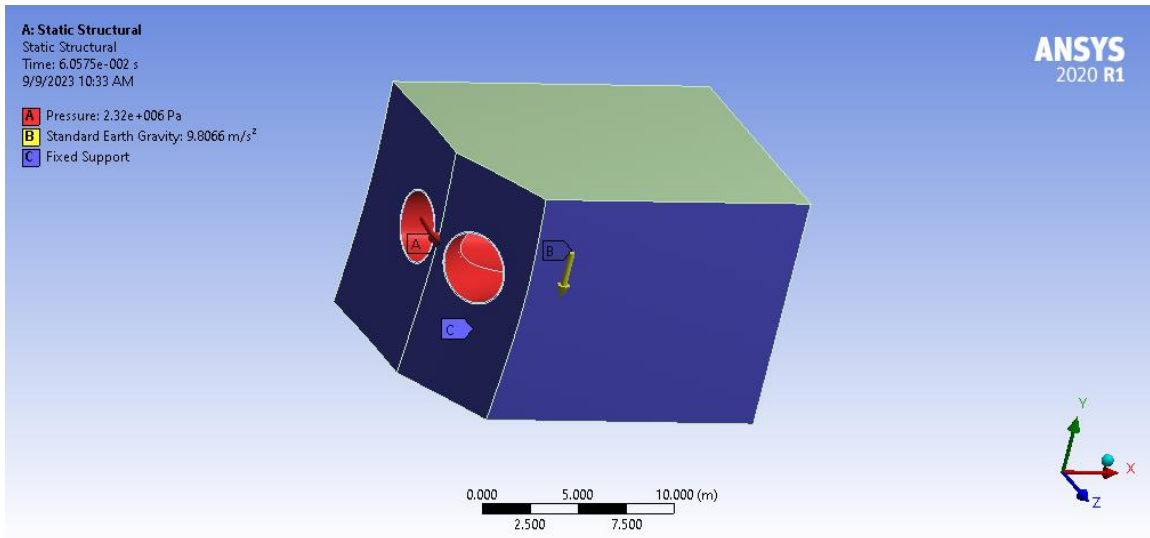
Figure 3.15 Boundary conditions used for the concrete block and pipe (second bifurcation)
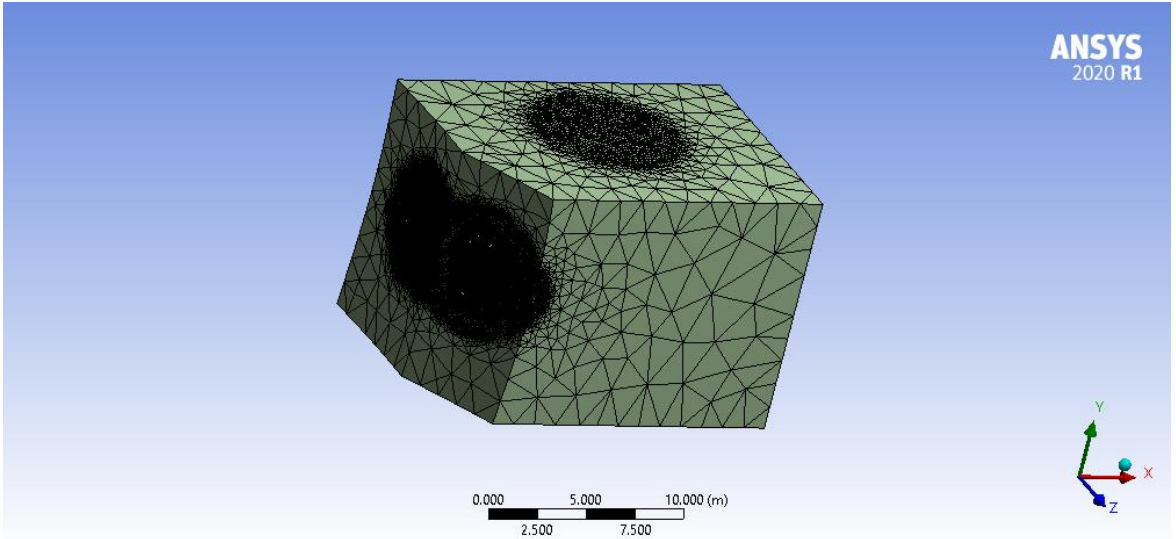
3.2.3 Result Analysis

The results of maximum stress and maximum deformation are analyzed after the optimum element size have been determined. The maximum stress value must be compared with allowable stress for the piped structure in two different conditions: normal condition and intermittent condition. Intermittent condition is added to safeguard the structure in cases of events such as abnormal vibration whereas the normal condition accounts for stresses under operating conditions. The material used is the same in both conditions and thus the values of yield strength and ultimate strength. In the case of normal conditions, the allowable stress is either 60 percent of yield stress or one third of ultimate strength; whichever is lower. For intermittent conditions, it is either 40 percent of the ultimate strength or two thirds of yield stress; whichever is lower (C. Z. Ji et al., 2012). Detailed calculations are shown in Table 3-3.

Table 3-3 Allowable stress calculation

Ultimate tensile strength	460 MPa
Yield strength	250 MPa
Normal condition	
60 percent of yield stress	150 MPa
One-third of Ultimate tensile strength	153.33 MPa
Allowable stress	150 MPa
Intermittent condition	
40 percent of Ultimate tensile strength	184 MPa
Two-third of yield stress	166.67 MPa

22

Allowable stress	166.67 MPa

Between the two cases, Intermittent condition allows more stress to be exerted on the structure, so it is taken as the reference value while analyzing the results. The ultimate factor of safety is also calculated using the ultimate tensile strength as the reference. Even though the ultimate tensile strength is 460 MPa as given in the Ansys library, the more realistic value of tensile strength is given by the type of steel chosen to construct at the site. In the original design, it is taken as 415 MPa and that is used here as well. It all depends on the project cost and the thickness range of the pipe being used when determining the type and strength range of the steel being used (Inc, 2018). The safety factor is given by dividing ultimate tensile stress with the maximum observed stress.

While analyzing the results of concrete, the allowable stress on the concrete due to the interaction with pipe is determined with respect to the ultimate compressive strength. The properties of concrete available are same as that of M40 grade concrete. There are two types of stresses acting on the concrete. i.e. Direct stress and Bending stress. Bending stress acts on the concrete if there are bending elements such as reinforcement bars covered by the concrete. Since there are no reinforcements used in the concrete modelled for this study, the permissible value of direct stress is considered. The limit for direct stress is 10 MPa whereas for bending stress is 13 MPa for M40 grade concrete.(Bhavan & Marg, 2000)

3.2.4 Modification of the geometry

If the calculated safety factor is found to be much higher than the target, then the thickness of the pipe is reduced, and the simulation procedure is repeated (J. Zhang & Li, 2011). In case if the safety factor is lesser or just nearer to 1, then either the grade of the concrete is changed to higher strength type, or the geometry of the rings attached is increased. After that, the simulation is repeated until the suitable value of factor of safety is reached.

The thickness of the pipes can't be less than the standard thickness values suggested by Indian standards which can be calculated by Equations 2.2 and 2.4 respectively.

Table 3-4 Calculations for thickness first bifurcation

Inlet branch minimum thickness	50.40 mm
Outlet branch 1 minimum thickness	41.09 mm
Outlet branch 2 minimum thickness	29.07 mm
Inlet branch minimum thickness (ASME)	50.87 mm

Outlet branch 1 minimum thickness (ASME)	41.48 mm
Outlet branch 2 minimum thickness (ASME)	29.35 mm
Adopted thickness with corrosion allowance	60 mm

Table 3-5 Calculations for thickness second bifurcation

Inlet branch minimum thickness	41.17 mm
Outlet branch 1 minimum thickness	29.13 mm
Outlet branch 2 minimum thickness	29.13 mm
Inlet branch minimum thickness (ASME)	41.56 mm
Outlet branch 1 minimum thickness (ASME)	29.40 mm
Outlet branch 2 minimum thickness (ASME)	29.40 mm
Adopted thickness with corrosion allowance	50 mm

In the calculations the joint efficiency is assumed as 0.9, Mean effective pressure as 2.32 MPa and Allowable stress as 167 MPa. At the end, the goal of the research is to find if geometry offers a significant cost reduction compared with the suggestions of previous research. A thinner pipe prompts a lower cost of construction of not only the bifurcation pipe but the sections of the manifold that lie downstream from the bifurcation point. The amount by which the cost of construction is brought down by using a thinner pipe.

CHAPTER 4: RESULTS AND DISCUSSION

4.1 Fluid Flow Analysis

4.1.1 Mesh independence test

Pressure and velocity are the variables chosen for the mesh independence test. The sections where the values of these variables are taken are at the section before the bifurcation named section0 and at the three outlets named outlet1, outlet2 and outlet3 respectively. The area weighted average values are recorded with increasing element number. The values of pressure for mesh independence are graphed as shown.
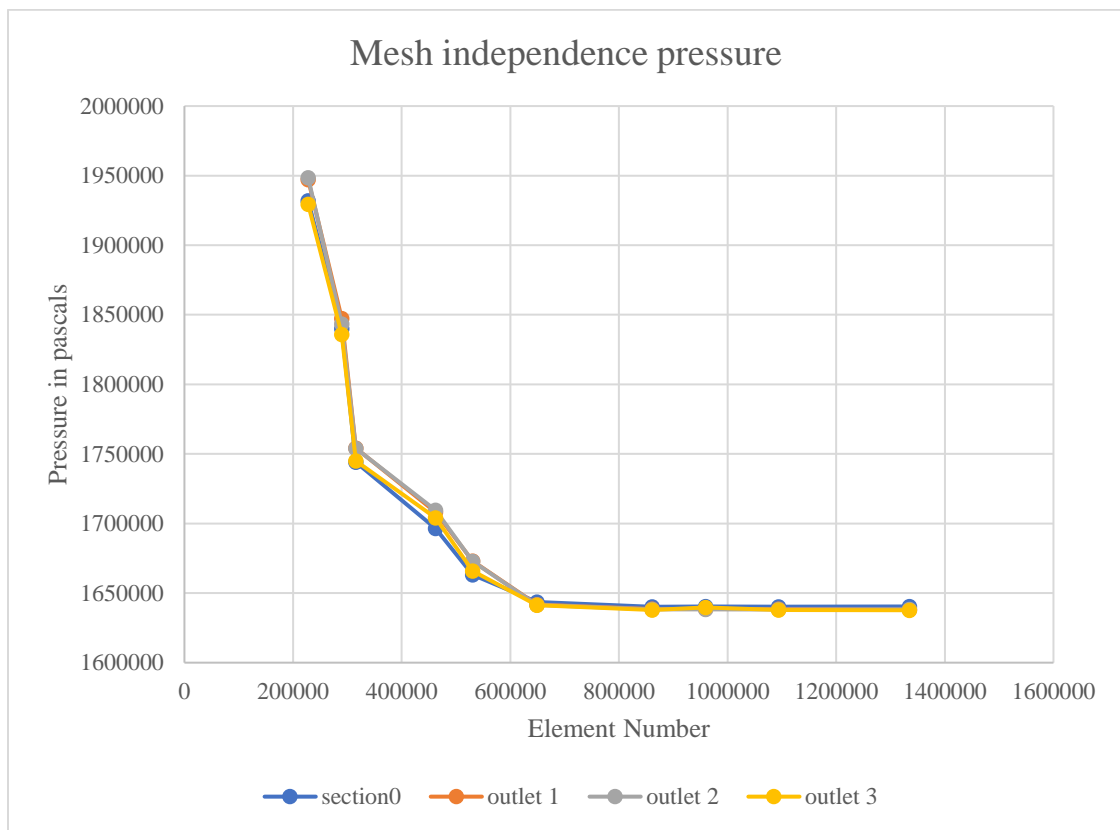
Figure 4.1 Mesh independence graph for pressure

Similarly, the mesh independence graph for the velocity is given below.
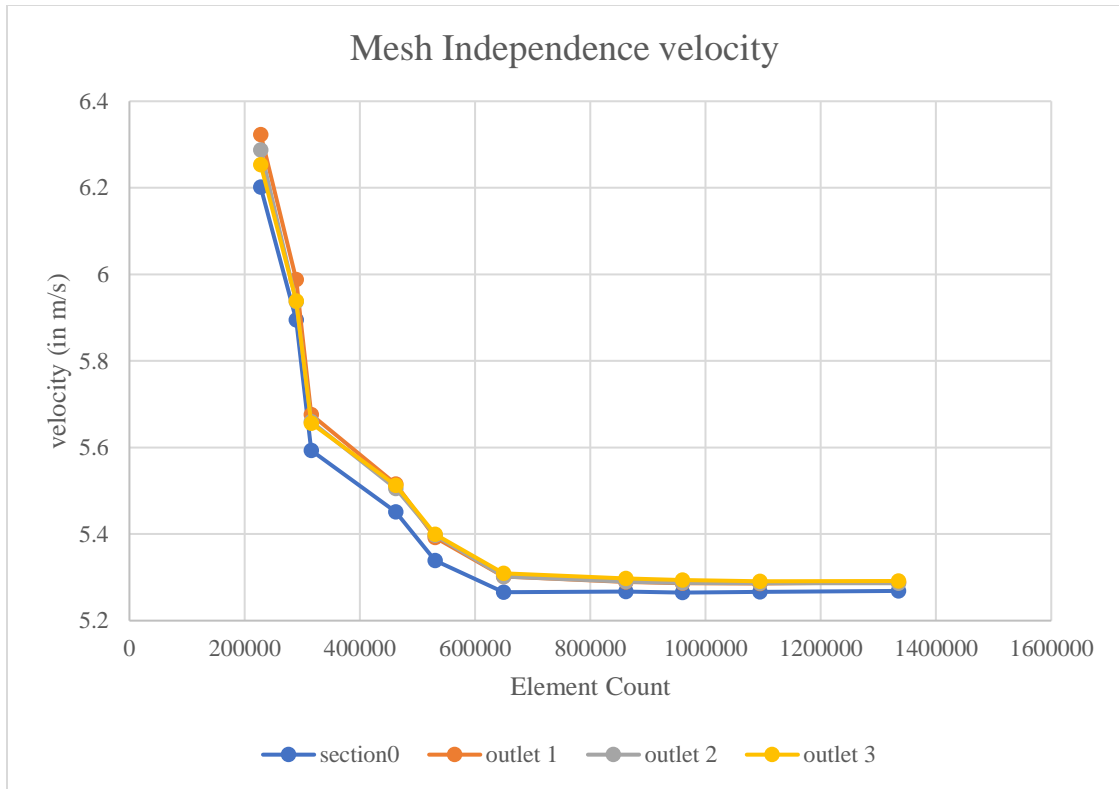
Figure 4.2 Mesh independence graph for velocity

The error is calculated between consecutive rounds of simulation are calculated and it is found that the error is very negligible after the number of cells in the domain is 861,423 so that is taken as the optimum element count.

4.1.2 Contours

The contours of pressure and velocity at the mid plane are shown below for the optimum cell count.

Figure 4.3 Pressure contour at the mid plane in the manifold

The contour shows that the pressure head drops greatly at the point of bifurcation points and slightly at bends.

Figure 4.4 Velocity contour at the mid plane in the manifold
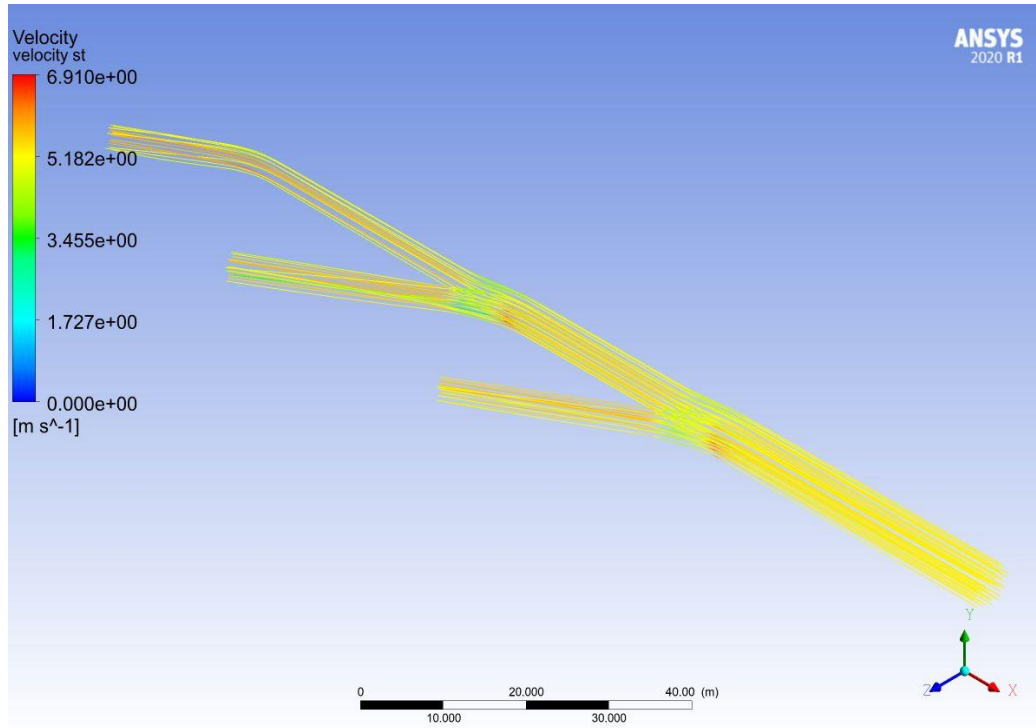
Figure 4.5 Velocity streamlines at the mid plane in the manifold

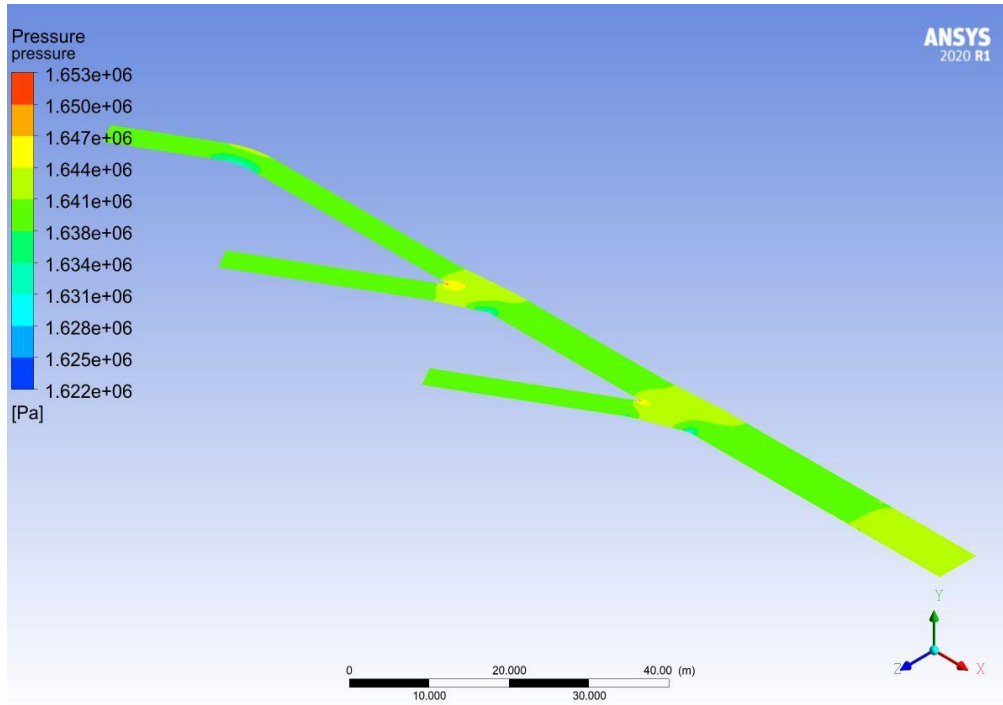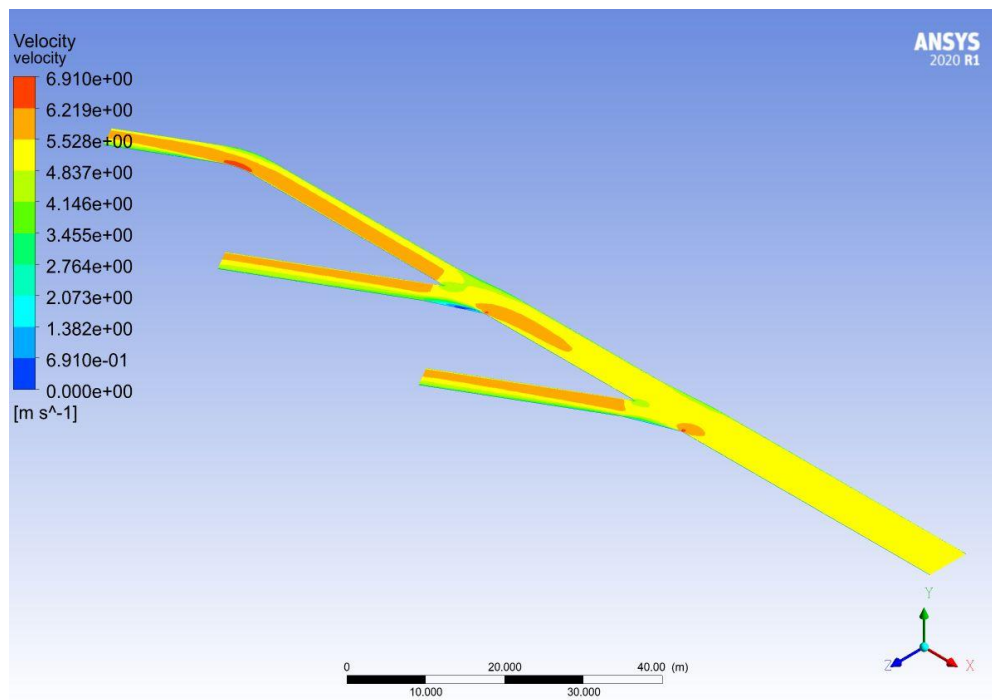The velocity contour shows that the velocity at surfaces nearer to the point of bifurcation is higher than at the layer far from the bifurcation point. That is due to the acceleration of flow after the flow is divided.

4.1.3 Head loss calculation

Three sections are created as shown in figure 9 where the respective values of area weighted average pressure and velocities are calculated. Those sections are named section1, section2 and section3 respectively. The head losses are to be calculated with the formula mentioned in equation 1.

Table 4-1 Pressure head loss values

Sections	Section0	Section1	Section2	Section3
Recorded values (pressure) (Pa)	1640324	1638565	1638931	1638129
Δp		1759	1393	2195
Δp/specific weight of water		0.17931	0.142	0.2238

The drop in average pressure in the three sections is calculated in comparison to the value of section0. The pressure difference values are divided by the specific weight of water taken as 9810 N/m^3 to get the loss in pressure head.

Table 4-2 Velocity head loss values

Sections	Section0	Section1	Section2	Section3
Recorded values (velocity) (m/s)	5.24818	5.19698	5.09131	5.16826
Δv^2		0.534792	1.621956	0.832482
$\Delta v^2 /2g$		0.027285	0.082753	0.04245

The velocities are squared, and the change seen in the velocities at the three sections is deducted from that of section0. That difference is then divided by 2g where g is the acceleration due to gravity taken as 9.81 m/s^2 which gives the velocity head loss.

The loss in potential head is not taken into consideration as the manifold model is created at the same elevation and thus there is no difference in elevation of the different sections as well. The head loss calculated by adding the different head loss values which can be summarized as

Table 4-3 Total head loss calculation and comparison

Head loss	Section 0-1	Section 0-2	Section 0-3
Pressure head loss	0.17931	0.14200	0.22375
velocity head loss	0.02729	0.08275	0.04247
Total head loss	0.20659	0.22475	0.26622
Total head loss in previous research	0.13	0.46	0.31

When comparing the head loss values of the three sections with the initial section just before the first bifurcation, the losses are comparable with each other hence the energy is divided equivalently in all the three turbines.

4.2 Structural Analysis

The mean internal pressure value that is required for the calculation of the thickness of the pipe and used as the boundary condition for the simulation purpose is dependent on three values; specific weight which is 9810 N/m^3 for water, design head with reference to bifurcation elevation which is 169 m available from the design data and allowable transient head rise which is taken as 40%. This value depends on the control system used for operation of turbines (Adamkowski & Kwapisz, 2004). The head rise percentage ensures that the structure can bear pressure much higher than that exerted by fluid in steady flow.

$$MP = w \; x \; \left(1 + \frac{r}{100}\right) x \; h \qquad \text{.........................} \qquad \text{Equation 4.1}$$

Where,

MP = Mean Internal Pressure

w = specific weight

r = allowable transient head rise (%)

h = design head

The formula is taken from design guidelines of water conveyance systems.

Using the values, the mean internal pressure is calculated as 2.32 MPa.

The thickness of the bifurcations is calculated using formula of equation 2.2. For that the allowable stress is required. In the original design, allowable stress is calculated from the yield stress of steel as 415 MPa with the safety factor taken as 2.5. Based on that the adopted thickness in case of the first bifurcation is 60 mm whereas it is 50 mm for second bifurcation.

Previous research enhanced upon that design values by conducting fluid flow analysis and analyzed the head loss values. In terms of the varying cone length and bifurcation angle, the head loss was found to be minimum for 30° and 9m model, the pipe of 130 mm thickness was recommended for first bifurcation and 70 mm for the second bifurcation. Based on that the models of the pipes are created.

4.2.1 Analysis of model with pipes only

The two bifurcations are modelled along with sickle plate and different rings are modelled and simulation is run to conduct mesh independence tests.

4.2.1.1 First Bifurcation

The results of mesh independence tests are shown below for the first bifurcation.

Table 4-4 Mesh independence test for first bifurcation (130mm)

Element count	Average stress on inlet (MPa)	Average stress on outlet 1 (MPa)	Average stress on outlet 2 (MPa)
223671	39.369	32.981	25.477
270108	41.712	35.389	26.978
794931	40.522	34.779	27.052
946896	40.347	35.069	27.178
1568517	40.222	34.883	27.281

The graphs of the change percentage of the variables shown in the above table is shown below.
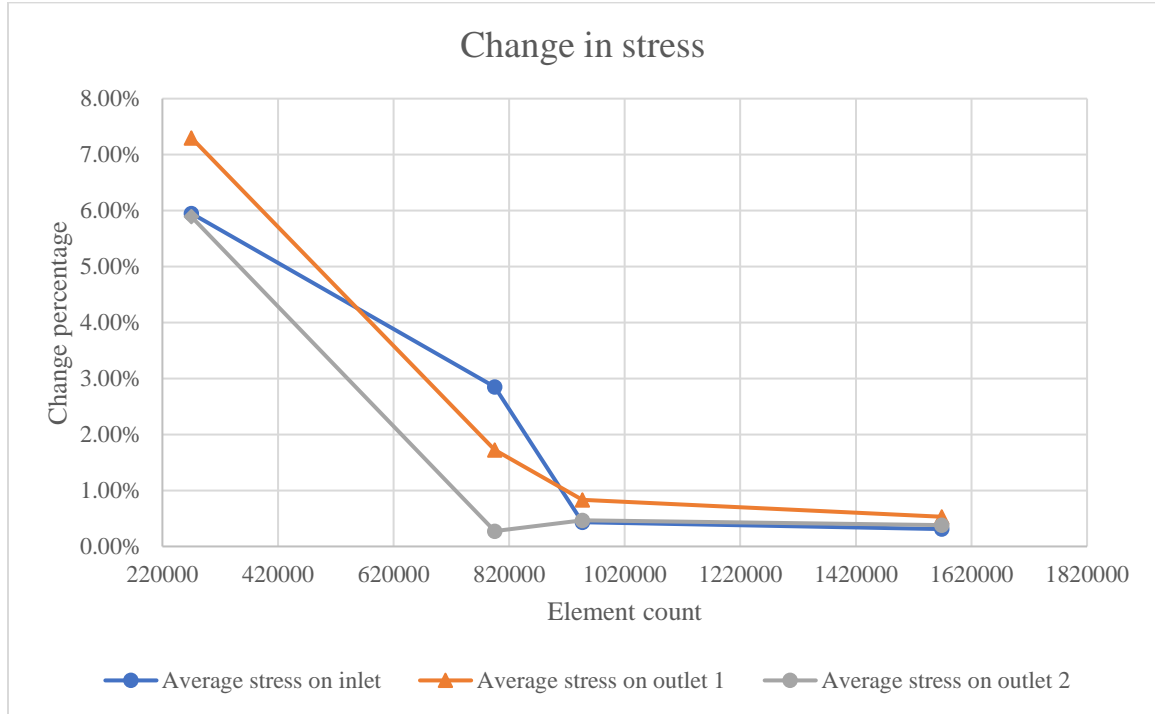

Figure 4.6 Mesh independence graph for change percentage bifurcation 1 (130mm)

31

The change percentage in all variables drops below 1 percent at element count 794,931. So, that is the optimum mesh setting. The deformation and equivalent von-mises contours of the first bifurcation are shown below.
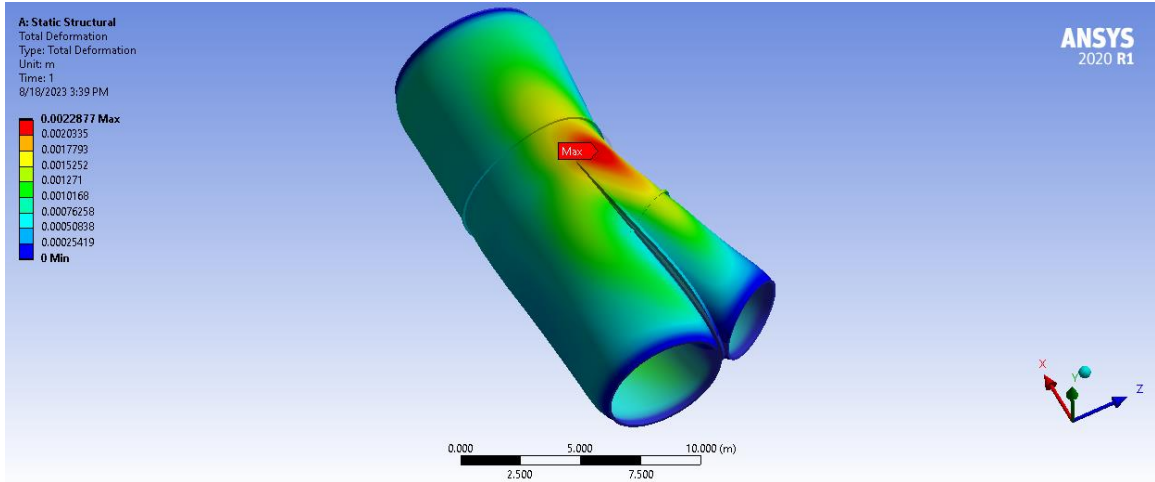

Figure 4.7 Deformation contour for the first bifurcation (130mm)

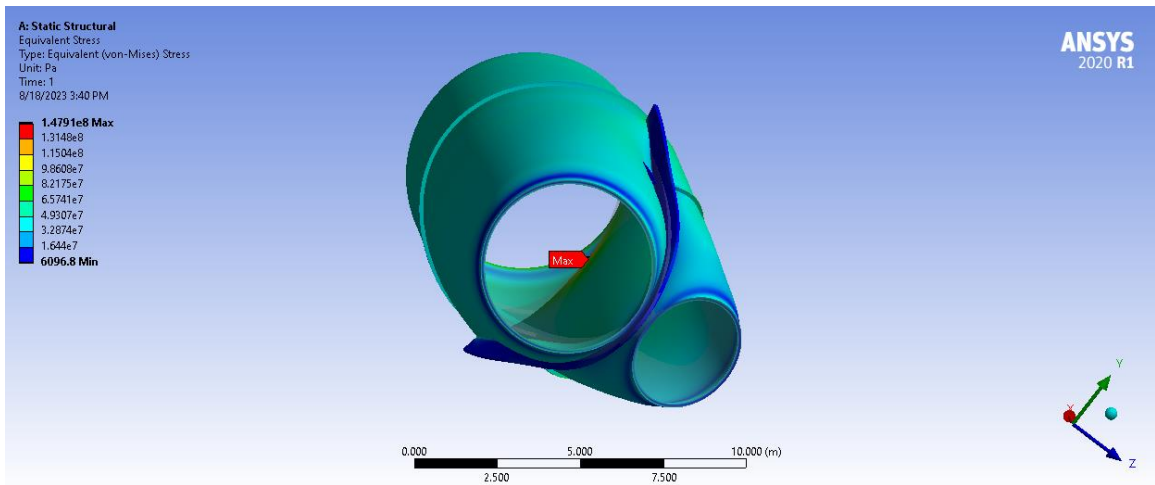Deformation of 2.3mm is less than that of the model that was simulated in previous research.

Figure 4.8 Equivalent von-mises stress contour for the first bifurcation (130mm)

The factor of safety calculation is shown below.

Table 4-5 Factor of safety for first bifurcation (130mm)

Exerted maximum stress	147.91 MPa
Allowable Stress	166.67 MPa
Ultimate tensile strength	460 MPa

Factor of safety	460/147.91 =3.11
Target factor of safety	2.5

The exerted maximum stress is slightly lesser than the allowable values whereas the maximum deformation is bettered with previous research's findings.

4.2.1.2 Second Bifurcation

The same process is followed for the second bifurcation.

Table 4-6 Mesh independence test for second bifurcation (70mm)

Element count	Average stress on inlet (MPa)	Average stress on outlet 1 (MPa)	Average stress on outlet 2 (MPa)
156909	51.154	36.267	37.336
185913	58.795	42.178	42.474
424031	66.555	48.441	48.384
572061	67.809	49.466	49.377
737104	68.311	49.333	49.329
837206	68.241	49.44	49.242

The graphs of the absolute values of change percentage of the variables shown in the above table are shown below.
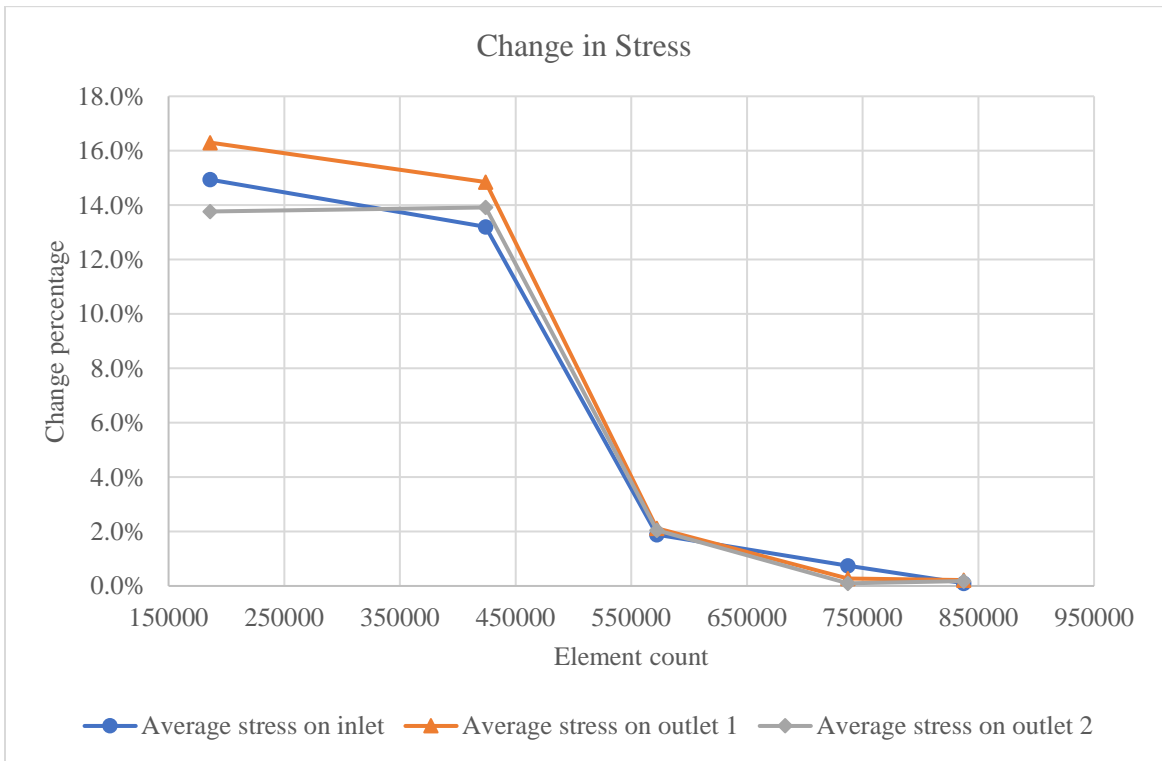

Figure 4.9 Mesh independence graph for change percentage bifurcation 2 (70mm)

The change percentage in all variables drops below 1 percent at element count 572,061. So, that is the optimum mesh setting for the second bifurcation. The deformation and equivalent von-mises contours of the second bifurcation are shown below.
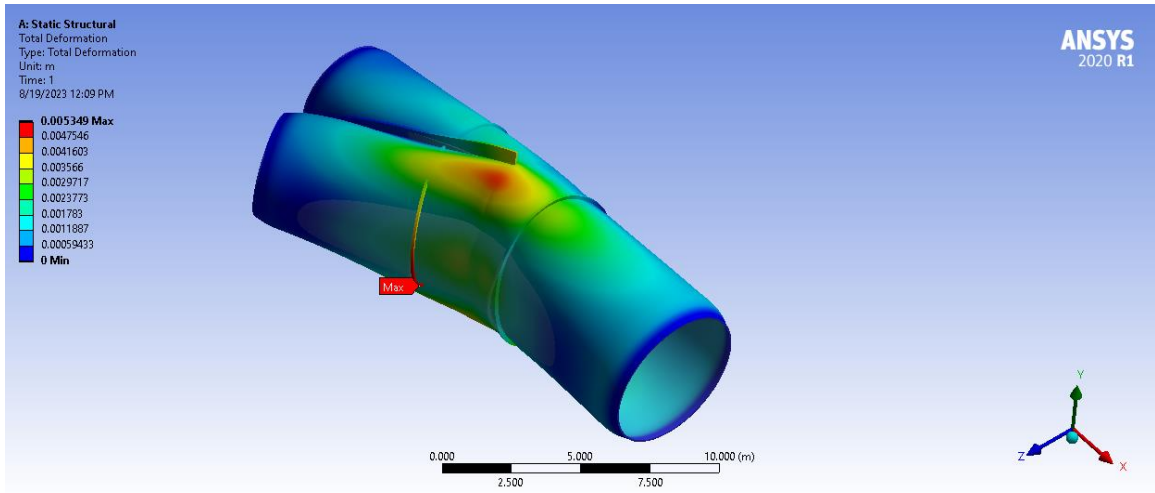

Figure 4.10 Deformation contour for the second bifurcation (70mm)

The maximum deformation found in the model is about 5 mm and it is lesser than the observed value in previous research.
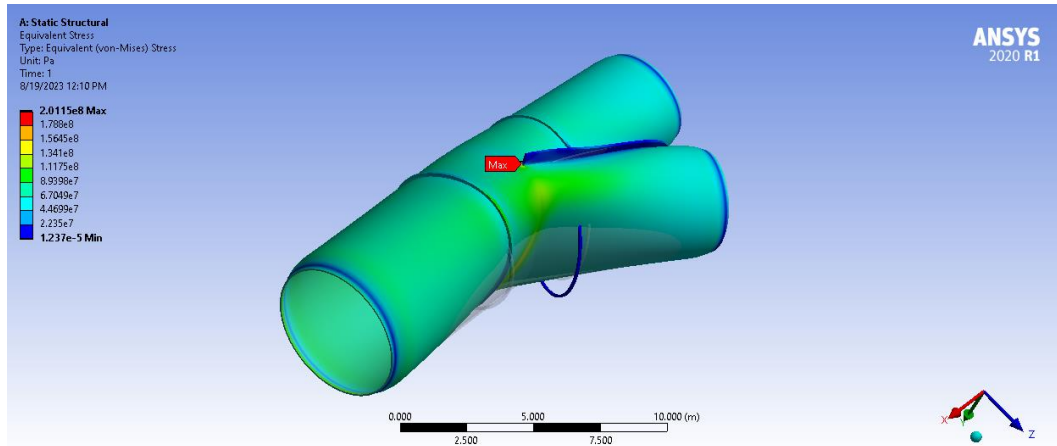

Figure 4.11 Equivalent von-mises stress contour for the second bifurcation (70mm)

Table 4-7 Factor of safety for second bifurcation (70mm)

Exerted maximum stress	201.15 MPa
Allowable Stress	166.67 MPa
Ultimate tensile strength	460 MPa
Factor of safety	460/201.15 =2.2868
Target factor of safety	2.5

The observed factor of safety is lesser than the target factor of safety. The geometry must be modified.

4.2.2 Analysis of model with pipe with concrete

As the concrete block is modelled to cover the pipe shown above, it is found to bear high stress on the rings, thus, to avoid that, the rings are removed from the model and the simulation is done of the pipe and block together. When the meshing is done for the pipe covered in concrete consisting of sickle plate, it is found that automatic meshing isn't enough to produce good quality tetrahedron mesh on the cavity made by the sickle plate, thus sickle plate is also eliminated from the model.

4.2.2.1 First Bifurcation

The average value of stresses observed in the first outlet of the first bifurcation are noted and can be represented in graph as shown below.
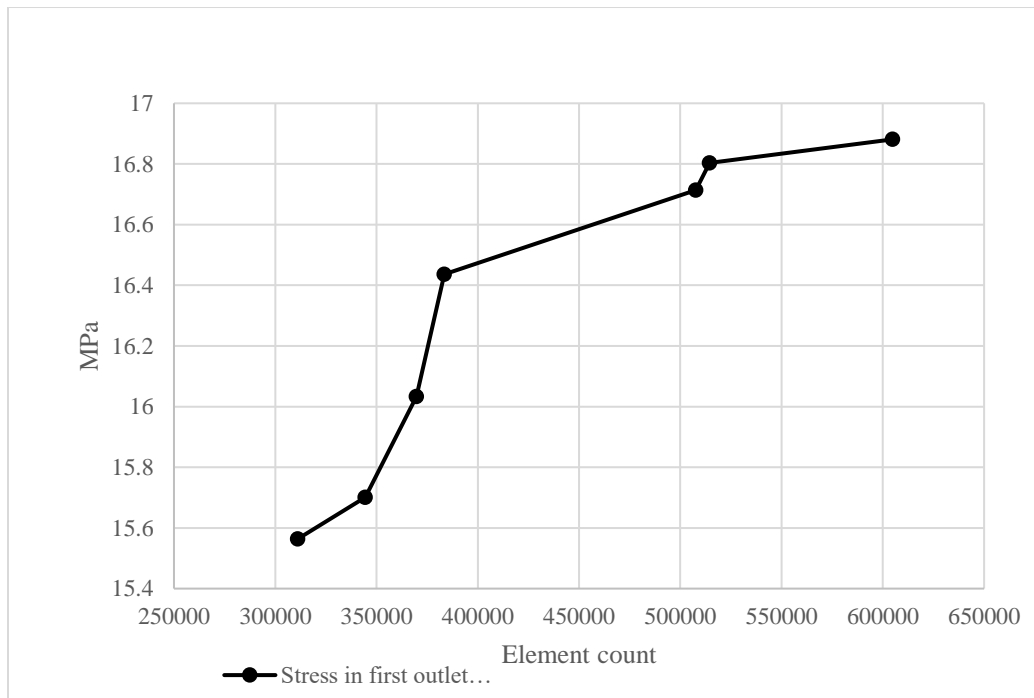

Figure 4.12 Mesh independence graph for first bifurcation (130mm) covered in concrete.

From the graph above it is found that the optimum element count for the given model is 507,704.

The contours of stress and displacement on the concrete block and the first bifurcation pipe are shown below.
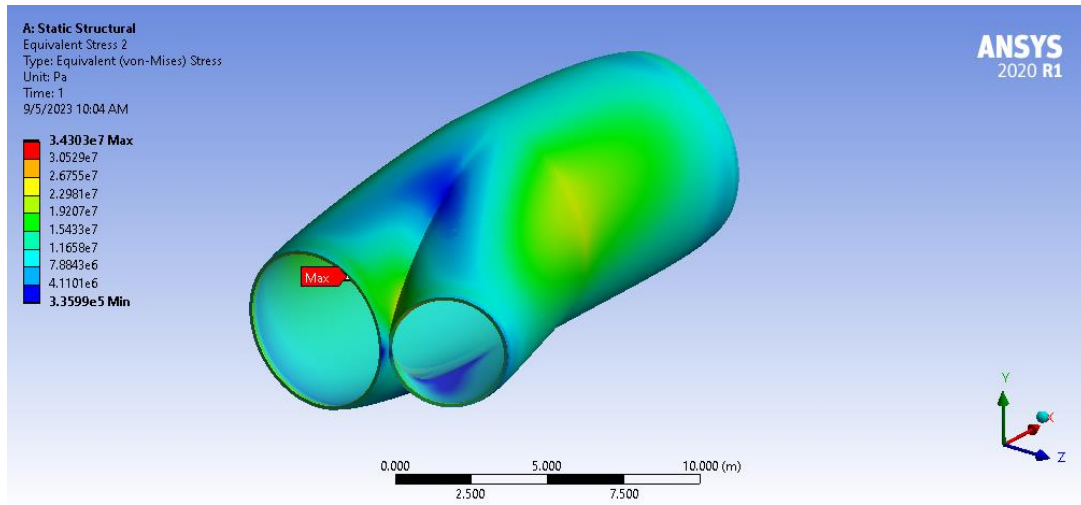
Figure 4.13 Equivalent von-mises stress observed in first bifurcation (130 mm) covered in concrete.

The stress is found to decrease drastically as the concrete shares the force exerted on the inner walls of the pipe. Thus, the factor of safety also changes sharply for the pipe.
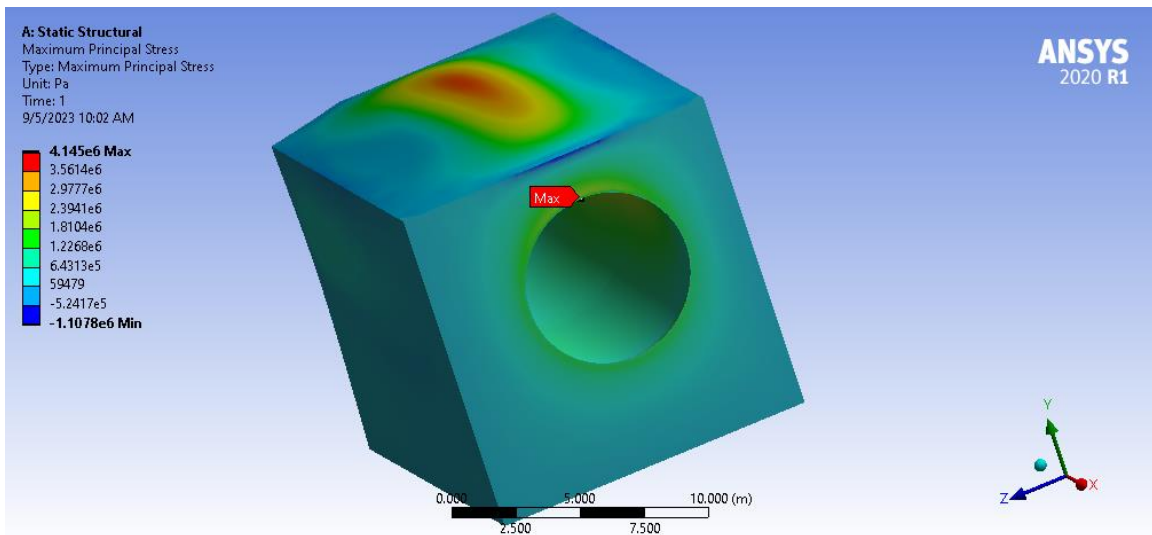

Figure 4.14 Maximum Principal stress on concrete covering first bifurcation (130mm)

The maximum principal stress on the concrete is found as 4.145 MPa which is less than both the permissible values of bending and direct stresses for M40 grade concrete.

Table 4-8 Factor of safety calculation for first bifurcation (130 mm) covered in concrete.

Exerted maximum stress	4.145 MPa
Allowable Stress	10 MPa

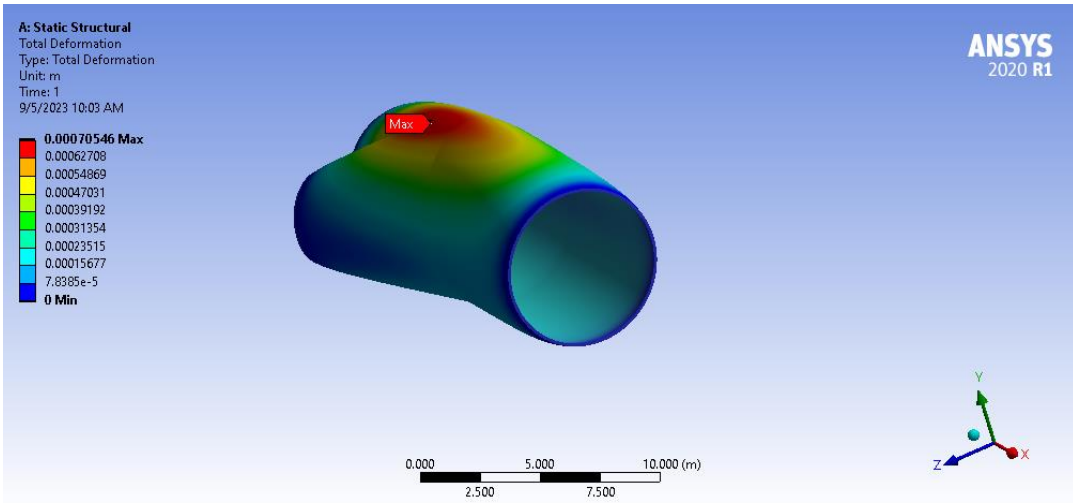|	
Ultimate strength	40 MPa
Factor of safety	10/4.145 = 2.4125

Figure 4.15 Deformation observed in first bifurcation (130 mm) covered in concrete

The deformation can be seen near the sickle plate on the outer surface of the pipe but it is reduced to 0.705 mm. The deformation observed can be explained by the deformation on the interface of the pipe and concrete.

4.2.2.1 Second Bifurcation

Similarly, the mesh independence graph for the second bifurcation and block is given below.
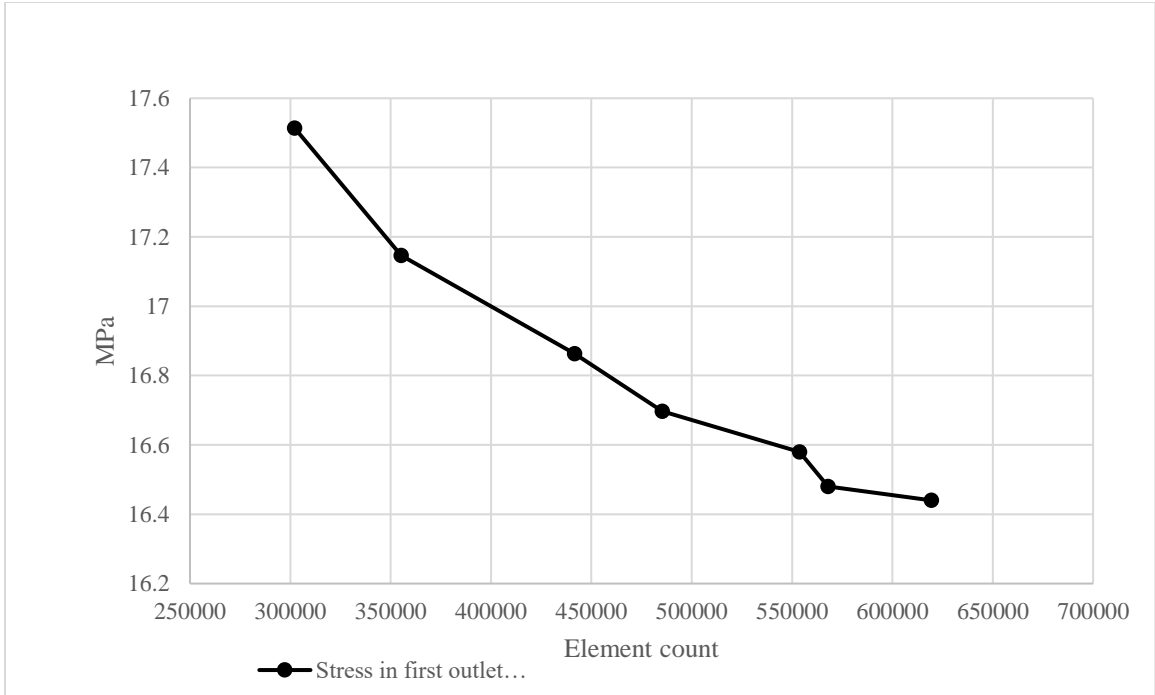
Figure 4.16 Mesh independence graph for second bifurcation (70mm) covered in concrete

The optimum element count is 553,771 for the second bifurcation model as seen in the graph above that the change percentage decreases below 1 percent beyond that point.

The contours of stress and displacement on the concrete block and the second bifurcation pipe are shown below.
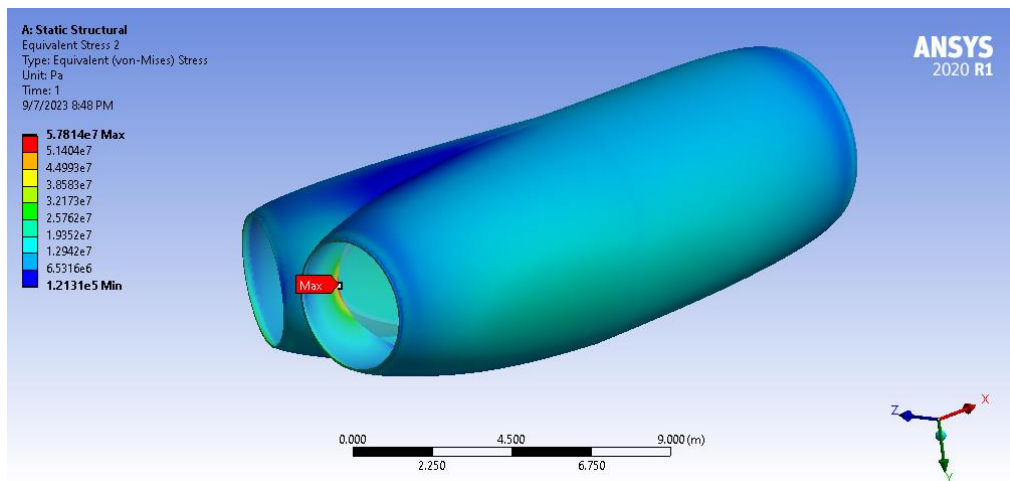

Figure 4.17 Equivalent von-mises stress observed in second bifurcation (70 mm) covered in concrete

The stress is found to decrease drastically as the concrete shares the force exerted on the inner walls of the pipe. Thus, the factor of safety also changes sharply for the pipe.
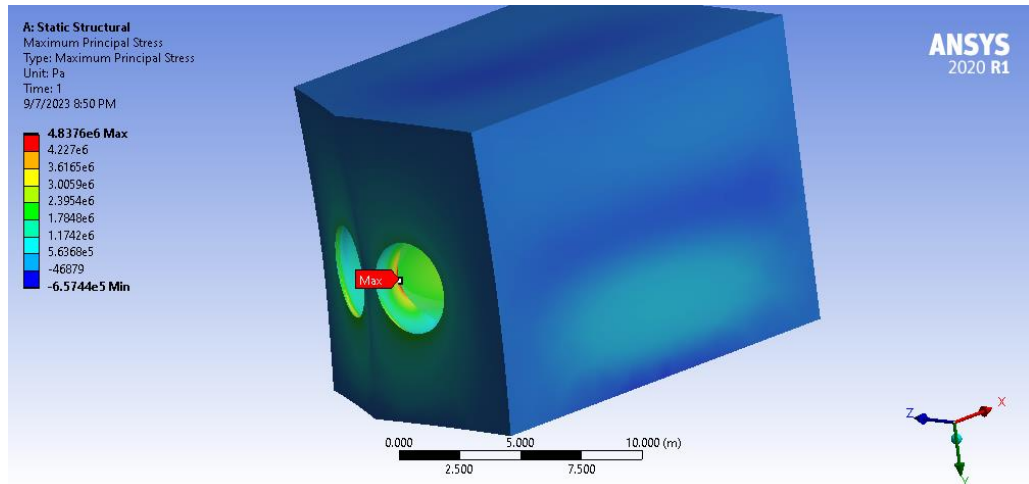
Figure 4.18 Maximum Principal stress on concrete covering second bifurcation (70mm)

The maximum principal stress on the concrete is 4.8376 MPa is less than the permissible value of both direct and bending stresses of M40 concrete.

Table 4-9 Factor of safety calculation for second bifurcation (70 mm) covered in concrete.

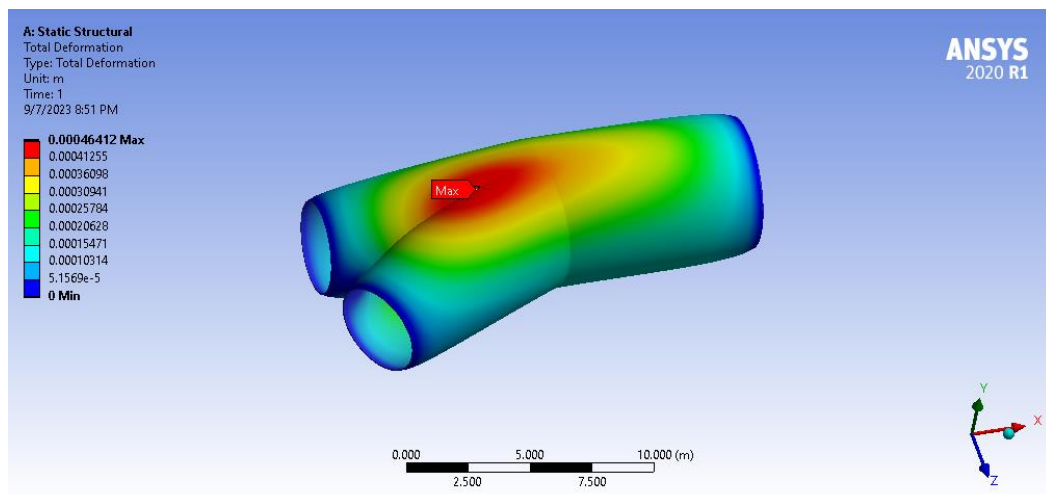| Exerted maximum stress	4.8376 MPa
Allowable Stress	10 MPa
Ultimate strength	40 MPa
Factor of safety	10/4.8376 = 2.067

Figure 4.19 Deformation observed in second bifurcation (70 mm) covered in concrete

The deformation can be seen near the sickle plate on the outer surface of the pipe but it is reduced greatly to just 0.464 mm.

Since the factor of safety is found to be greater than the target for both pipe and concrete, the same analysis is repeated for thinner pipe. The models are recreated decreasing the thickness by 10 mm and the simulation is done again.

The following graphs (Figure 4.20 and Figure 4.21) are generated with the results of the stresses in pipe and concrete from the simulation for the first bifurcation.
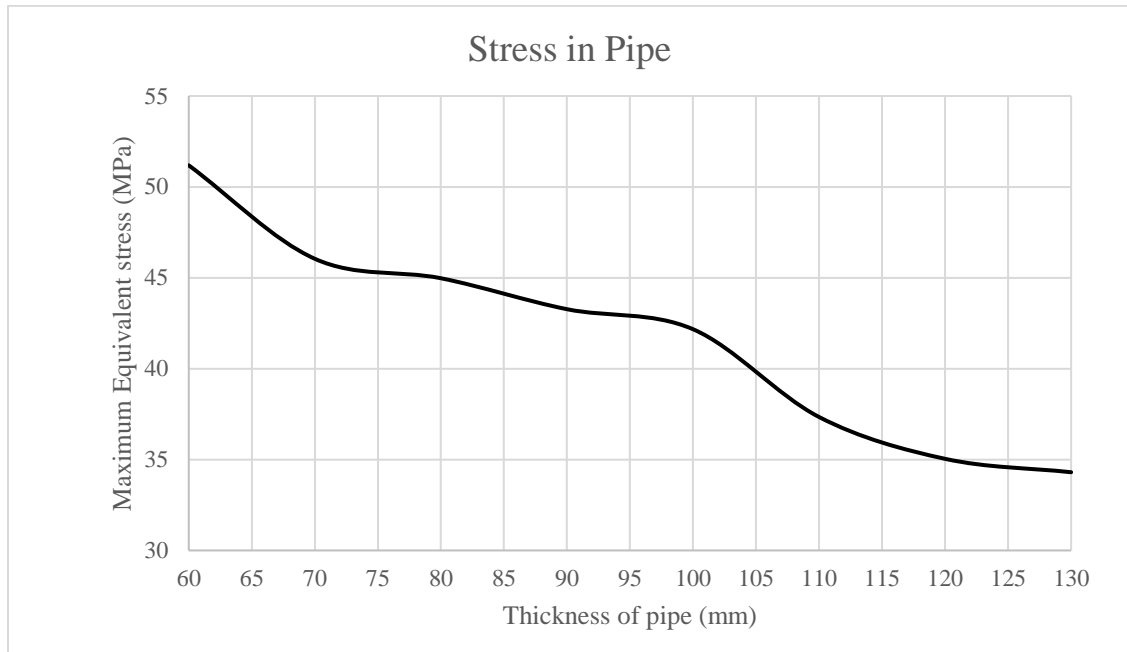

Figure 4.20 Variation of Maximum equivalent von mises stress on first bifurcation w.r.t. its thickness
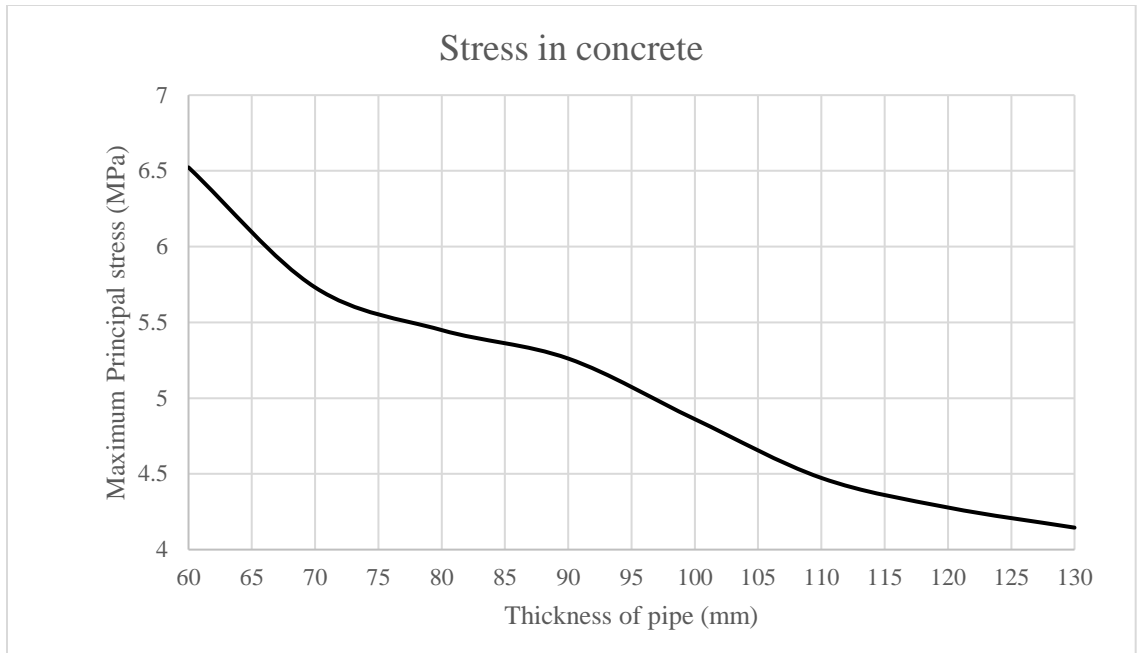
Figure 4.21 Variation of Maximum equivalent principal stress on concrete covering first bifurcation w.r.t. its thickness

The values above are taken to calculate the factor of safety taking 10 MPa as the reference permissible stress and plotted as below in Figure 4.22.

Figure 4.22 Varying factor of safety for concrete plotted against thickness of pipe (first bifurcation)

The target factor of safety for concrete is taken as 2 and the thickness of the pipe that corresponds to FOS higher than that is 100 mm hence it is taken as the recommended thickness for the first bifurcation.

Similarly, the results of the second bifurcation are graphed as below in Figure 4.23 and Figure 4.24 respectively.

41

Figure 4.23 Variation of Maximum equivalent von mises stress on second bifurcation w.r.t. its thickness

Figure 4.24 Variation of Maximum equivalent principal stress on concrete covering second bifurcation w.r.t. its thickness

The values above are taken to calculate the factor of safety taking 10 MPa as the reference permissible stress and graphed as below in Figure 4.25.
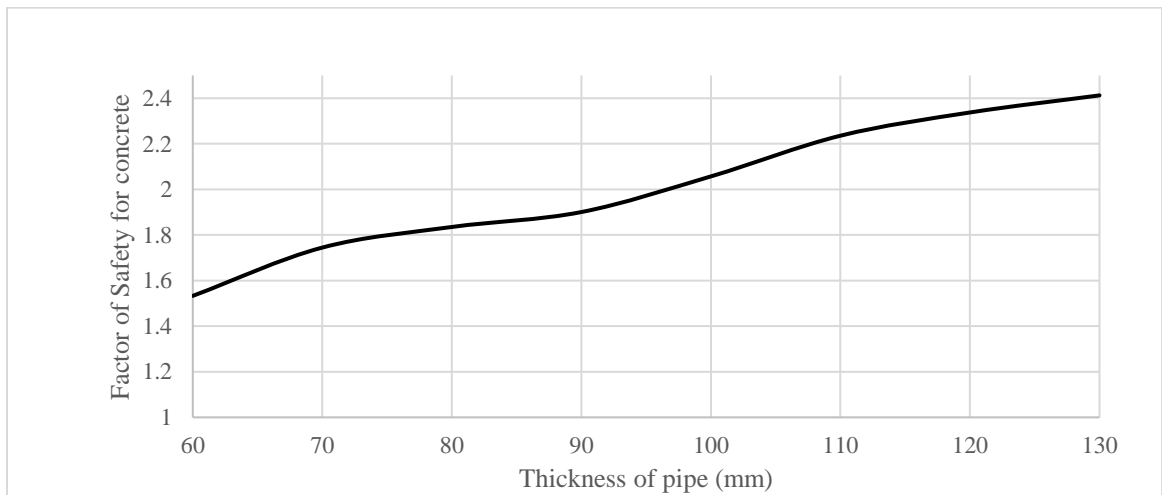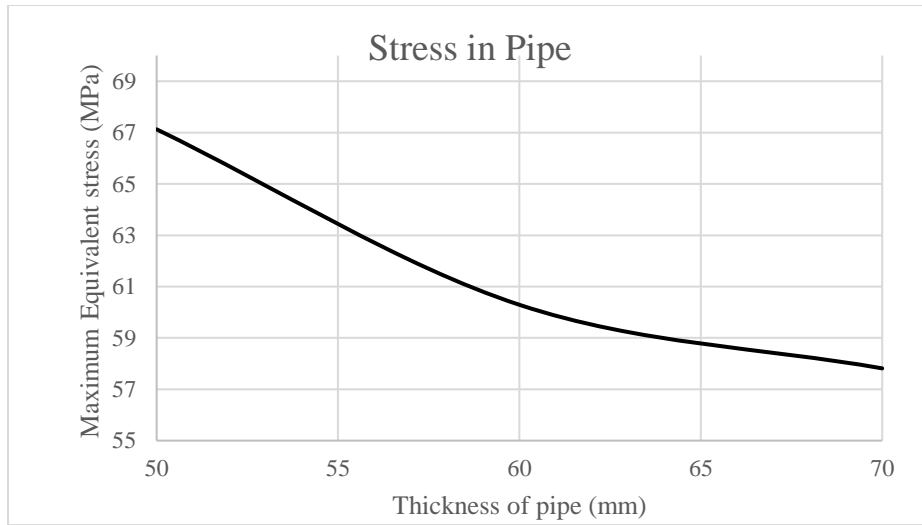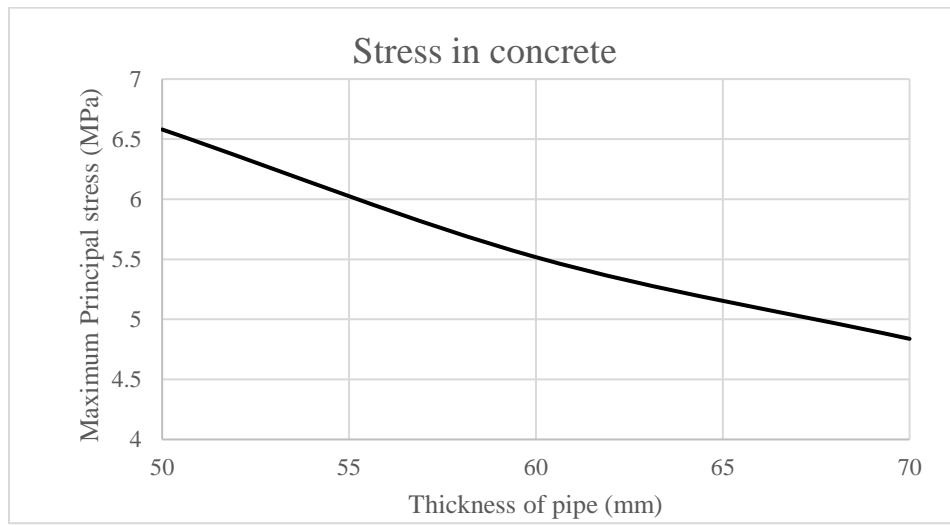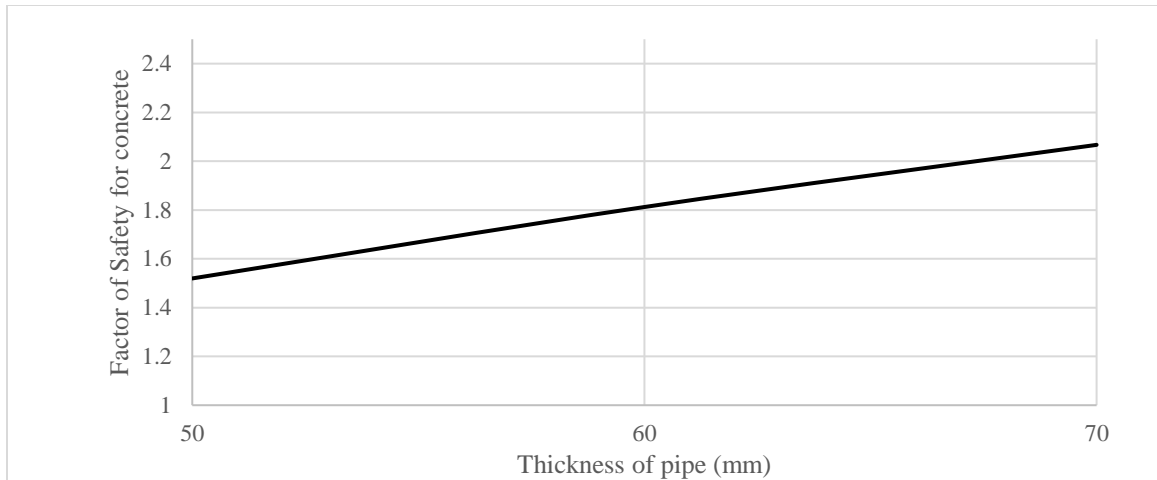
Figure 4.25 Varying factor of safety for concrete plotted against thickness of pipe (second bifurcation)

The target FOS for concrete which is taken as 2 is bettered by 70 mm thick pipe only so it is the recommended thickness for the second bifurcation.

The cost of the first bifurcation is calculated for both thicknesses recommended in previous research and the one suggested in this research. For that the volume of the pipes is found by Ansys SpaceClaim.

Volume of pipe with 130 mm thickness =51.269 m^3

Volume of pipe with 100 mm thickness =39.283 m^3

Difference in volume = 51.269-39.283 m^3

$$\delta v = 11.986 \text{ m}^3$$

Difference in mass of the two pipes = $\delta v \times \rho$ = 11.986 x 7850 = 94,090.1 kg

If the cost of steel per metric ton is taken as $105

Cost saved = 94.09 x 105 = $ 9879.45

The weight reduction percentage due to the use of thinner pipe is given by

$$\frac{94{,}090.1 \text{ kg}}{(51.269 \ m^3 \text{ x } 7850 \text{ kg}/ \ m^3)} \ x \ 100\% = \ 23.3786 \ \%$$

CHAPTER 5: CONCLUSIONS AND RECOMMENDATIONS

5.1 Conclusions

The analysis can be concluded in the following points.

- The total head loss in the three outlets of the pipe are 0.207, 0.22475 and 0.26622 meters respectively that shows there is similar head loss for all the turbines.
- The deformation on the pipes with the addition of reinforcement rings is found as 2.3mm for the first bifurcation and 5mm for the secondd bifurcation however the maximum stress observed are 147.91 MPa and 201.15 MPa respectively.
- Taking a safety factor of 2 for M40 grade concrete, the first bifurcation with 100 mm thickness exerts 4.86 MPa maximum principal stress on the concrete which gives safety factor of 2.06 times below the permissible reference value of 10 MPa which is higher than usual FOS value for concrete. In the case of second bifurcation, the thickness of 70mm was suitable to get a safety factor above 2.

5.2 Recommendations

The recommendations from the analysis are as follows.

- The presence of the sickle plate and ring enforcement also affects the overall stress on the pipe and on the concrete. Thus, the analysis with concrete can be repeated by adding those members in the pipe.
- The thickness of the reinforcements and sickle plate is subject to change with the thickness of the pipe, hence the effect of their varying thickness on the bifurcations can be analyzed separately.
- The structural analysis can be conducted on the whole manifold using the boundary conditions that are very near to the ones available at the actual site.
- The analysis can also be proceeded with different materials for different values of allowable transient head rise.

REFERENCES

Adamkowski, A. (2001). Case Study: Lapino Powerplant Penstock Failure. *Journal of Hydraulic Engineering-Asce - J HYDRAUL ENG-ASCE*, *127*. https://doi.org/10.1061/(ASCE)0733-9429(2001)127:7(547)

Adamkowski, A., & Kwapisz, L. (2004). STRENGTH ANALYSIS OF PENSTOCK BIFURCATIONS IN HYDROPOWER PLANTS. *Transactions of the Institute of Fuid - Flow Machinery ISSN 0079-3205*, 113–124.

Aguirre, C. A., Ramirez Camacho, R. G., de Oliveira, W., & Avellan, F. (2019). Numerical analysis for detecting head losses in trifurcations of high head in hydropower plants. *Renewable Energy*, *131*, 197–207. https://doi.org/10.1016/j.renene.2018.07.021

Aguirre Rodriguez, C., & Camacho, R. (2014, April 9). *HEAD LOSSES ANALYSIS IN SYMMETRICAL TRIFURCATIONS OF PENSTOCKS - HIGH PRESSURE PIPELINE SYSTEMS CFD*.

Bai, X. L., Jia, Q. P., & Su, H. L. (2013). Optimal Design of the Stiffener Penstock Structure in a Hydropower Station. *Applied Mechanics and Materials*, *438–439*, 561–564. https://doi.org/10.4028/www.scientific.net/AMM.438-439.561

Bhavan, M., & Marg, B. S. Z. (2000). *BUREAU OF INDIAN STANDARDS IS 456: 2000*.

Bureau of Indian Standards. (1995). *IS 11639-2: Structural Design of Penstocks - Criteria, Part 2: Buried/Embedded Penstocks in Rock*. http://archive.org/details/gov.in.is.11639.2.1995

Dangi, B., Bajracharya, T., Timilsina, A., Chhantyal, B., & Bista, S. (2022, July 24). *Numerical Analysis of Manifold: A Case Study of Phukot Karnali Hydroelectric Project*.

Dhakal, R., & Shrestha, R. (2023). Computational Analysis of Bifurcation of Raghuganga Hydropower Project. *Journal of Advanced College of Engineering and Management*, *8*(2), 27–37. https://doi.org/10.3126/jacem.v8i2.55940

Ferziger, J. H., & Perić, M. (2002). *Computational methods for fluid dynamics* (3rd, rev. ed ed.). Springer.

Inc, A. (2018). *Fluent Tutorial Guide*.

Ji, C. Z., Wu, X. M., Meng, J. B., Xu, J. T., Chen, W. B., & Zhang, X. (2012). Numerical Simulation of Hydraulic Shape Optimization for Bifurcated Pipe of Hydropower Station. *Applied Mechanics and Materials*, *170–173*, 3507–3511. https://doi.org/10.4028/www.scientific.net/AMM.170-173.3507

Ji, D., & Li, L. (2014). *Structure Force Analysis for Reinforced Concrete Bifurcation Pipe of Dongjiang Hydropower Station:* 2014 International Conference on Mechatronics, Electronic, Industrial and Control Engineering (MEIC-14), Shenyang, China. https://doi.org/10.2991/meic-14.2014.261

Kandel, B., & Luintel, M. (2019). Computational Fluid Dynamics Analysis of Penstock Branching in Hydropower Project. *Journal of Advanced College of Engineering and Management*, *5*, 37–43. https://doi.org/10.3126/jacem.v5i0.26676

Karakouzian, M., Karami, M., Nazari-Sharabian, M., & Ahmad, S. (2019). Flow-Induced Stresses and Displacements in Jointed Concrete Pipes Installed by Pipe Jacking Method. *Fluids*, *4*(1), 34. https://doi.org/10.3390/fluids4010034

Koirala, R., Chitrakar, S., Neopane, H., Chhetry, B., & Thapa, B. (2017). Computational Design of Bifurcation: A Case Study of Darundi Khola Hydropower Project.

International Journal of Fluid Machinery and Systems, *10*, 1–8. https://doi.org/10.5293/IJFMS.2017.10.1.001

Kumar, A., & Singhal, M. (2015). Optimum Design of Penstock for Hydro Projects. *International Journal of Energy and Power Engineering*, *4*, 216–226. https://doi.org/10.11648/j.ijepe.20150404.14

Mallik, R., & Paudel, P. (2010). 3D Flow Modeling of the First Trifurcation Made in Nepal. *Hydro Nepal: Journal of Water, Energy and Environment*, *5*. https://doi.org/10.3126/hn.v5i0.2493

Nepal Government, D. (2006). *Water conveyance manual*. http://www.doed.gov.np/pages/guidelines-and-manuals

Neupane, P., & Luitel, M. C. (2022). *Flow Analysis in Asymmetric and Symmetric Bifurcation with Varied Layout: A Case Study of Daram Khola HEP*. https://www.researchgate.net/publication/371071205_Flow_Analysis_in_Asymmetric_and_Symmetric_Bifurcation_with_Varied_Layout_A_Case_Study_of_Daram_Khola_HEP

Penstock Branch Design. (2009). Bureau of Indian Standards. https://dokumen.tips/documents/53948734-penstock-branch-design.html

Sharma, K. R., & Neupane, S. (2023). *A study on flow and structural analysis on bifurcation of Seti Nadi Hydropower Project (25MW)* [Academic]. IOE Pulchowk Campus.

Standard 2062, I. (2011). *IS 2062 Hot Rolled Medium and High Tensile Structural Steel*.

Thapa, D., Bajracharaya, T. R., & Luintel, M. C. (2016). *Flow Analysis and Structural Design of Penstock Bifurcation of Kulekhani III HEP*.

Vidhyut Utpadan Company Limited. (2023, August). https://www.vucl.org/projects/phukot-karnali-pror-hep

Wang, Y., Su, K., Wu, H., & Qian, Z. (2017). Flow Characteristics of Large Hydropower Bifurcation Under Structure Rounding Optimization. *International Journal of Civil Engineering*, *15*(4), 515–529. https://doi.org/10.1007/s40999-016-0091-5

Welded Steel Penstocks—USBR Monograph 3. (1977). United States Bureau of Reclamation. https://dokumen.tips/documents/welded-steel-penstocks-usbr-monograph-3.html

Wingate, J. A. (2007). *Applying the ASME Codes: Plant Piping and Pressure Vessels*. ASME Press.

Zhang, J., & Li, X. (2011). Three-dimensional finite element simulative analysis on reinforced concrete bifurcation pipe of hydropower station. *2011 International Conference on Electric Technology and Civil Engineering (ICETCE)*, 6382–6385. https://doi.org/10.1109/ICETCE.2011.5774335

Zhang, Z., Fang, H., Li, B., & Wang, F. (2020). Mechanical Properties of Concrete Pipes with Pre-Existing Cracks. *Applied Sciences*, *10*(4), 1545. https://doi.org/10.3390/app10041545

Annex-A DESIGN FEATURES OF HYDROPOWER PROJECT

Feature category	Parameters	Details
General	Project Name	Phukot Karnali Hydroelectric Project
	Location	Kalikot, Karnali Province
	Climate	Moderate
	Source river	Karnali
	All weather airport	Surkhet (160 km from site) and Nepalgunj (260km from site)
	Nearest Highway	Karnali highway
Firms	Consultant firm	NEA Engineering Company Limited
	Developers	Vidhyut Utpadan Company Limited
Energy	Total Annual Energy harvest dry season	750.55 Gigawatt-hour
	Annual Energy harvest in dry season (off peak)	269.5 Gigawatt-hour
	Annual Energy harvest in dry season (peak)	481.05 Gigawatt-hour
	Energy harvest in wet season	1704.63 Gigawatt-hour
	Total Energy	2455.19 Gigawatt-hour
Hydrology	Catchment Area	16,902 square kilometers
	Minimum Monthly flow	77 cubic meter per second
	Maximum Monthly flow	881.50 cubic meter per second
	Average yearly flow	328 cubic meter per second
	Maximum Discharge	361 cubic meter per second
	Design Discharge	348 cubic meter per second
	1 in 10000 years flood Q_{10000}	5956 cubic meter per second
	1 in 1000 years flood Q_{1000}	4813 cubic meter per second

	1 in 100 years flood Q_{100}	3648 cubic meter per second
	Probable Maximum Flood	15882 cubic meter per second
Gross Storage Volume	Storage required for 6 hrs peaking	7.52 cubic millimeters
	Minimum draw down level	904 masl
	Reservior live storage volume upto 904 masl	14.29 square millimeters
	Dry season full supply level	910 masl
	Length of reservoir at FSL	11 kilometers
	Surface area at FSL	2.51 square kilometers
River Diversion	Upstream Coffer dam Location	235 meter upstream from Dam Axis
	Coffer dam Height	36 m
	Lining for tunnel	Concrete lining
	Tunnel Diameter	11 meter
	Number of Tunnels	2
Dam	Dam type	Roller Compacted concrete
	Dam height	160 and 109 meter from foundation bed and river bed respectively
	Dam width at top	10
	Dam length	313 meters
	Elevation of Dam top	915 masl
Sediment By-pass tunnel	Number of tunnels	1
	Tunnel Diameter	8 meters
	Location of tunnel	775 meters from axis of dam
	Length	660 meters
Trash Overflow Spillway	Type	Ogee
	Width	4 meters
	Height	3 meters
	Number	1

	Dissipation of Energy	Flip Bucket
	Crest Elevation	902.5 masl
Sluice Spillway	Type	Ogee
	Width	7 meters
	Height	13 meters
	Number	3
	Dissipation of Energy	Flip Bucket
	Crest Elevation	860 masl
Overflow Spillway	Type	Gated Ogee
	Width	13.5 meters
	Height	19 meters
	Number	3
	Dissipation of Energy	Flip Bucket
	Crest Elevation	891 masl
Main Intake	Type	Side intake embedded in dam
	Design discharge (wet)	361 cubic meter per second
	Design discharge (dry)	348 cubic meter per second
	Deck level	915 masl
	Invert level	883 masl
Intake Gate	Type	Vertical lift gate
	Number	2
	Width	8.4 meters
	Height	8.4 meters
Trash Rack Openings		
	Width	4.8 meters
	Height	28 meters
	Inclination	80 degrees with horizontal
	Number	8
Surge Tunnel	Number	2
	Slope	1:10
	Diameter	6.5 meters
	Length	848 and 869 meters
	Down surge level	871.15 masl
	Upsurge level	935.43 masl
	Number	2

Headrace Tunnel	Type	Circular
	Diameter	8.4 meters
	Length	6043.9 and 5878.5 meters
	Max velocity	3.3 m/s
	Lining type	Reinforced concrete
	Lining thickness	300 mm
Pressure Shaft and Tunnel	Number	2
	Length	366 and 477.8 meters
	Diameter	Main 6.5 meters, 5.3 meters and 3.75 meters after first and 3.75 meters after second bifurcation
	Lining	Concrete
Tailrace Tunnel	Diameter	9.5 meters
	Number	2
	Lining type	Concrete
	Lining thickness	500 mm
Main Powerhouse	Rate net head	159.6 meters
	Gross head	168.62 meters
	Power house type	Underground
	Normal Tail water level	741.38 masl
	Length	156 meters
	Width	20 meters
	Height	44.6 meters
Main Powerhouse Turbine	Type	Vertical axis Francis turbine
	Number	6
	Capacity of one turbine	79 Megawatts
	Turbine floor level	733.64 masl
	Generator floor level	737.94 masl
	Turbine center line level	734.7 masl
	Machine floor level	742.54 masl
Secondary Powerhouse	Rate net head	88.88 meters
	Gross head	95 meters
	Power house type	Surface
	Normal Tail water level	815 masl

	Length	37.15 meters
	Width	10.5 meters
	Height	15.75 meters
Secondary Powerhouse Turbine	Type	Horizontal axis francis turbine
	Number	2
	Capacity of one turbine	3
	Turbine floor level	813.7 masl
	Generator floor level	813.7 masl
	Turbine center line level	813.7 masl
	Machine floor level	813.7 masl
Total Capacity	Total Installed capacity	474 + 6 = 480 Megawatts
Transmission line	Voltage	400 kV
	Connection length	2300 meters

Annex-B GEOMETRY USED IN MODEL FOR ANALYSIS
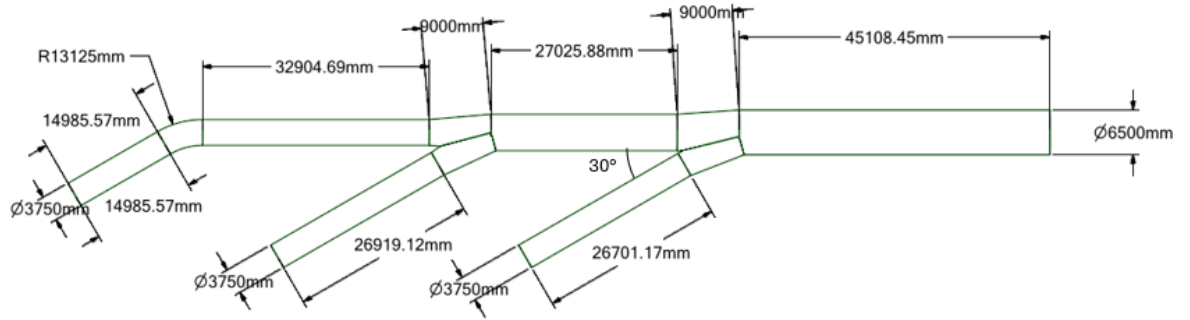
Figure B 1 Intake manifold Geometry used in CFD simulation
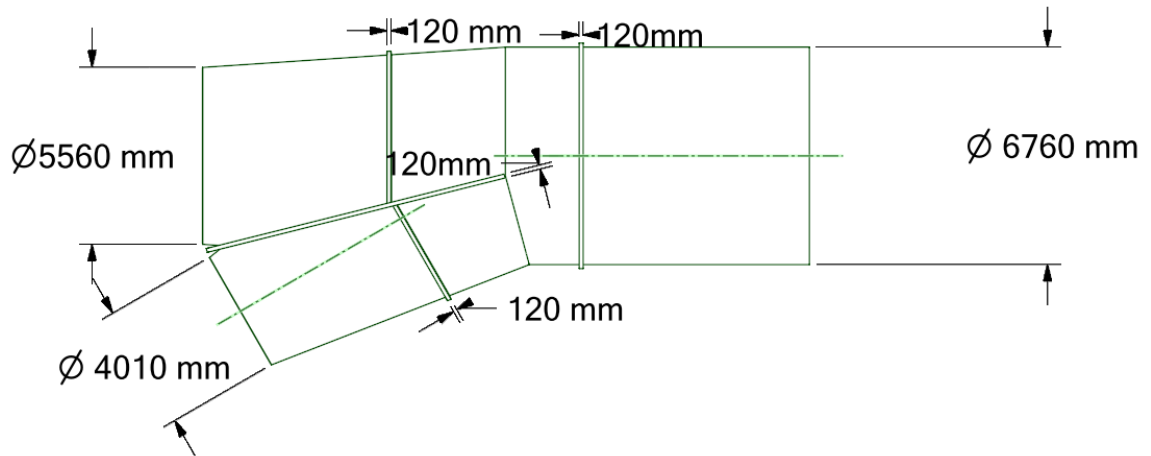
Figure B 2 130 mm thick first Bifurcation with reinforcement without the concrete block used for simulation
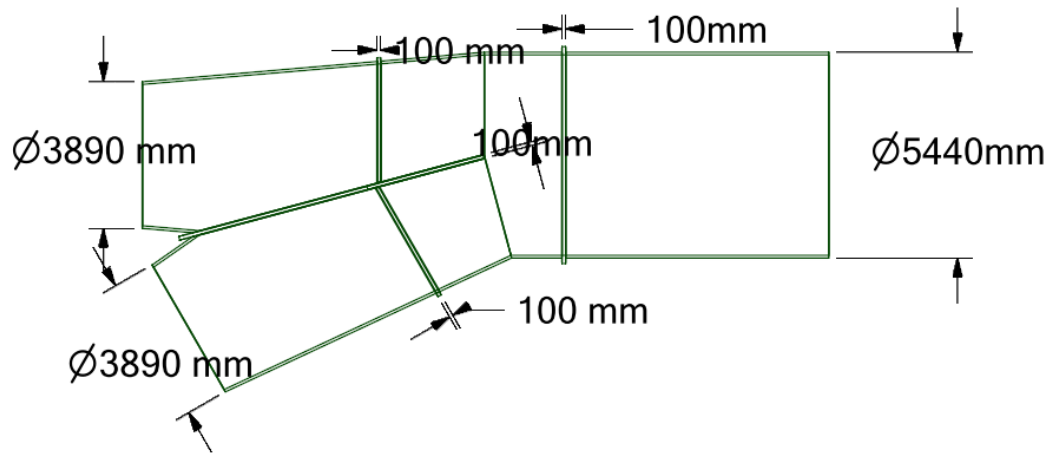
Figure B 3 70 mm thick second Bifurcation with reinforcement without the concrete block used for simulation
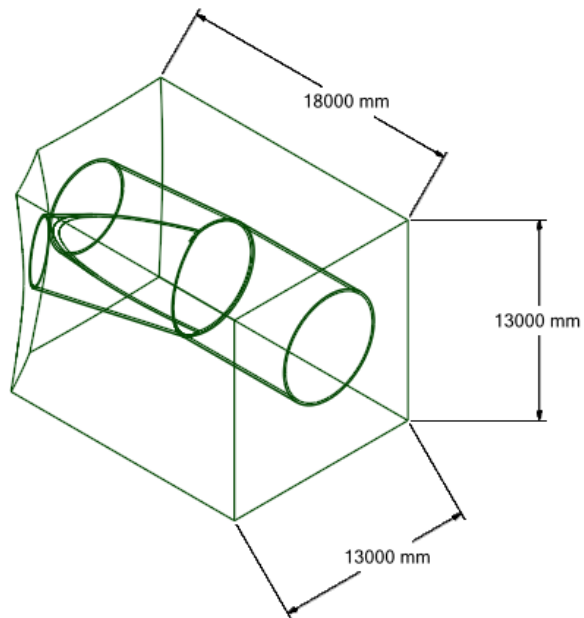
Figure B 4 Dimensions of concrete block covering first bifurcation without reinforcement
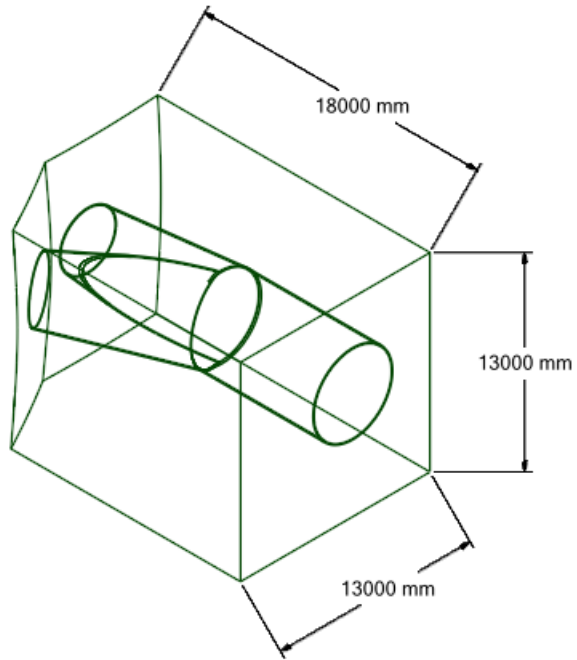
Figure B 5 Dimensions of concrete block covering second bifurcation without reinforcement

Annex-C MESH INDEPENDENCE TESTS

C-A CFD Analysis

Table C 1 Pressure values recorded for CFD analysis of manifold

Element number	Pressure (in Pascals)			
	Section0	Outlet 1	Outlet 2	Outlet 3
227886	1931934	1947048	1948613	1929383
289576	1839937	1847294	1843532	1835759
315648	1744016	1754315	1754074	1745018
462107	1696514	1708194	1709624	1704119
530775	1663249	1673060	1672822	1665806
649105	1643526	1641864	1641631	1641188
861423	1640246	1638587	1638354	1637912
959650	1640271	1638640	1638315	1639714
1094099	1640232	1638447	1638218	1637861
1334594	1640450	1638122	1638351	1637670

Table C 2 Velocity values recorded for CFD analysis of manifold.

Element number	Velocity (in m/s)			
	section0	outlet 1	outlet 2	outlet 3
227886	6.201659	6.323355	6.287246	6.25366
289576	5.895113	5.988026	5.936965	5.938898
315648	5.593086	5.675854	5.659642	5.656094
462107	5.451351	5.515893	5.505489	5.512762
530775	5.339227	5.39188	5.397538	5.399375
649105	5.26551	5.30175	5.3021	5.30912
861423	5.26706	5.28951	5.29017	5.29736
959650	5.26483	5.28675	5.28725	5.29415
1094099	5.26621	5.28578	5.28654	5.29101
1334594	5.26856	5.288695	5.286751	5.291838

C-B Structural Analysis

Table C 3 Mesh independence graph for first bifurcation (130mm) covered in concrete.

Element count	Stress in first outlet (MPa)
311162	15.564
344511	15.701
369713	16.033
383455	16.436

507704	16.714
514465	16.803
604789	16.881

Table C 4 Stress values at second outlet with varying element numbers for first bifurcation 120 mm

Elements	Stress at second outlet (MPa)
251229	17.44
324455	16.333
372587	15.675
409398	15.303
467456	15.518
545195	15.319
609142	15.345
688332	15.341
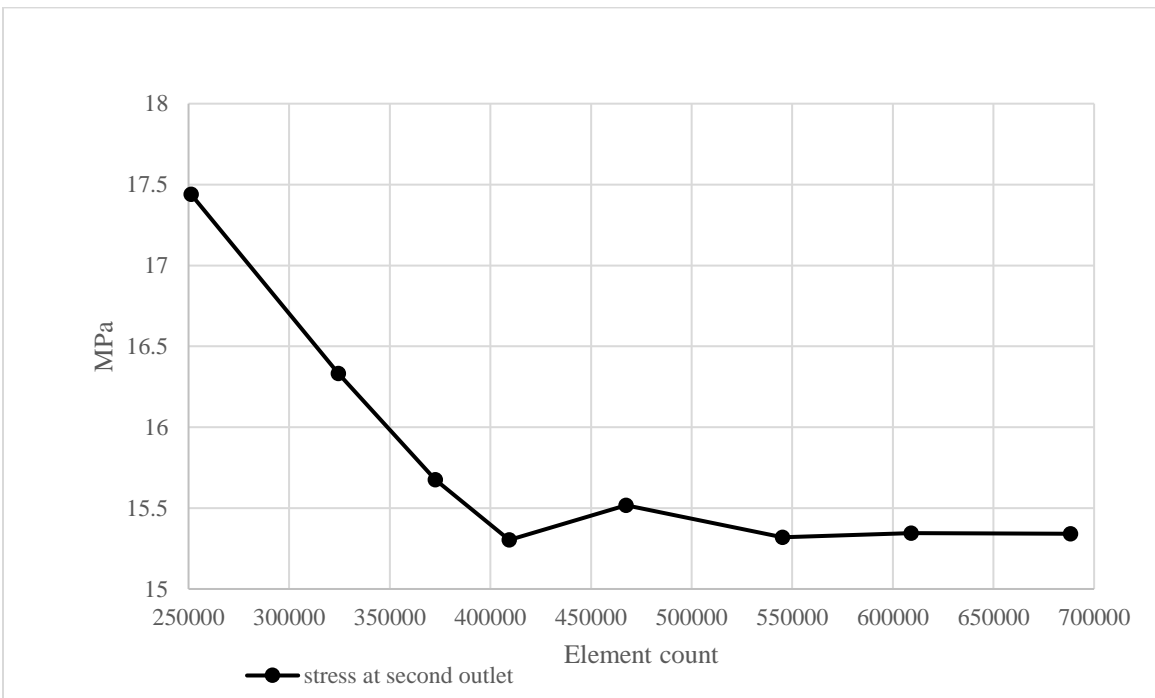
Figure C 1 Mesh independence graph for first bifurcation 120 mm

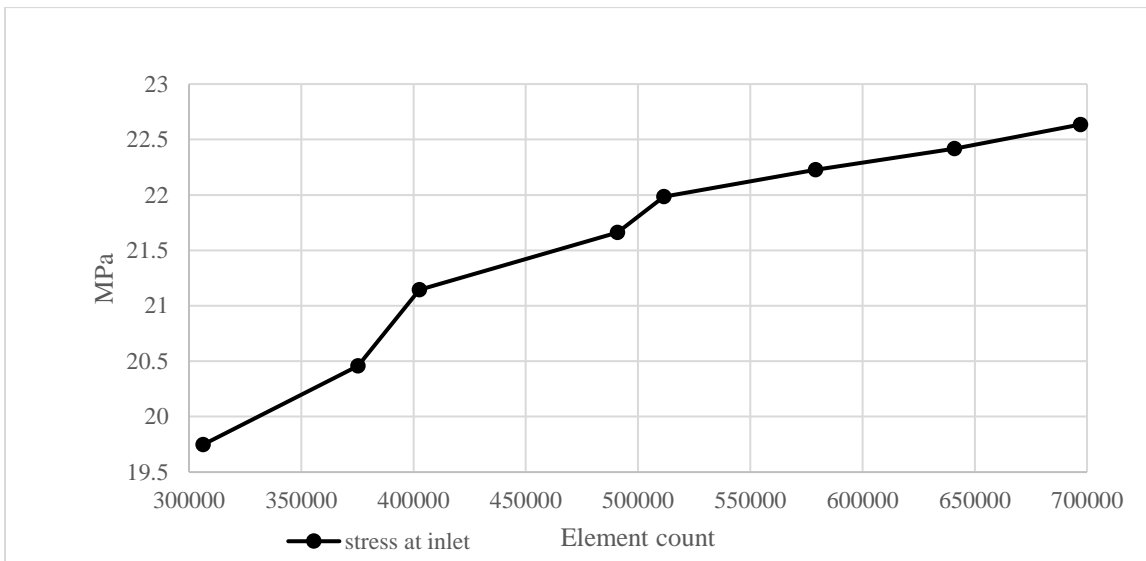| Elements	Stress at second outlet (MPa)
287687	17.974
321767	17.37
387248	16.85
447136	16.64
495913	16.41
568751	16.198
610629	16.167
687054	16.145
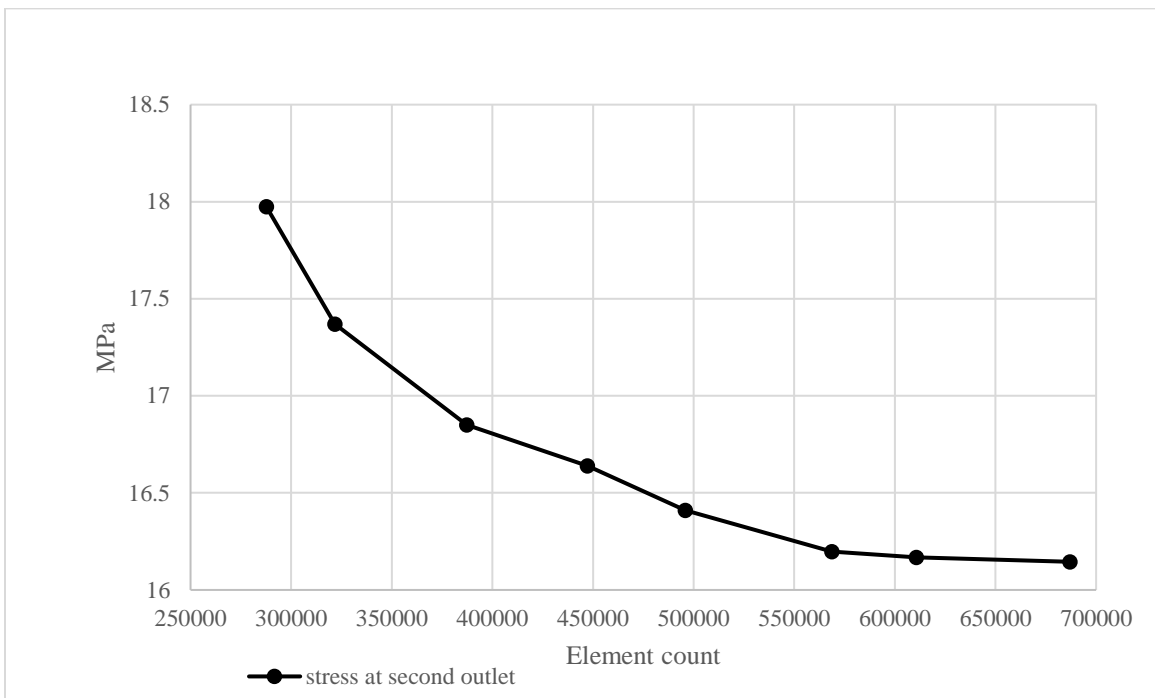
Figure C 2 Mesh independence graph for first bifurcation 110 mm

Table C 6 Stress values at first outlet with varying element numbers for first bifurcation 100 mm

Elements	Stress at first outlet (MPa)
243312	19.791
287908	19.105
353266	18.587
380314	18.177
443682	17.726
508026	17.288
582896	16.991
613086	16.887
690551	16.851
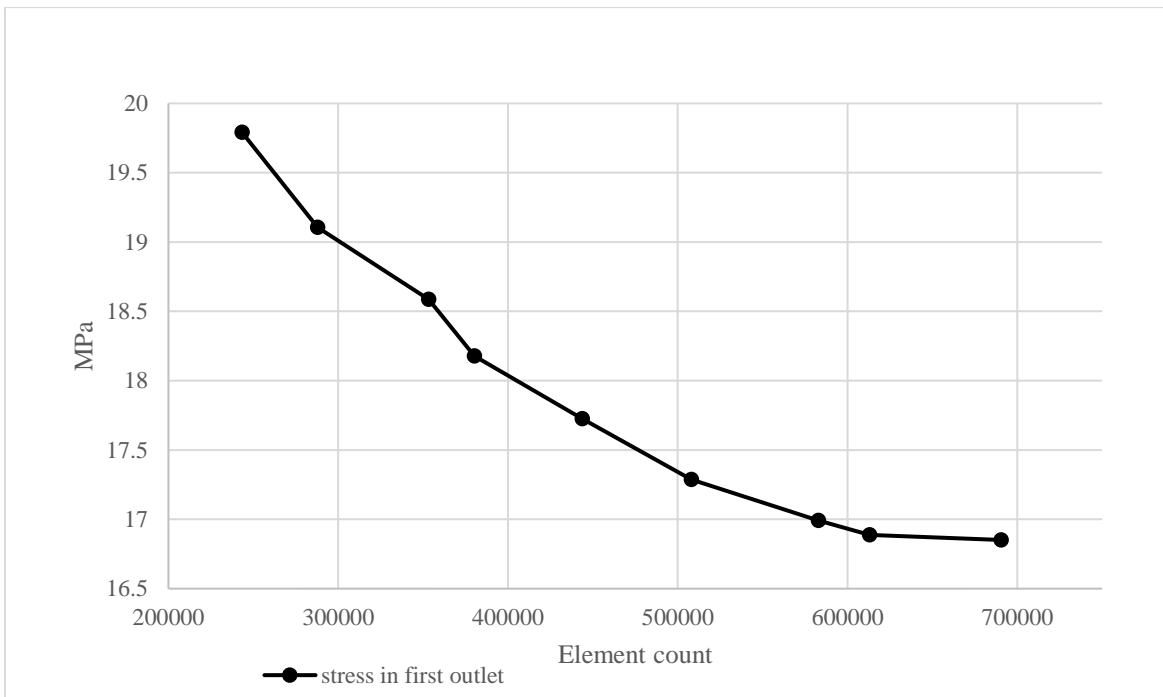
Figure C 3 Mesh independence graph for first bifurcation 100 mm

Table C 7 Stress values at inlet with varying element numbers for first bifurcation 90 mm

Elements	Stress at inlet (MPa)
338436	19.523
404868	18.897
446982	18.844
485009	18.742
581580	18.407
633349	18.317
692103	18.216
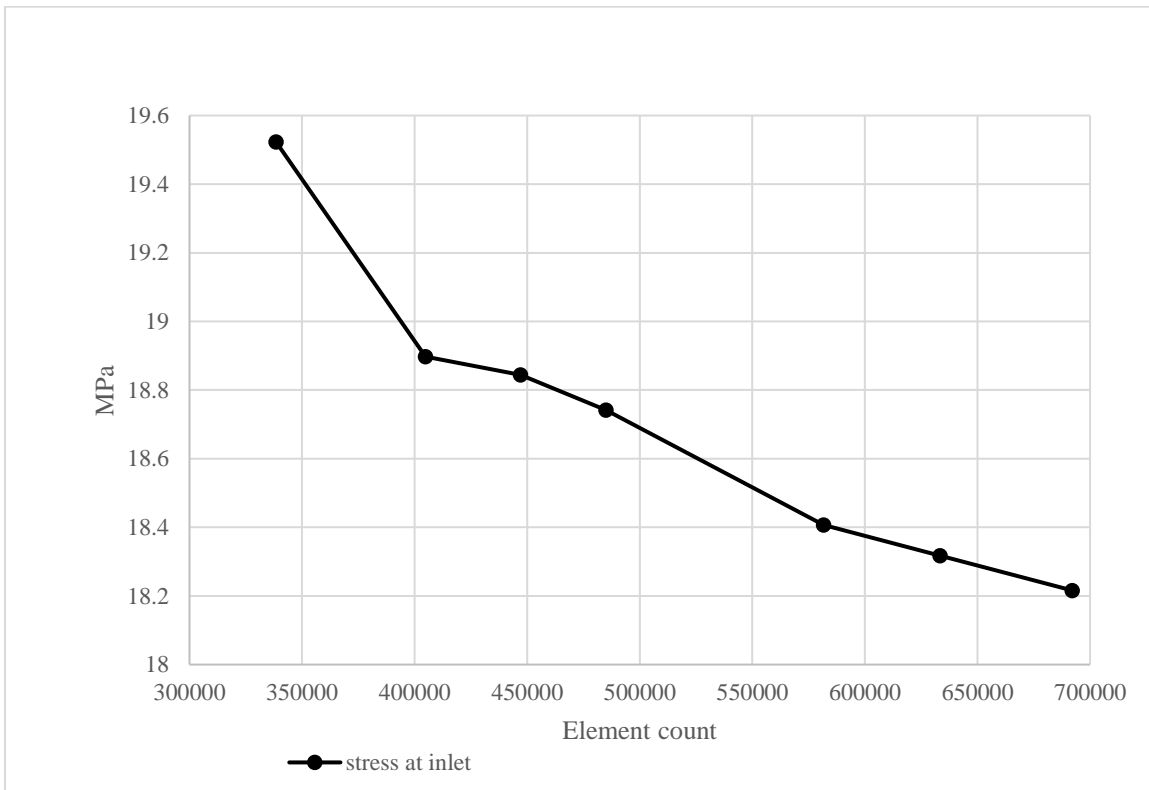
Figure C 4 Mesh independence graph for first bifurcation 90 mm

Table C 8 Stress values at inlet with varying element numbers for first bifurcation 80 mm

Elements	Stress at inlet (MPa)
304055	22.487
379820	20.948
442874	19.987
486692	19.584
550345	19.345
653009	19.199
688384	19.187
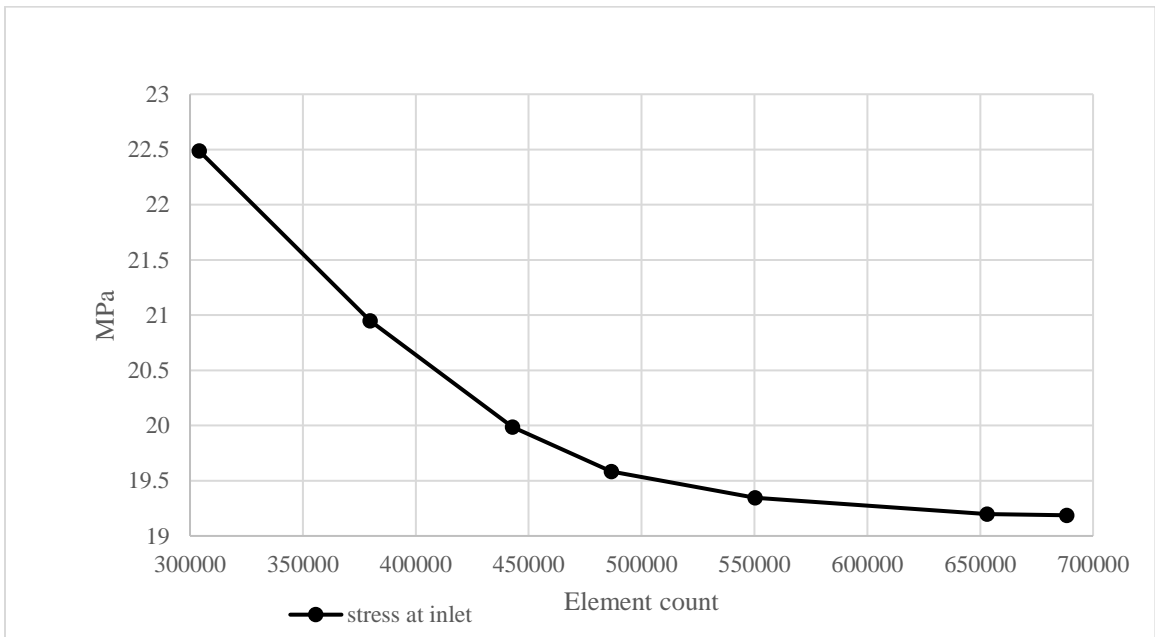
Figure C 5 Mesh independence graph for first bifurcation 80 mm

Elements	Stress at second outlet (MPa)
285750	16.7894
302639	17.148
362335	17.545
412998	18.181
473070	18.417
575667	18.626
613533	18.648
668802	18.74
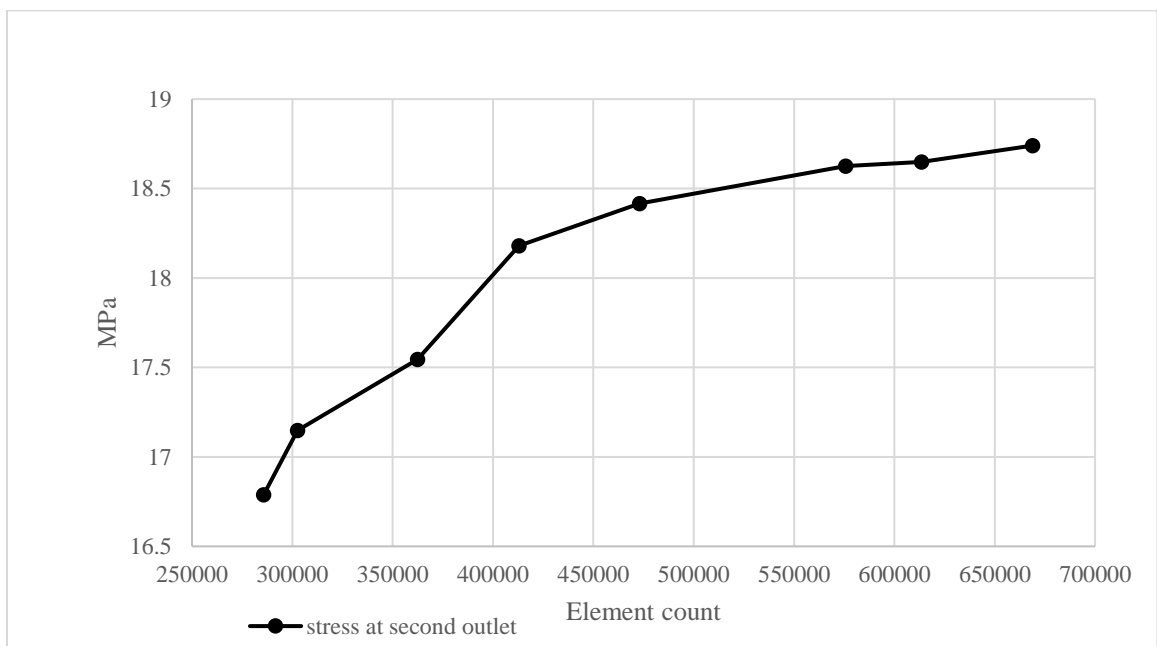
Figure C 6 Mesh independence graph for first bifurcation 70 mm

Table C 10 Stress values at inlet with varying element numbers for first bifurcation 60 mm

Elements	Stress at inlet (MPa)
334177	26.01
373213	24.647
411636	23.814
454812	23.279
505297	22.778
606993	22.422
644319	22.231
688739	22.331
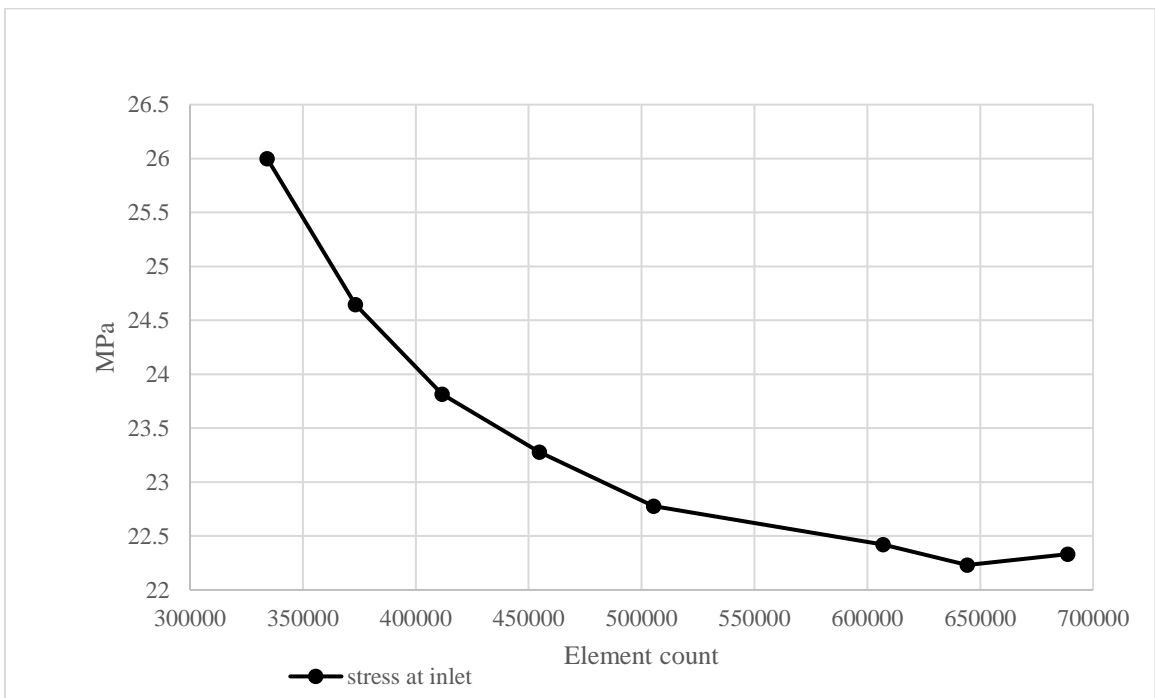
Figure C 7 Mesh independence graph for first bifurcation 60 mm

Table C 11 Mesh independence graph for second bifurcation (70mm) covered in concrete

Element count	Stress in first outlet (MPa)
302136	17.514
355162	17.147
441576	16.863
485276	16.697
553711	16.58
567948	16.48
619460	16.44

Table C 12 Stress values at first outlet with varying element numbers for second bifurcation 60 mm

Elements	Stress at first outlet (MPa)
290860	19.747
300511	20.456
395163	21.145
423991	21.661
479895	21.9845
512627	22.226
588140	22.418
640305	22.635
726488	19.747

Figure C 8 Mesh independence graph for second bifurcation 60 mm

Elements	Stress at inlet (MPa)
268800	22.8745
306212	23.747
375326	22.456
402602	21.78145
490787	22.461
511472	21.9845
579026	22.226
640896	22.418
697056	22.635
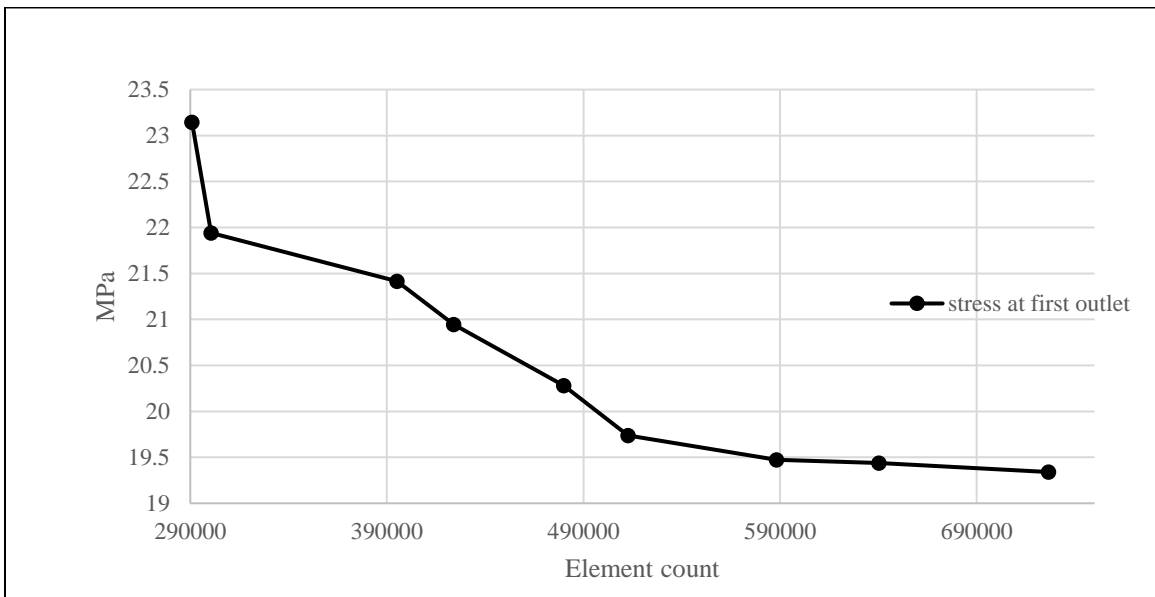
Figure C 9 Mesh independence graph for second bifurcation 50 mm

Annex-D STRESS CONTOURS IN CONCRETE
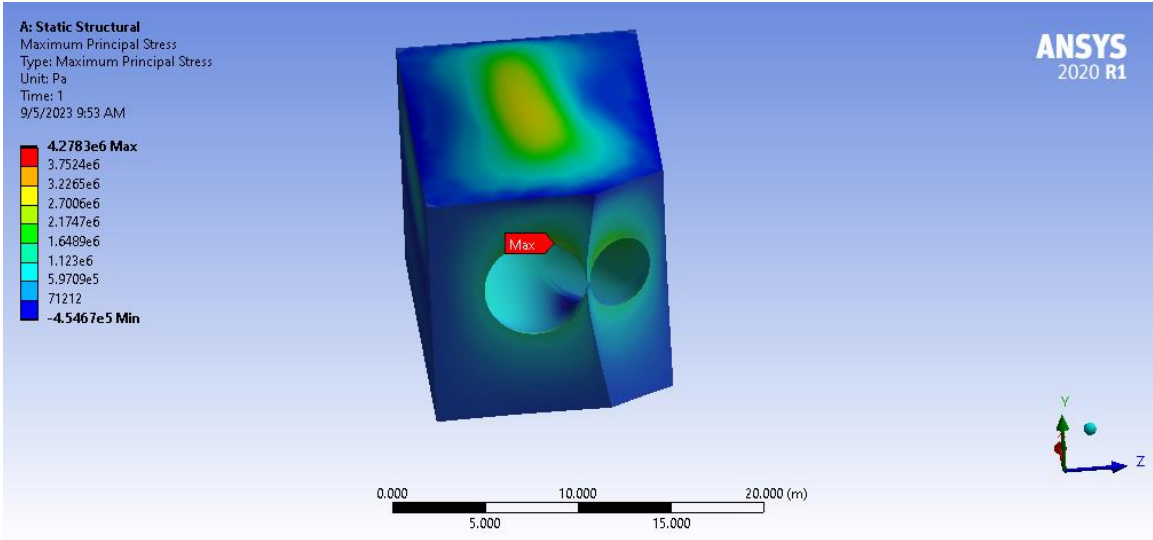
Figure D 1 Maximum Principal stress in concrete covering first bifurcation(120mm)
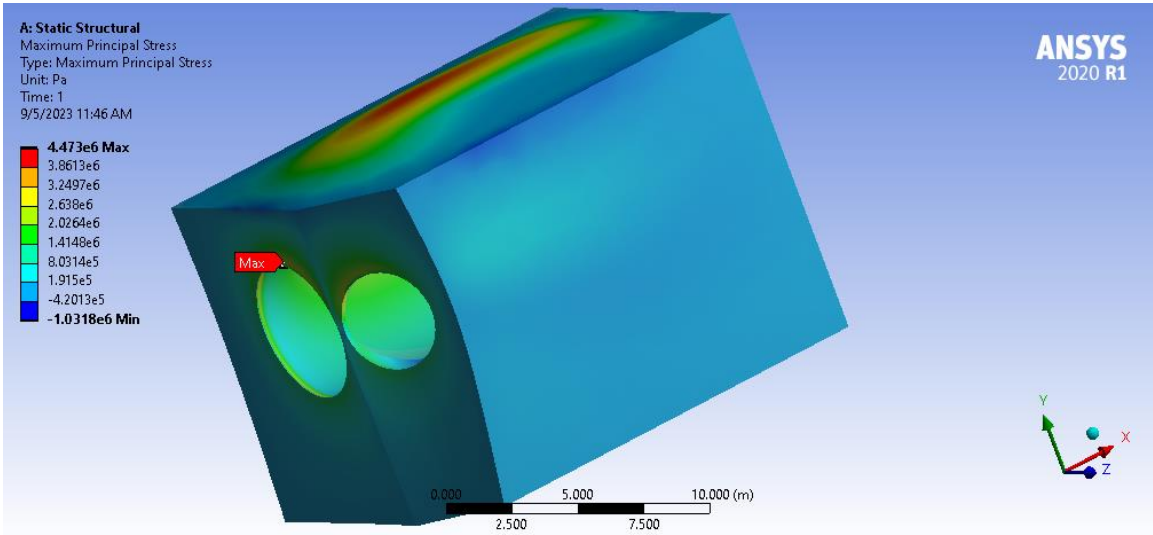
Figure D 2 Maximum Principal stress in concrete covering first bifurcation(110mm)
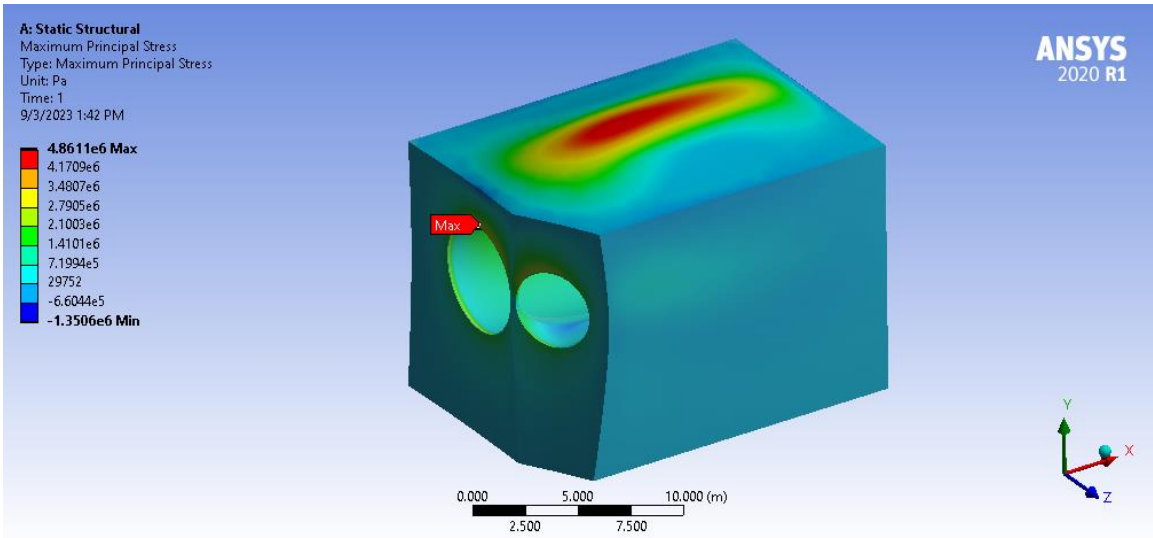
Figure D 3 Maximum Principal stress in concrete covering first bifurcation(100mm)
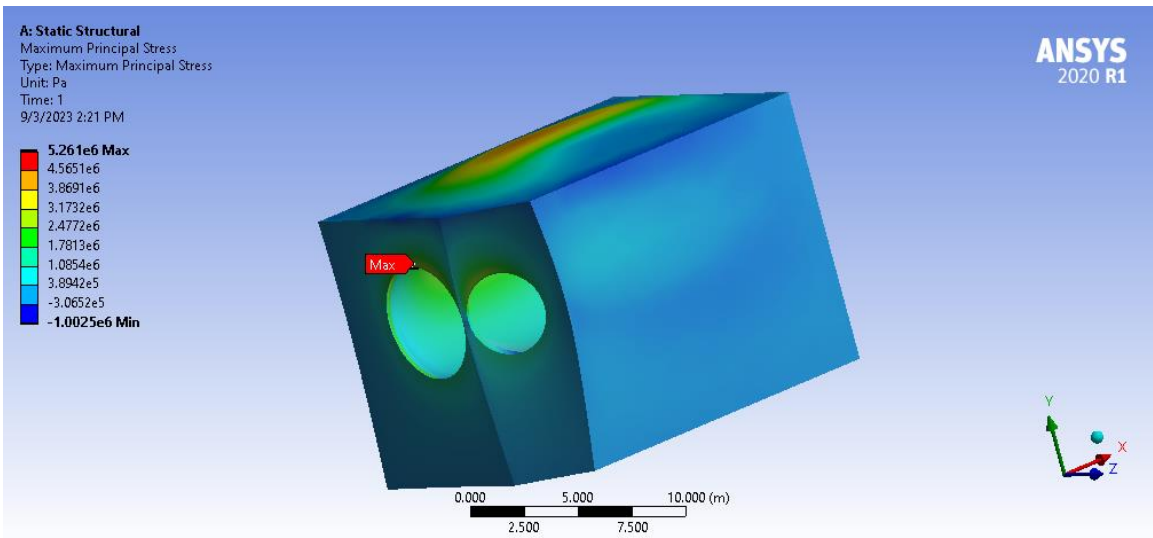
Figure D 4 Maximum Principal stress in concrete covering first bifurcation(90mm)
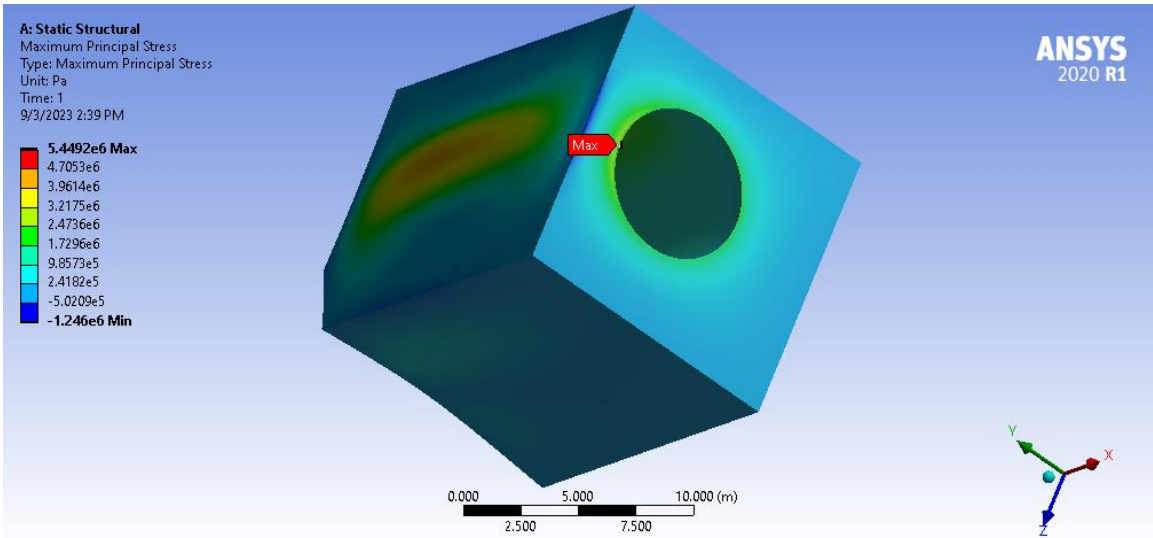
Figure D 5 Maximum Principal stress in concrete covering first bifurcation(80mm)
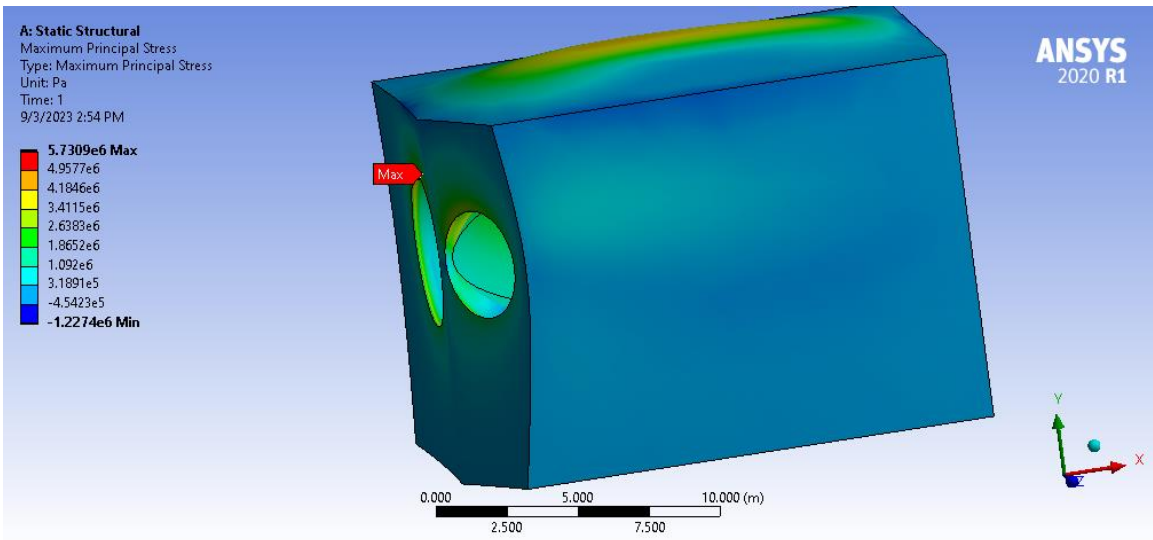
Figure D 6 Maximum Principal stress in concrete covering first bifurcation(70mm)
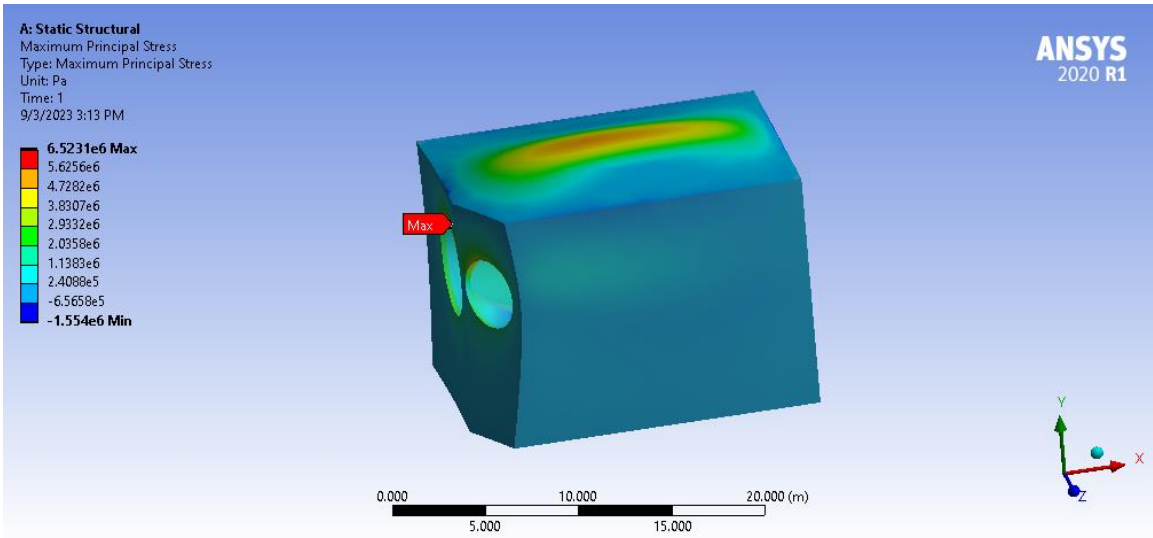
Figure D 7 Maximum Principal stress in concrete covering first bifurcation(60mm)
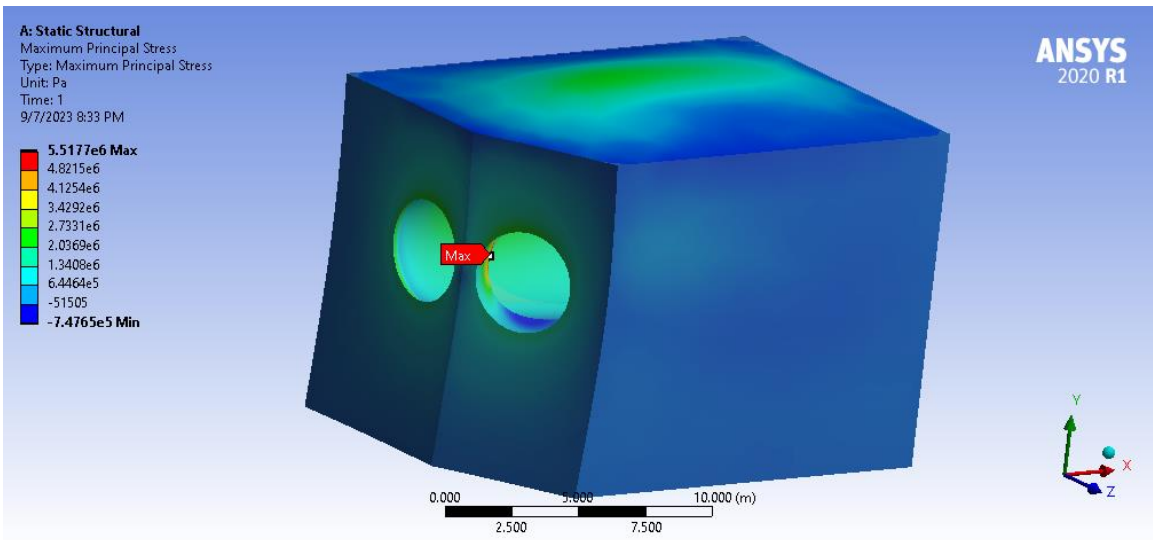
Figure D 8 Maximum Principal stress in concrete covering second bifurcation(60mm)
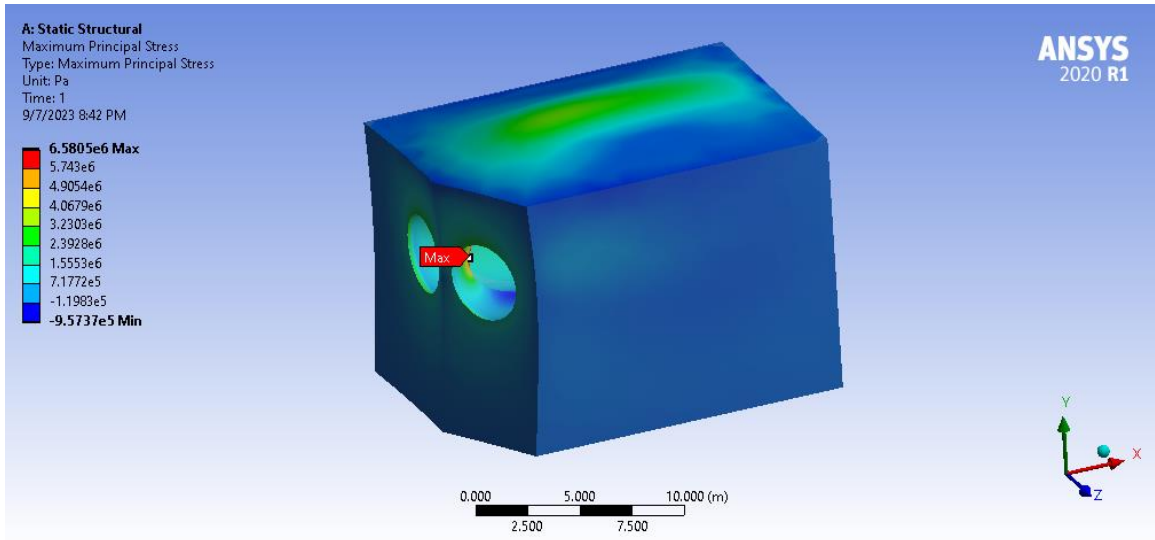
Figure D 9 Maximum Principal stress in concrete covering second bifurcation(50mm)
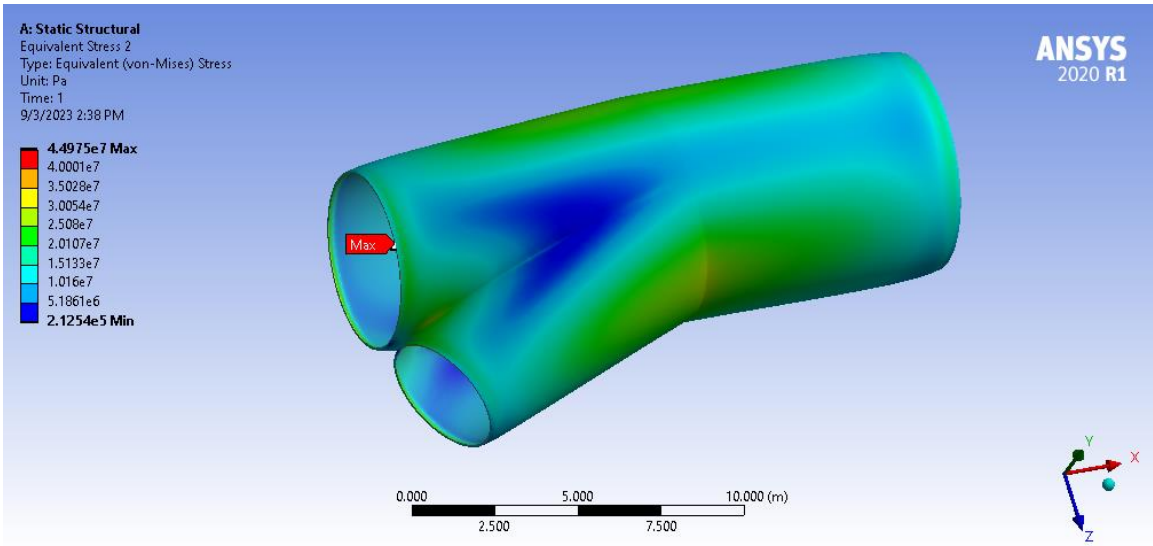
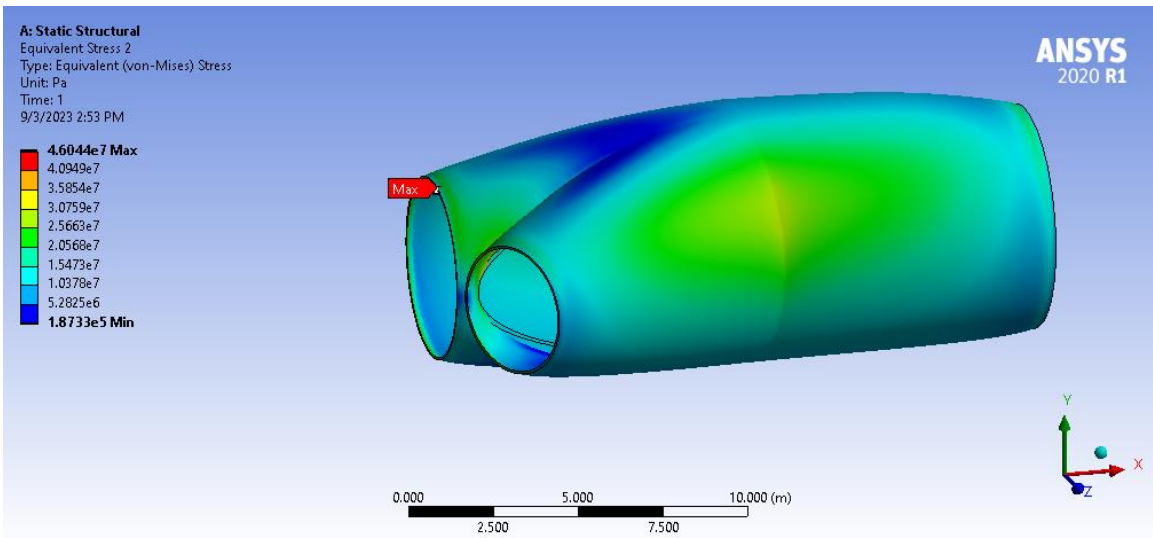**Annex-E STRESS CONTOURS IN PIPE**
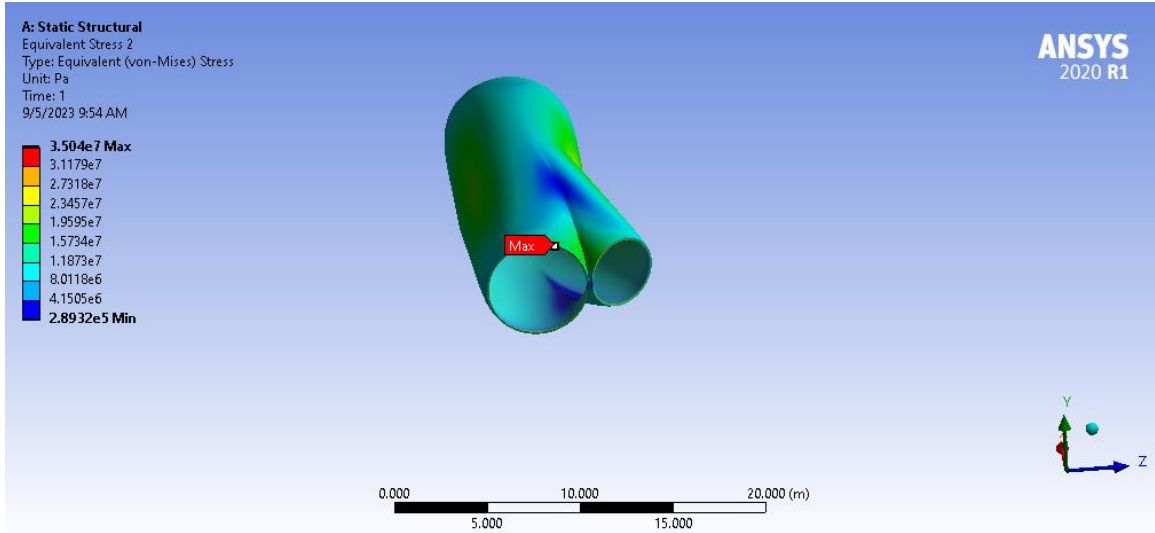
Figure E 1 Maximum Equivalent von-mises stress in first bifurcation(120mm) covered by concrete
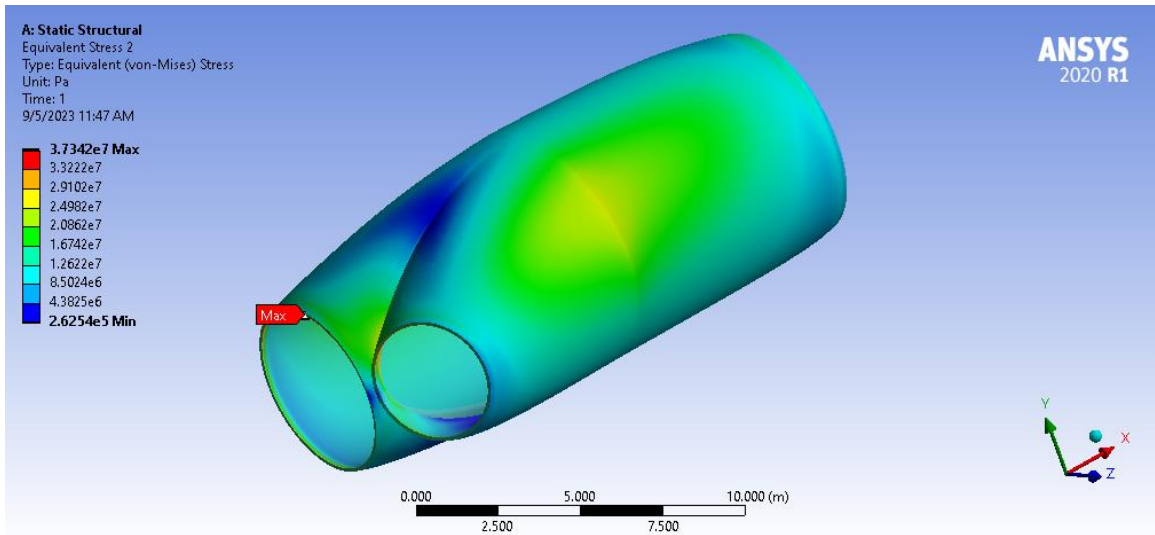
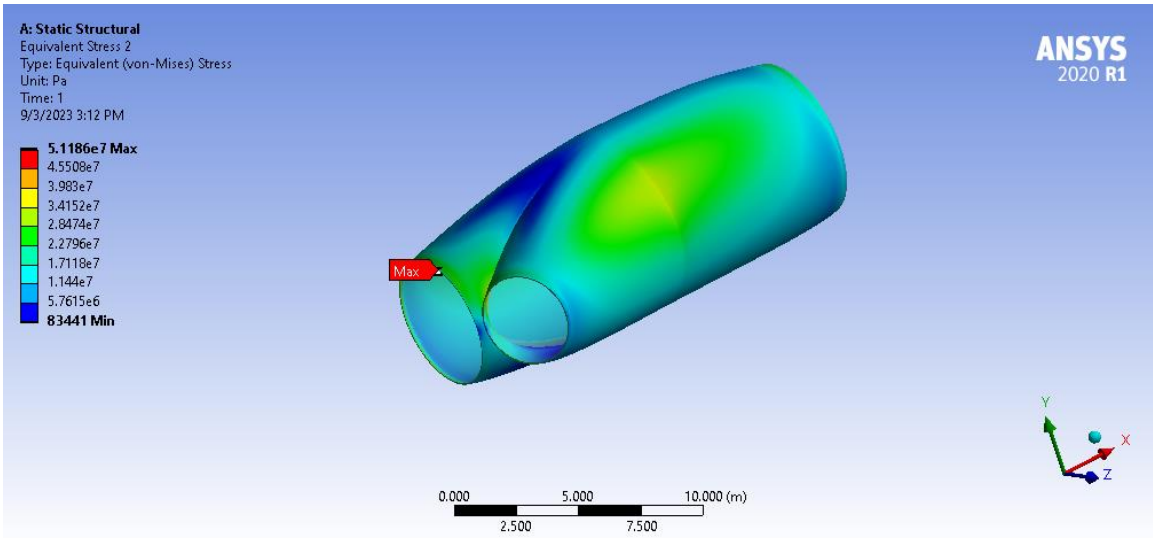*Figure E 2 Maximum Equivalent von-mises stress in first bifurcation(110mm) covered by concrete*
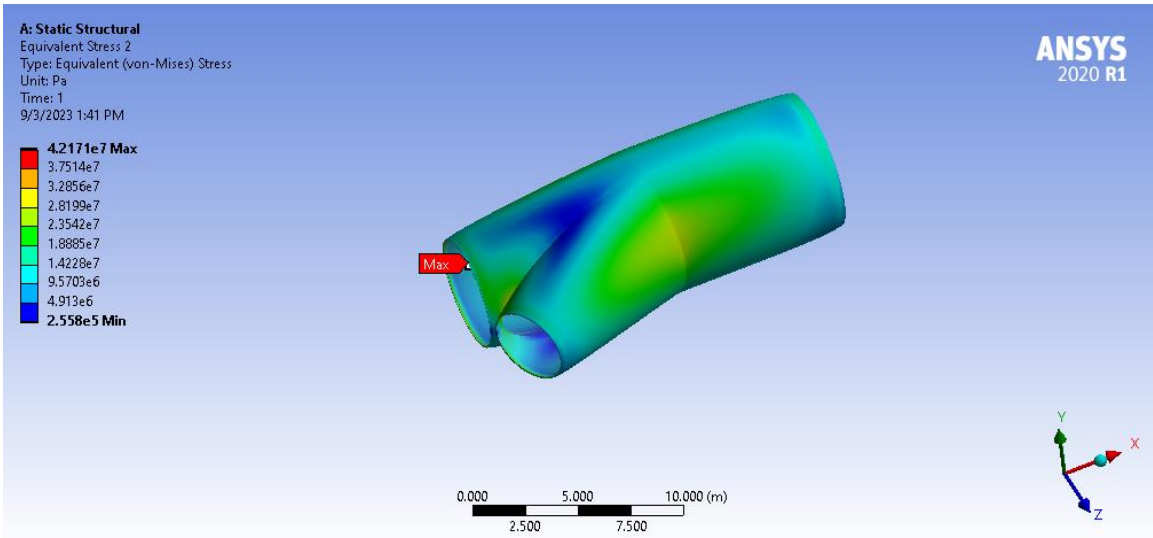
Figure E 3 Maximum Equivalent von-mises stress in first bifurcation(100mm) covered by concrete
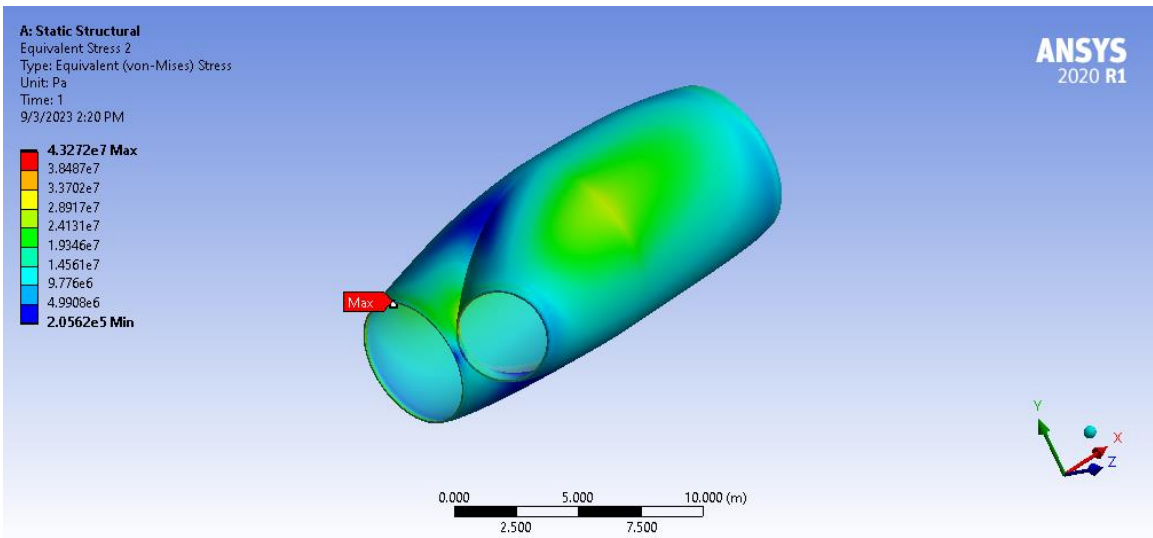
Figure E 4 Maximum Equivalent von-mises stress in first bifurcation(90mm) covered by concrete

Figure E 5 Maximum Equivalent von-mises stress in first bifurcation(80mm) covered by concrete

Figure E 6 Maximum Equivalent von-mises stress in first bifurcation(70mm) covered by concrete

Figure E 7 Maximum Equivalent von-mises stress in first bifurcation(60mm) covered by concrete
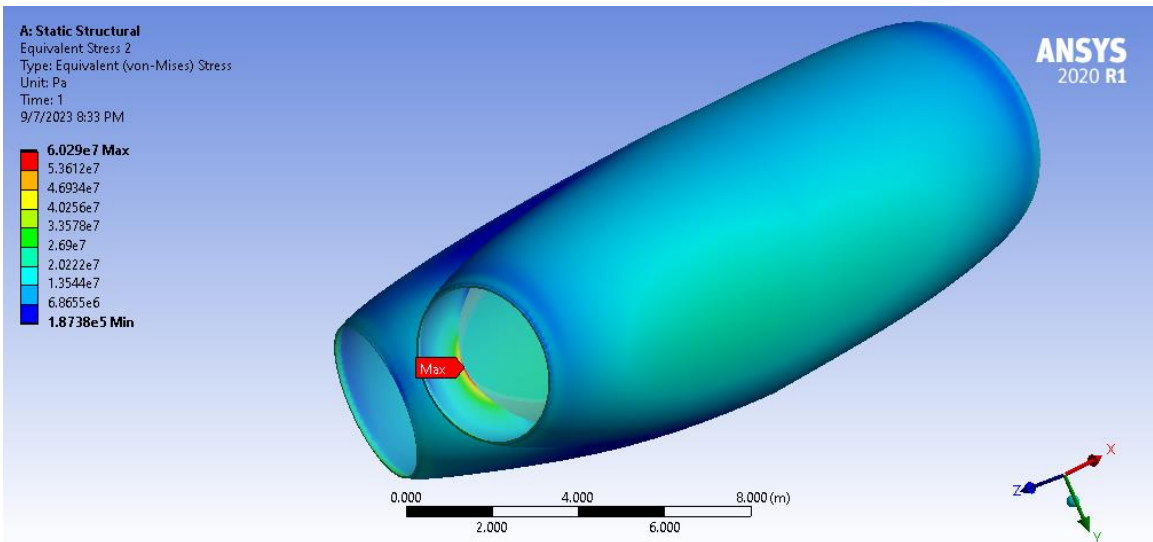

Figure E 8 Maximum Equivalent von-mises stress in second bifurcation(60mm) covered by concrete
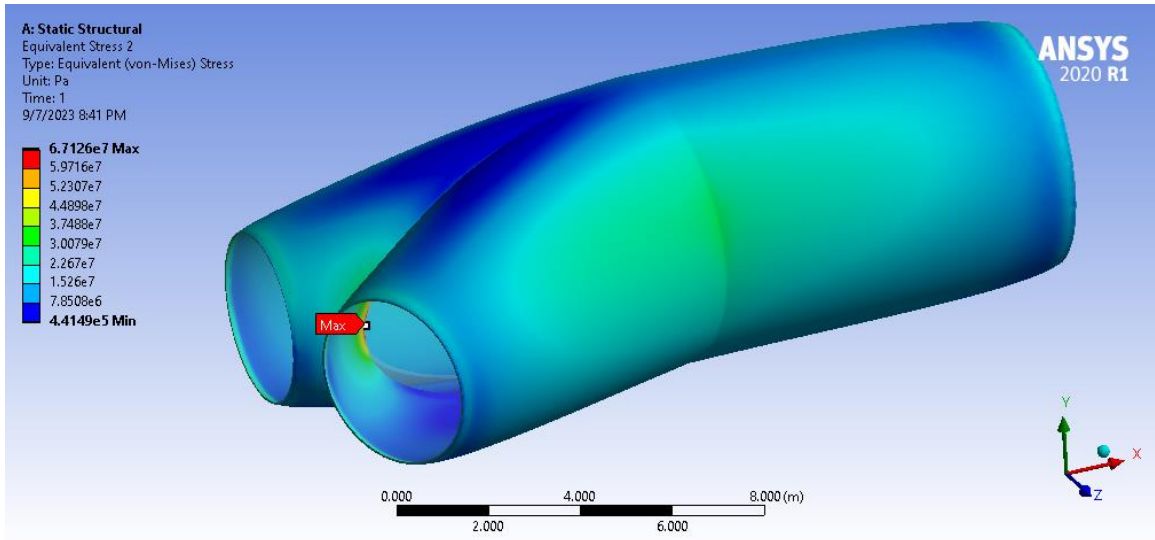
Figure E 9Maximum Equivalent von-mises stress in second bifurcation(50mm) covered by concrete

Annex-F STRESS RESULTS OF STRUCTURAL ANALYSIS

Table F 1 Variation of stress on pipe and concrete with thickness of first bifurcation

Thickness (mm)	Max Equivalent stress in pipe (MPa)	Max Principal stress in concrete (MPa)
130	34.303	4.145
120	35.04	4.278
110	37.342	4.473
100	42.171	4.8611
90	43.272	5.261
80	44.975	5.449
70	46.044	5.7309
60	51.186	6.5231

Table F 2 Safety Factor calculation for concrete (first bifurcation)

Thickness (mm)	Safety factor
130	2.412545
120	2.337541
110	2.235636
100	2.057148
90	1.900779
80	1.835199
70	1.744927
60	1.533013

Table F 3 Variation of stress on pipe and concrete with thickness of second bifurcation

Thickness (mm)	Max Equivalent stress in pipe (MPa)	Max Principal stress in concrete (MPa)
70	57.814	4.8376
60	60.29	5.5177
50	67.126	6.5805

Table F 4 Safety Factor calculation for concrete (second bifurcation)

Thickness (mm)	Safety factor
70	2.067141
60	1.812349
50	1.519641

Thesis

Internet   10 words — < 1%

23   www.ircwash.org
Internet   10 words — < 1%

24   archiv.ub.uni-heidelberg.de
Internet   9 words — < 1%

25   atrium.lib.uoguelph.ca
Internet   9 words — < 1%

26   kuscholarworks.ku.edu
Internet   9 words — < 1%

27   ledsgp.org
Internet   9 words — < 1%

28   www.ijfms.org
Internet   9 words — < 1%

29   Karakouzian, Chavez, Hayes, Nazari-Sharabian. "Bulbous Pier: An Alternative to Bridge Pier Extensions as a Countermeasure against Bridge Deck Splashing", Fluids, 2019
Crossref   8 words — < 1%

30   Koser, David Ryan. "Assessment of flood mitigation strategies for the city of Kalona, IA.", Proquest, 2016.
ProQuest   8 words — < 1%

31   Lee, Zeh. "Geosynthetic-reinforced soil walls under multidirectional seismic shaking", Proquest, 2012.
ProQuest   8 words — < 1%

32 Moses Karakouzian, Mohammad Nazari-Sharabian, Mehrdad Karami. "Effect of Overburden Height on Hydraulic Fracturing of Concrete-Lined Pressure Tunnels Excavated in Intact Rock: A Numerical Study", Fluids, 2019
Crossref

8 words — < 1%

33 Onsorynezhad, Saeed. "Analytical Study of Impact-Driven Frequency Up-Conversion Piezoelectric Energy Harvester", Southern Illinois University at Carbondale, 2022
ProQuest

8 words — < 1%

34 commons.erau.edu
Internet

8 words — < 1%

35 erepository.uonbi.ac.ke:8080
Internet

8 words — < 1%

36 essay.utwente.nl
Internet

8 words — < 1%

37 ethiopianchamber.com
Internet

8 words — < 1%

38 nec.edu.np
Internet

8 words — < 1%

39 pubag.nal.usda.gov
Internet

8 words — < 1%

40 soar.wichita.edu
Internet

8 words — < 1%

41 www.grafiati.com
Internet

8 words — < 1%

42 www.researchgate.net
Internet
8 words — < 1%

43 Proceedings of the International Symposium on Engineering under Uncertainty Safety Assessment and Management (ISEUSAM - 2012), 2013.
Crossref
6 words — < 1%

44 Siddhant Singh Yogesh, Arun Saco Selvaraj, Dinesh Kumar Ravi, Thundil Karuppa Raj Rajagopal. "Heat transfer and pressure drop characteristics of inclined elliptical fin tube heat exchanger of varying ellipticity ratio using CFD code", International Journal of Heat and Mass Transfer, 2018
Crossref
6 words — < 1%

EXCLUDE QUOTES	ON	EXCLUDE SOURCES	< 6 WORDS
EXCLUDE BIBLIOGRAPHY	ON	EXCLUDE MATCHES	OFF